REGULATION OF RENAL ORGANIC ANION TRANSPORTERS

by

HAOXUN WANG

A dissertation submitted to the

School of Graduate Studies

Rutgers, The State University of New Jersey

In partial fulfillment of the requirements

For the degree of

Doctor of Philosophy

Graduate Program in Pharmaceutical Sciences

Written under the direction of

Guofeng You

And approved by

_____

_____

_____

_____

New Brunswick, New Jersey

May, 2019

ABSTRACT OF THE DISSERTATION

Regulation of Renal Organic Anion Transporters

by HAOXUN WANG

Dissertation Director:

Guofeng You

Organic anion transporters (OATs) are a group of membrane proteins that are mainly involved in the body disposition of organic anionic molecules or zwitterions, including a diverse array of clinical therapeutics, environmental toxins, and endogenous molecules. OATs are present in multiple tissues. OATs in the kidney is responsible for removing various organic anion molecules from blood to proximal tubule lumen for subsequent elimination through urine.

The regulation of OATs can be classified into multiple levels such as transcriptional regulation, translational regulation, and post-translational regulation. My thesis work focuses on the investigation of post-translational modification/regulation of OATs by ubiquitination and SUMOylation as well as their upstream signaling pathways.

This thesis consists of 8 chapters. Chapter 1 gives an overview on the general properties of OATs. Chapters 2-6 describe our investigation on the molecular mechanisms underlying the regulation of OATs by post-translational modification ubiquitination and SUMOylation as well as their upstream signaling pathways including proteins kinases (sgks and PKA) and hormones (dexamethasone and insulin).

ACKNOWLEDGEMENTS

First and foremost, I would like to express my sincere gratitude to my advisor, Professor Guofeng You, who gave me such a great opportunity to conduct my PhD research in her laboratory and supported me through my PhD study with her comprehensive knowledge, logic thinking, patient guidance, and valuable suggestions in both science and social life. Without her kindly encouragement and numerous supports, this dissertation wouldn't have been possible.

I would also like to thank other committee members Professor Bozena B. Michniak-Kohn, Professor Arash Hatefi, and Professor Luca Cartegni for their helpful suggestions and critical review on my dissertation.

I am also grateful to all the current and previous colleagues in Dr. You's group for their generous help on my PhD study, particularly Dr. Qiang Zhang, Dr. Shanshan Li, Dr. Peng Duan and Dr. Da Xu for teaching me the technical skills and philosophical insights at the beginning of my PhD study. I also want to present my deep appreciation to my fellow students and colleagues Jinghui Zhang, Dr. Yunzhou Fan, Chenchang Liu, Zhou Yu, Dr. May Fern Toh and other members in the Pharmaceutical Science program.

It is a pleasure for me to thank the entire department of pharmaceutics, particularly Ms. Marianne Shen, Hui Pung, Fei Han, Sharana Taylor. I acknowledge the financial support from Department of Pharmaceutics during my first three years PhD study.

Last, I would like to express my deep love and gratitude to my beloved family. I am so grateful to my parents for their selfless and unconditional love that only parents can give. Specially, to my dear wife, Shuang, who gave me endless love and encouraged me since the first day we met. To my loving son, Antong Wang, who is the greatest gift I ever received in my life.

TABLE OF CONTENTS

LIST OF FIGURES

Chapter 1

Chapter 2

Chapter 3

ABBREVIATION

Bt2-cAMP –Dibutyryl cyclic AMP

BUO –Bilateral ureteral obstruction

CA-sgk –Constitutive active serum and glucocorticoid regulated kinase

DHEAS –Dehydroepiandrosterone sulfate

DMEM –Dulbecco's modified Eagle's medium

ES –Estrone sulfate

EMA –European Medicines Agency

FDA –Food and drug administration

hERG –Human ether-a-go-go related gene

IB –Immunoblotting

IGF-1 – insulin-like growth factor 1

IN-sgk –Inactive serum and glucocorticoid regulated kinase

IP –Immunoprecipitated

Nedd4-2 –Neural precursor cell expressed, developmentally down-regulated 4-2

NEM –N-ethylmaleimide

NHE –Na+/H+exchanger

NS –Statistically not significant

OAT –Organic anion transporter

NS –Statistically not significant

PAH–Para-aminohippurate

PBS –Phosphate-buffered saline

PKA –Protein kinase A

PKC –Protein kinase C

PMA –Phorbol 12-myristate 13-acetate

SDCT2–Na+/dicarboxylate cotransporter

Sgk –Serum and glucocorticoid regulated kinase

siRNA –small interfering Ribonucleic acid

SLC transporter –Solute carrier transporter

Ub –Ubiquitin

WT-sgk –Wild type serum and glucocorticoid regulated kinase

α-KG –α-ketoglutarate

Chapter 1

Overview

Portions of the information presented in this chapter are currently in preparation for the following article:

Haoxun Wang, Jinghui Zhang, Yunzhou Fan and Guofeng You.

Post-translational Regulation of Organic Anion Transporters - An Update

1. Drug Transporters

Drug transporters are membrane proteins that are localized on the physiological barriers of different tissues (e.g., intestine, liver, brain and kidney). They are the key players for the translocation of a variety of chemicals into and out of cells, and play critical roles in drug absorption, distribution, tissue-specific targeting, and drug elimination, thus affecting the pharmacokinetics and pharmacodynamics of the drug profile (1). One of the characteristics of these drug transporters is their broad substrate spectrums. As a result, co-administered drugs that are either substrates or potent inhibitors of drug transporters could cause serious side effects through drug-drug interaction (DDI) (1). In 2012, the US Food and Drug Administration (FDA) issued the industry draft guidance on drug interaction, which listed several major human drug transporters with clinical significance and outlined the recommendation on transporter-based DDI studies (2-4). As the field of drug transporter develops, in 2017, the FDA updated the draft guidance on DDI studies involving transporter-based inhibition and substrate studies (e.g., including Multi-antimicrobial extrusion proteins (MATE1 and MATE2-K) for inhibition and substrate studies) (5).

2. Organic Anion Transporters

Among the tissues involved in the ADME (absorption, distribution, metabolism and elimination) of clinical relevant therapeutics, kidney is one of the vital organs responsible for drug elimination after oral or intravenous administration, which basically includes three processes: glomerulus filtration, secretion and reabsorption (6). Renal drug transporters participate in the latter two processes and are responsible for the transfer of the drugs between blood and proximal tubule lumen (Figure 1-1) (2, 6-9). Among those renal transporters, organic anion transporters (OATs) are solute carrier (SLC) transporters that mainly interact with organic anionic molecules or zwitterions. The substrates of OATs consist not only a diverse array of important clinical therapeutics, including antivirals, anti-cancer drugs, antibiotics, anti-hypertensives, and anti-

inflammatories (10-15), but also endogenous physiological substances, like blood pressure regulator Thymidine(16), neurotransmitter metabolite 3,4-dihidroxymandelic acid (DHMA)(17), and dicarboxylic acid ketoglutarate (18). In addition, multiple nephrotoxins are also OAT substrates, such as the uremic toxins of indoxyl sulfate and Ochratoxin A (19, 20). OAT1-3 are expressed at the basolateral membrane of proximal tubule cell and are responsible for the uptake of anionic drug from blood into the proximal tubule cells. OAT4 is expressed at the apical membrane and functions as a bidirectional transporter (2, 12).

Figure 1-1. Membrane transporters expressed on human renal proximal tubule cells.

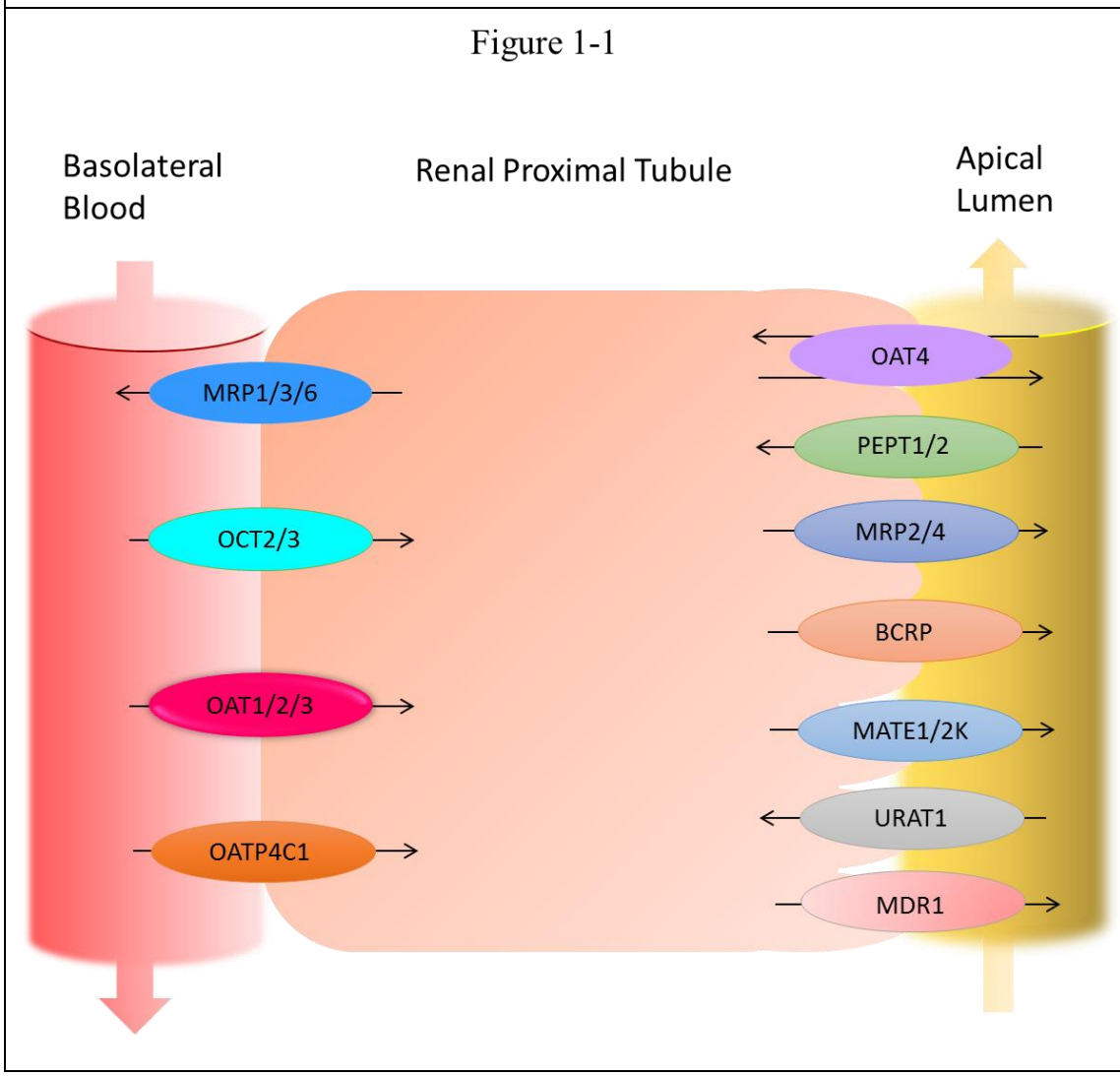

2.1 Transport Mechanism of OATs

Figure 1-2 illustrates the mechanism underlying OAT-mediated organic anion transport in the renal proximal tubule cells (6, 21). A tertiary transport mechanism is applied by OAT1-3 to bring the organic anions into the proximal tubule cells through the basolateral membrane: Na^+,K^+-ATPase on the basolateral membrane first creates the inwardly directed (blood-to-cell) Na^+ gradient, which promotes a sodium dicarboxylate cotransporter to move both sodium and dicarboxylates (e.g. α-ketoglutarate for OAT1/3, succinate for OAT2) into the cell. Eventually, an outwardly directed (cell-to-blood) dicarboxylate gradient facilitates the OAT1–3 mediated uptake of organic anions into the cell through organic anion (OA)/dicarboxylate exchange (11, 22-24). The apical OAT4 is a bi-directional transporter, which can mediate the influx of organic anions into the cell via OA/OH^- exchange mode and pump the organic anions out of cell through PAH/Cl^- exchange mechanism (6).

Figure 1-2. Model for OAT pathway. $SDCT_2$: Na+-coupled dicarboxylate cotransporter2; OAT: organic anion transporter; OA^-:organic anion; α-KG: α-ketoglutarate

Figure 1-2

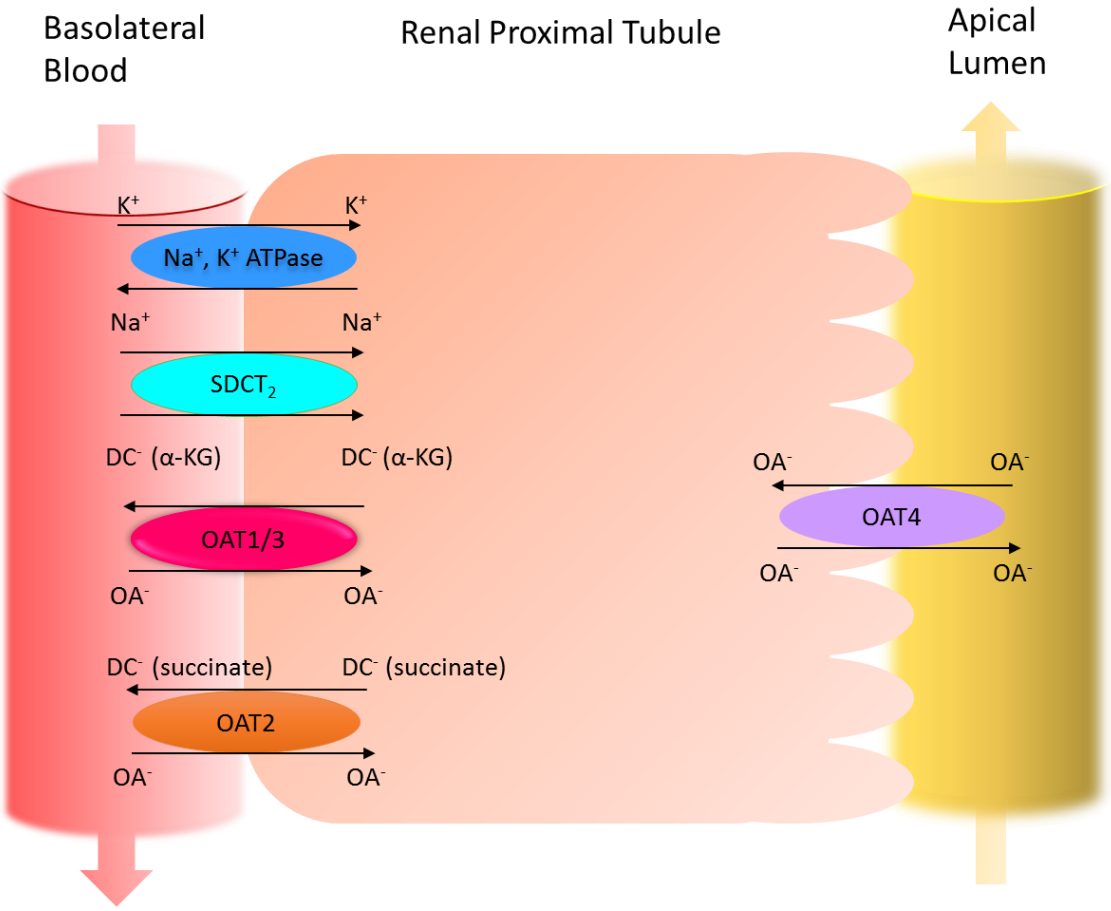

2.2 Clinical Relevance of OATs

In addition to the importance of OATs in drug disposition, their physiological role has also been revealed in certain physiology and disease conditions (21). One of the major focuses is the expression level and transport activity of OATs in renal failure and diseases, since kidney dysfunction will directly influence the elimination of clinical therapeutics which are OAT substrates (25, 26). It has been reported that rOat1 and rOat3 expression levels and transport activities were reduced in rats with chronic renal failure and acute renal failure (27-30). In the case of bilateral ureteral obstruction (BUO), which is a disease that blocks the urine to pass from

kidney to bladder, the transport activity and surface expression of renal rOat1/3 are also reduced (31). The relationship between Oats and diabetes in animal models has been extensively studied during the past decade. The observation made by Phatchawan et al. showed that the transport activity and expression level of rOat3 but not rOat1 were diminished in renal cortical slice of diabetic rats, which could be restored by Insulin treatment (32). Analysis of kidney transporters in Ins2Akita mouse model revealed decreased mRNA and protein expression of mOat1, mOat2, and mOat3 (33). Also, both ob/ob mice and db/db mice reduced mOat2 mRNA expression (34, 35). Interestingly, in rats fed a high-fat diet and injected a low dose of streptozotocin, elevated protein expression of rOat2 was revealed (36). The reason(s) for these observed discrepancies is still unclear. The difference in experimental conditions, such as different animal models might contribute to the disparate results. Besides diabetes, cholestasis, a liver disease in which the flow of bile from the liver is reduced or blocked, was also reported to affect renal Oats. Administration of alpha-naphthylisothiocyanate (ANIT) to induce biliary obstruction in rats resulted in reduced protein expression of rOat1 and rOat3 (37).

Given the crucial roles OATs play in determining the therapeutically effects of many clinical drugs, elucidating the molecular and cellular mechanisms underlying OAT regulation has a great physiological significance.

3. Regulations of OATs

OATs, like other proteins, are delicately regulated to maintain their normal activities. OATs can be controlled at both gene levels and protein levels by signaling pathway activators such exogenous chemicals and endogenous hormones (21).

During the past decade, our lab focused on the studies to uncover the mechanisms of several post-translational modifications of OATs, such as Glycosylation, Phosphorylation, and Ubiquitination (38-41). Our laboratory previously illustrated that OATs are dynamic membrane

proteins, which can constitutively internalize from and recycle back to the cell surface. Changes of the trafficking kinetics (internalization rate and recycling rate) may contribute to an alteration of amount of surface OATs, which usually accompanies a change in OAT transport activity. For example, short term activation of protein kinase C (PKC) increases the OAT internalization rate without altering the OAT recycling rate. As a result, OAT surface expression is decreased and OAT transport activity is also reduced (42, 43).

Further studies from our laboratory illustrated that the conjugation of ubiquitin, a polypeptide of 76 amino acids, to the surface OAT is a pre-requisite for PKC-stimulated OAT internalization (41, 44). Internalization machinery can recognize the ubiquitin-conjugation of transporter and therefore triggers the internalization process. Ubiquitination of OAT has been identified to be catalyzed by an E3 ubiquitin ligase, namely Nedd4-2. From our study, Nedd4-2 showed inhibitory effect on OAT transport activity through stimulating OAT ubiquitination, and internalization, and eventually decreasing OAT surface expression. Prolonged OAT ubiquitination leads to the degradation of the transporters in proteolytic systems. Therefore, Nedd4-2 is an important mediator in the regulation of OAT (45-47) (Figure 1-3).

Figure 1-3. The Mechanistic Links between Nedd4-2, PKC, and OAT. U: ubiquitin.

Figure 1-3

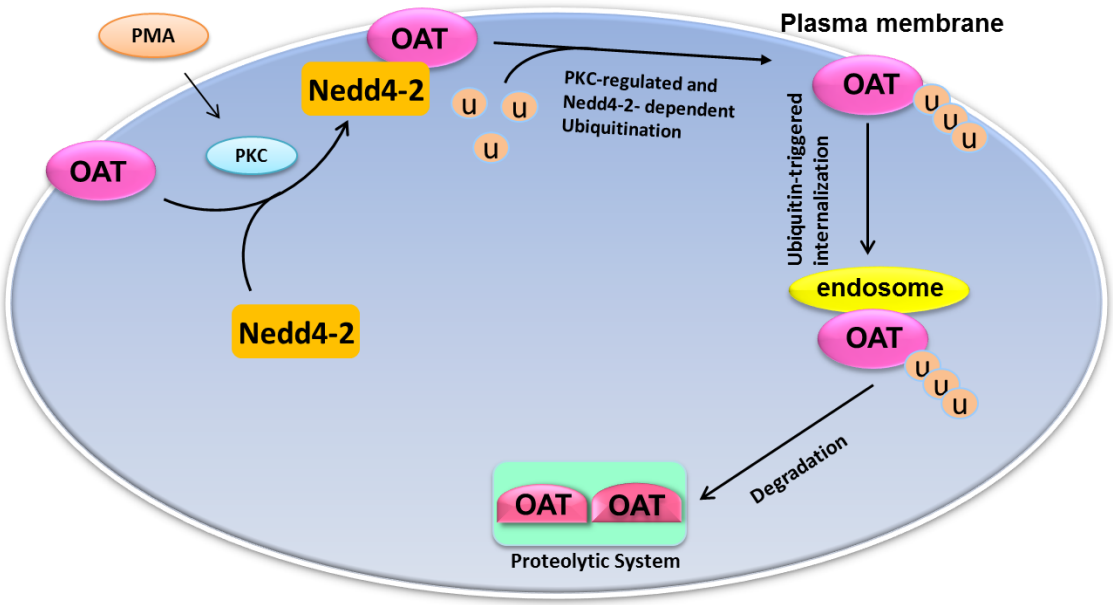

4. **Project goal and Rationale**

Although our lab has previously studied the detailed mechanism of Ubiquitination in the regulation of OATs, the upstream regulators of Ubiquitination, such as endogenous hormones and exogenous chemicals were largely unknown. Besides, other Post-translational modifications, like SUMOylation, which may have a cross talk with ubiquitination would be particularly interesting to be investigated (48). Therefore, during my PhD study, I investigated the upstream regulators of Ubiqutination and another Post-translational modification, SUMOylation.

Chapter 2

Serum- and glucocorticoid-inducible kinase SGK2 regulates human organic anion transporters 4 via ubiquitin ligase Nedd4-2

Majority of the work presented in this chapter has been published in the following articles:

Haoxun Wang, Da Xu, May Fern Toh, Alan C. Pao, and Guofeng You.

Serum- and Glucocorticoid-Inducible Kinase SGK2 Regulates Human Organic Anion Transporters 4 via Ubiquitin Ligase Nedd4-2.

Biochemical Pharmacology, 2016, 102, pp 120-129. doi: 10.1016/j.bcp.2015.11.024.

Haoxun Wang, Jinghui Zhang, and Guofeng You.

The mechanistic links between insulin and human organic anion transporter 4.

Int J Pharm. 2019 Jan 30;555:165-174. doi: 10.1016/j.ijpharm.2018.11.040

As collaboration, part of the data was generated by Da Xu and Haoxun Wang together.

1. Introduction

As mentioned in the section of overview, human organic anion transporter 4 (hOAT4) belongs to a class of organic anion transporters, that exert critical function in the body secretion, absorption, and distribution of numerous drugs, such as antiviral drugs, anti-cancer therapeutics, antibiotics, antihypertensive medicine, and anti-inflammatory drugs. The activity of these membrane proteins can be regulated at many levels such as transcriptional, translational, and posttranslational modulation (21). OAT4-mediated transport was suggested to be bidirectional (49) and sodium-independent (20). hOAT4 is richly existent in the kidney and placenta (20). In the kidney, hOAT4 is expressed at the apical membrane of the proximal tubule cells and participates in renal excretion and reabsorption of endogenous substances in addition to numerous drugs and xenobiotics. In the placenta, hOAT4 is expressed at the basolateral membrane of syncytiotrophoblasts (50). Placenta utilizes dehydroepiandrosterone sulfate (DHEAS), a precursor generated by the fetal adrenals, to synthesize estrogen. Buildup of extra DHEAS is linked with intrauterine growth retardation (51). DHEAS is a hOAT4 substrate (52). Therefore, hOAT4 may exert a significant role in placental uptake of DHEAS for making estrogens and for protecting fetus from the DHEAS cytotoxicity. OAT4 has also been found to be expressed in choroid plexus epithelial cells and brain microvessel endothelial cells through RT-PCR assay (53, 54). However, whether OAT4 protein is expressed in these cells are not known.

Due to such a critical role, delineating how hOAT4 is regulated has deep clinical significance. We formerly established that members of OAT family constitutively internalizes from and recycles back to plasma membrane and the transport activity of OAT can be modulated by changing the trafficking kinetics of these transporters (42, 43). An important event preceding OAT internalization is the ubiquitin conjugation to the transporter, catalyzed by an ubiquitin ligase Nedd4-2. Enhancement of Nedd4-2-dependent OAT ubiquitination leads to an acceleration

of OAT internalization/removal from plasma membrane and subsequent degradation (47). As a result, OAT expression at the plasma membrane, and therefore OAT transport activity is reduced.

The serum- and glucocorticoid-inducible kinases (sgk) participate in governing many cellular processes including sodium Na+ balance, renal transport, and cell proliferation (55-60). The family of the sgk protein kinases has three members: sgk1, sgk2 and sgk3. Sgk1 and sgk3 are richly present in every tissue, whereas sgk2 is expressed mainly in the liver, brain, kidney, and pancreas (61). Immunochemical characterization localized sgk1 protein to distal convoluted tubule, cortical and medullary collecting duct, whereas sgk2 protein was highly expressed in kidney proximal tubule cells, where it modulates the function of membrane proteins such as Na+/H+ exchanger (61). Based on the distinct characteristics of sgk2, we investigated whether hOAT4, also highly expressed in proximal tubule cells, is regulated by sgk2. We demonstrated a new regulatory mechanism that sgk2 modulates hOAT4 expression and function through an ubiquitin ligase Nedd4-2.

2. Results

2.1 Effect of sgk2 on hOAT4 transport activity

To explore the role of sgk2 in hOAT4 function, we transfected COS-7 cells with wild type sgk2 (WT-sgk2) or with its constitutive active form CA-sgk2. hOAT4-mediated uptake of [^{3}H] estrone sulfate was then measured. As shown in Fig. 2-1, wild type sgk2 stimulated ~ 40% increase in the uptake as compared to that in control cells, and CA-sgk2 significantly augmented the effect of sgk2, resulting in an additional 30% increase in the uptake. To examine the mechanism of sgk2-induced stimulation on hOAT4 transport activity, we measured hOAT4-mediated [^{3}H] estrone sulfate uptake at various substrate concentrations. An Eadie-Hofstee analysis of the derived data (Fig. 2-2) showed that transfection of CA-sgk2 resulted in an increased maximal transport velocity V_{max} of hOAT4 (48.66 ± 1.53 pmol·mg^{-1}·3min^{-1} with control cells and 80.59 ± 4.74 pmol·mg^{-1}·3min^{-1} with cells transfected with CA-sgk2) with no significant change in the substrate-binding affinity K_m of the transporter (5.32 ± 0.32 μM with control cells and 5.43 ± 0.46 μM with cells transfected with CA-sgk2).

Figure 2-1. Effect of sgk2 on hOAT4 transport activity (a) COS-7 cells were co-transfected with hOAT4 and control vector, or with hOAT4 and wild type sgk2 (WT-sgk2), or hOAT4 and the constitutive active form of sgk2 (CA-sgk2). 3-min uptake of [^{3}H]-estrone sulfate (0.1 μM) was then measured. Uptake activity was expressed as a percentage of the uptake measured in control cells. The data represent uptake into hOAT4-transfected cells minus uptake into mock cells (parental COS-7 cells). Values are mean ± S.E. (n = 3). *P<0.05

Figure 2-1

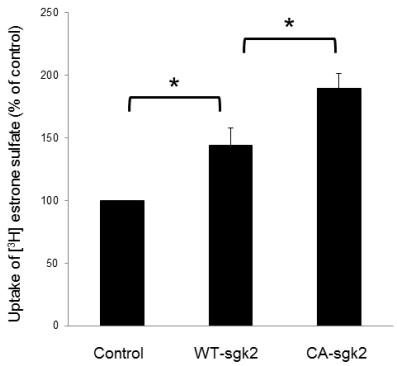

Figure 2-2. Effect of sgk2 on the kinetics of hOAT4-mediated estrone sulfate transport. COS-7 cells were co-transfected with hOAT4 and the constitutive active form of sgk2 (CA-sgk2), or with hOAT4 and control vector. Initial uptake (3 min) of [^{3}H] estrone sulfate was measured at the concentration of 0.1–10 μM. The data represent uptake into hOAT4-transfected cells minus uptake into mock cells (parental COS-7 cells). Values are means ± S.E. (n = 3). V, velocity; S, substrate concentration. (Figure 2-2 were generated by Da Xu and Haoxun Wang together)

Figure 2-2

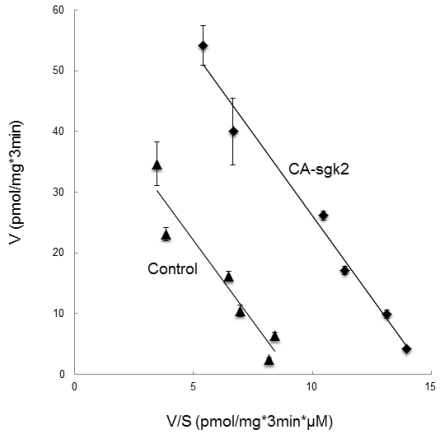

2.2 Effect of sgk2 on hOAT4 Expression

Either an increased number of the transporter at the plasma membrane or an increased transporter turnover rate could contribute to an increased Vmax. Therefore, we conducted biotinylation assay to differentiate between these two possibilities by measuring transporter expression both at the plasma membrane and in the total cell lysates. We showed that overexpression of sgk2 resulted in an increase of hOAT4 expression both at the cell surface (Fig. 2-3a) and in the total cell lysate (Fig. 2-3c). Such a change in hOAT4 total expression was not due to the general perturbation of cellular proteins because the expression of the house-keeping protein β-actin was similar under these conditions (Fig. 2-3e).

Figure 2-3. Effect of sgk2 on hOAT4 expression (a). Cell surface expression of hOAT4. COS-7 cells were co-transfected with hOAT4 and control vector or with hOAT4 and the constitutive active form of sgk2 (CA-sgk2). Transfected cells were labeled with biotin. Biotinylated/cell surface proteins were separated with streptavidin beads, followed by immunoblotting (IB) with an anti-myc antibody. (b). Densitometry plot of results from Fig. 2-3a, as well as from other experiments. The values are mean ± S.E. (n = 3). *P<0.05. (c). Total cell expression of hOAT4. COS-7 cells were co-transfected with hOAT4 and control vector or with hOAT4 and the constitutive active form of sgk2 (CA-sgk2). Transfected cells were lysed, followed by immunoblotting (IB) with an anti-myc antibody. (d). Densitometry plot of results from Fig. 2-3c, as well as from other experiments. The values are mean ± S.E. (n = 3). *P<0.05. (e). Total cell expression of β-actin. COS-7 cells were co-transfected with hOAT4 and control vector or with hOAT4 and the constitutive active form of sgk2 (CA-sgk2). Transfected cells were lysed, followed by immunoblotting (IB) with an anti-actin antibody.

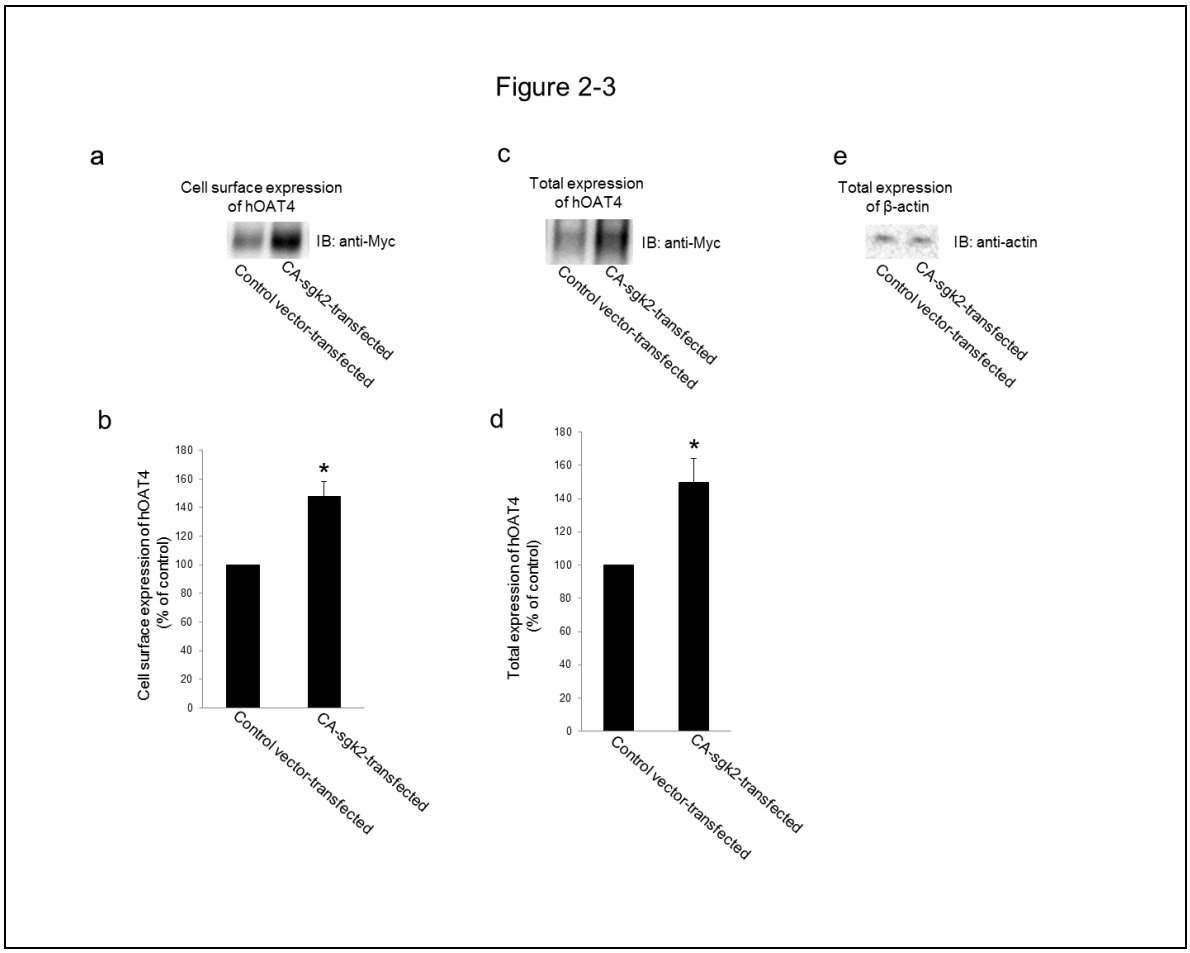

2.3 Effect of sgk2 on hOAT4 stability

Sgk2-induced increase in hOAT4 expression may reflect an increased stability of the transporter. In this experiment, we examined such possibility by measuring the degradation rate of cell surface hOAT4 in the presence or absence of sgk2. COS-7 cells were co-transfected with hOAT4 and control vector or with hOAT4 and CA-sgk2 for 48 hours and then biotinylated with membrane impermeable biotinylation reagent sulfo-NHSSS-biotin. Biotin-labeled cells were lysed at 2, 4, and 6 hour time point after the biotinylation, and cell surface proteins were isolated using streptavidin-agarose beads, followed by immunoblotting with anti-myc antibody (hOAT4 was tagged with myc at its carboxyl terminus). Our results (Figs. 2-4a, 4b) showed that the degradation rate of cell surface hOAT4 decreased significantly in the presence of sgk2 as

compared to that in control cells. The degradation rate change was not due to the general perturbation of the cellular proteins as evident when we measured the expression level of the house-keeping protein β–actin. β–actin was equally expressed in all samples tested (Fig. 2-4c).

Figure 2-4. Effect of sgk2 on the degradation of cell surface hOAT4 (a) COS-7 cells were cotransfected with hOAT4 and control vector (top panel) or with hOAT4 and the constitutive active form of sgk2 (CA-sgk2) (bottom panel). Cell surface hOAT4 degradation was then analyzed as described in "Materials and Methods" section followed by immunoblotting (IB) using anti-myc antibody. (b) Densitometry plot of results from Fig. 2-4a as well as from other experiments. The amount of undegraded cell surface hOAT4 was expressed as % of total initial cell surface hOAT4 pool. Values are mean ± S.E. (n = 3). (c). Total expression of sgk2 and house-keeping protein β-actin. COS-7 cells were co-transfected with hOAT4 and control vector or with hOAT4 and the constitutive active form of sgk2 (CA-sgk2). Transfected cells were lysed, followed by immunoblotting (IB) with anti-sgk2 antibody or anti-actin antibody.

Figure 2-4

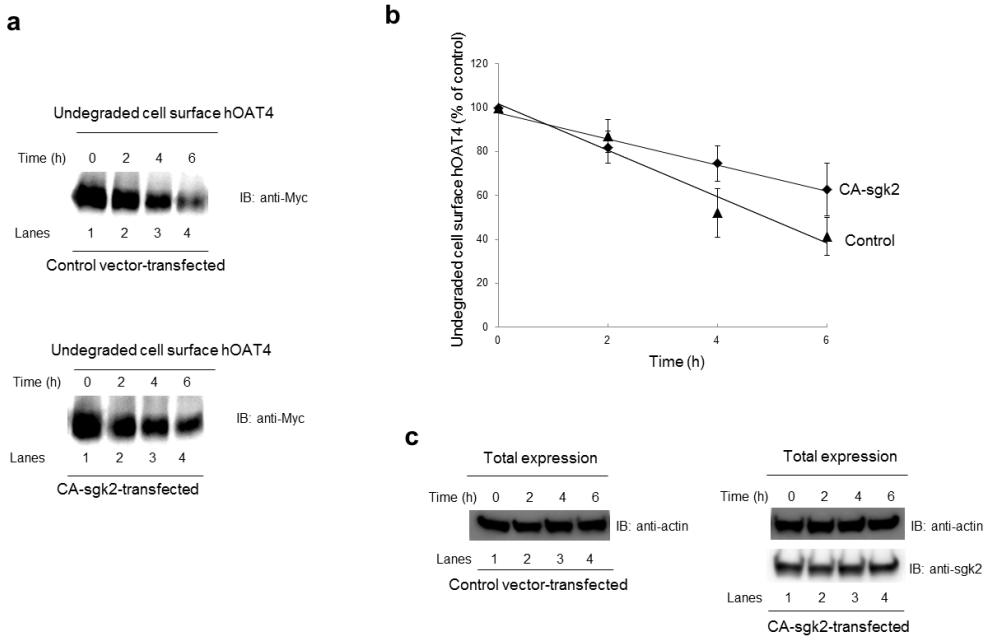

2.4 Effect of Nedd4-2 on hOAT4 ubiquitination and transport activity

It has been reported that one of the mediators for sgk regulation of membrane proteins is the ubiquitin ligase Nedd4-2 (62, 63). Nedd4-2 promotes the ubiquitination of many channels and transporters, and leads these membrane proteins to internalize from the cell surface and subsequently to be degraded (64-66). As a result, the expression of these membrane proteins at the cell surface is reduced, and their function is decreased. To examine whether Nedd4-2 is an ubiquitin ligase for hOAT4, we transfected Nedd4-2 into hOAT4-expressing COS-7 cells. Transfected cells were then lysed and hOAT4 was immunoprecipitated with anti-myc antibody (myc was tagged to hOAT4), followed by immunoblotting with anti-ubiquitin antibody to detect hOAT4 ubiquitination. As shown in Fig. 2-5a, hOAT4 ubiquitination was significantly enhanced

in cells transfected with Nedd4-2 as compared to that in control cells. Moreover, the differences in ubiquitination were not due to the differences in the amount of hOAT4 immunoprecipitated as similar amount of hOAT4 was immunoprecipitated between Nedd4-2 transfected sample and control (Fig. 2-5b). We then examined the effect of Nedd4-2 on hOAT4 transport activity. As shown in Fig. 2-5d, hOAT4 transport activity was decreased ~40% in cells transfected with Nedd4-2 as compared to that in control cells.

Figure 2-5. Effect of Nedd4-2 on hOAT4 ubiquitination and transport activity (a) hOAT4-expressing cells were transfected with or without wild type Nedd4-2. Transfected cells were then lysed, and hOAT4 was immunoprecipitated (IP) with anti-myc antibody (myc was tagged to hOAT4), followed by immunoblotting (IB) with anti-ubiquitin antibody (anti-Ub). (b) The same immunoblot from Fig. 2-5a was reprobed by anti-myc antibody. (c) Densitometry plot of results from Fig. 2-5a, as well as from other experiments. The values are mean ± S.E. (n = 3). *P<0.05. (d) COS-7 cells were co-transfected with hOAT4 and control vector or with hOAT4 and wild type Nedd4-2. 3-min uptake of [^{3}H]-estrone sulfate (0.1 μM) was then measured in these cells. The data represent uptake into hOAT4-transfected cells minus uptake into mock cells (parental COS-7 cells). Values are mean ± S.E. (n = 3). *P<0.05. (Figure 2-5 were generated by Da Xu and Haoxun Wang together)

Figure 2-5

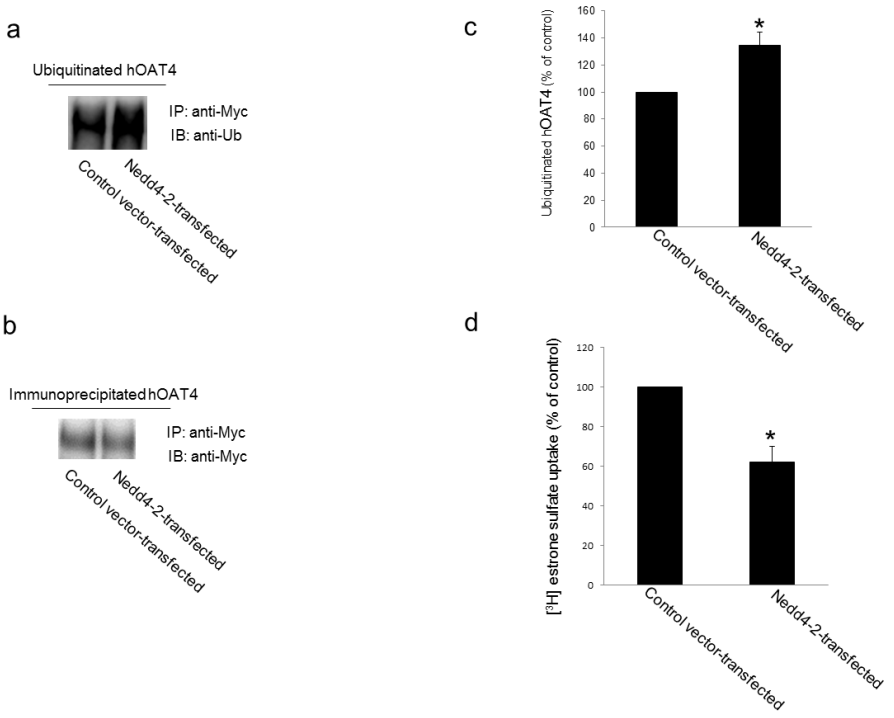

2.5 Effect of sgk2 on Nedd4-2 interaction with hOAT4

It has been reported that Nedd4-2 could interact either directly or indirectly with its target proteins (64, 65, 67, 68), and thus, we investigated whether there is an association between Nedd4-2 and hOAT4 through co-immunoprecipitation assay. As shown in Fig. 2-6a, when COS-7 cells were transfected with hOAT4, Nedd4-2 and control vector, significant amount of Nedd4-2 was observed in hOAT4 immunoprecipitates (lane 1), suggesting a direct association between these two proteins. However, in cells triple-transfected with hOAT4, Nedd4-2 and sgk2 (lane 2), the amount of Nedd4-2 detected in hOAT4 immunoprecipitates was much less than that in cells without sgk2. Furthermore, the differences in the amount of hOAT4 detected were not due to the differences in the amount of hOAT4 immunoprecipitated since similar amount of hOAT4 was

immunoprecipitated between CA-sgk2 transfected sample and control (Fig. 2-6b). These data suggest that sgk2 decreased the interaction between hOAT4 and Nedd4-2.

Figure 2-6. Effect of sgk2 on the interaction between Nedd4-2 and hOAT4 (a) COS-7 cells were transfected with hOAT4, Nedd4-2 and control vector or with hOAT4, Nedd4-2 and the constitutive active form of sgk2 (CA-sgk2). Transfected cells were then lysed, and hOAT4 was immunoprecipitated (IP) with anti-myc antibody, followed by immunoblotting (IB) with anti-Nedd4-2 antibody. (b) The same immunoblot from Fig. 2-6a was reprobed by anti-myc antibody. (c) Densitometry plot of results from Fig. 6a as well as from other experiments. The values are mean ± S.E. (n = 3). *P<0.05

Figure 2-6

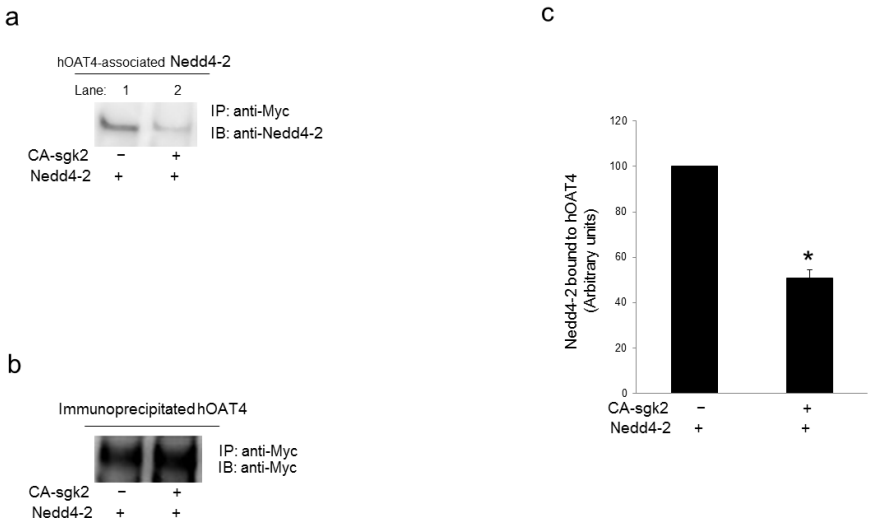

2.6 Effect of sgk2 on Nedd4-2-mediated cell surface expression of hOAT4

As mentioned above, Nedd4-2 ubiquitinates many membrane proteins, which leads these proteins to internalize from the cell surface. As a result, the amount of these proteins at the cell surface is reduced. In our current experiment, we further explored the relationship between sgk2 and Nedd4-2 in hOAT4 expression. We showed (Fig. 2-7a) that sgk2 significantly increased hOAT4 expression at the cell surface (lane 2 as compared to lane 1) in control cells. In cells transfected with Nedd4-2 for 48 hours, the initial amount of hOAT4 at the cell surface (lane 3) was already significantly decreased as compared to that in cells transfected with control vector, indicating that a portion of hOAT4 already went ubiquitination and therefore internalized from the plasma membrane during the 48-hour period of Nedd4-2 transfection. Such Nedd4-2-induced reduction of hOAT4 at the plasma membrane was abrogated by additional expression of sgk2 (lane 4). However, an ubiquitin ligase-dead mutant of Nedd4-2 (Nedd4-2/C821A) failed to reduce hOAT4 expression at the plasma membrane (lane 5), and furthermore, sgk2 was unable to enhance hOAT4 expression in the presence of Nedd4-2/C821A (lane 6). Therefore, these results suggest that stimulation of hOAT4 expression by sgk2 was via the ubiquitin ligase activity of Nedd4-2.

Figure 2-7. Effect of Nedd4-2 ligase activity on sgk2 regulation of hOAT4 cell surface expression (a). COS-7 cells were transfected with hOAT4, CA-sgk2 and control vector, or with hOAT4, CA-sgk2 and Nedd4-2, or with hOAT4, CA-sgk2 and ubiquitin ligase-dead Nedd4-2 mutant (Nedd4-2/C821A). Transfected cells were labeled with biotin. Biotinylated/cell surface proteins were separated with streptavidin beads, followed by immunoblotting (IB) with an anti-myc antibody. (b) COS-7 cells were transfected with hOAT4, CA-sgk2 and control vector, or with hOAT4, CA-sgk2 and Nedd4-2, or with hOAT4, CA-sgk2 and ubiquitin ligase-dead Nedd4-2 mutant (Nedd4-2/C821A). Transfected cells were then lysed, followed by immunoblotting with anti-actin antibody, anti-sgk2 antibody or anti-Nedd4-2 antibody, respectively. (c). Densitometry plot of results from Fig. 2-7a, as well as from other experiments. The values are mean ± S.E. (n =

3). *P<0.05, NS: statistically not significant.

Figure 2-7

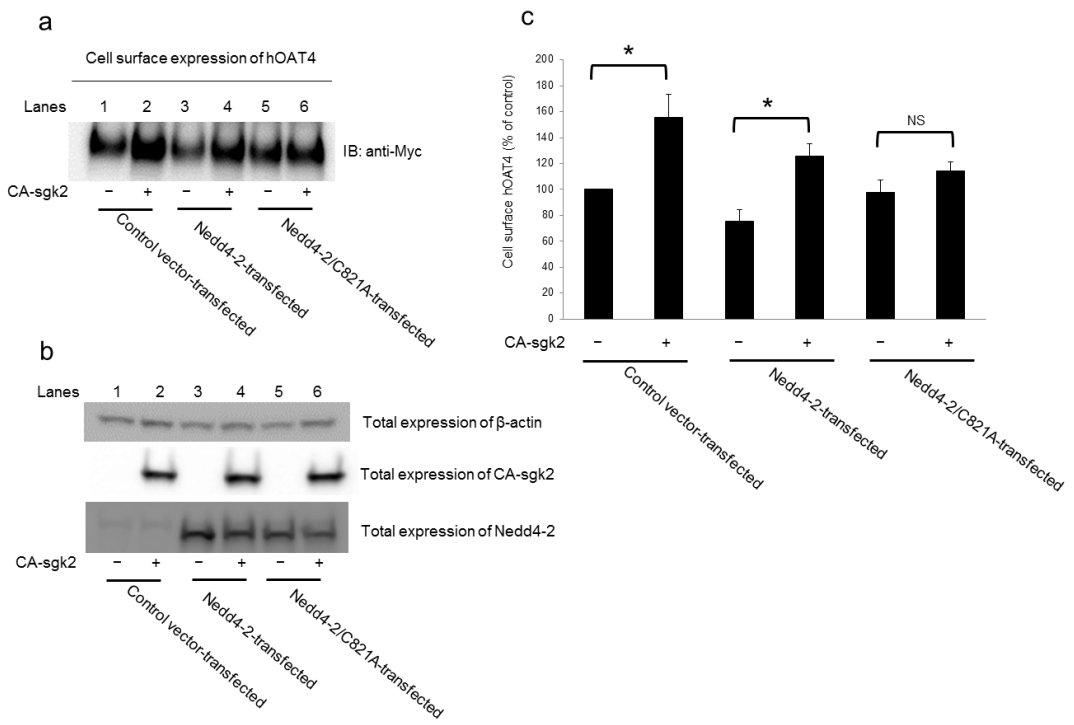

2.7 Effect of sgk2 on Nedd4-2-mediated transport activity of hOAT4

From the results described above, sgk2 and Nedd4-2 modulated hOAT4 expression at the cell surface. Therefore, we next investigated whether the altered surface expression will translate into a change in hOAT4 transport activity. As shown in Fig. 2-8, sgk2 stimulated hOAT4 transport activity by 44% in control cells. In cells transfected with Nedd4-2 for 48 hours, the initial hOAT4 transport activity was already significantly reduced as compared to that in control cells. This was consistent with the inhibition effect of Nedd4-2 on hOAT4 function (Fig. 2-5d). Additional expression of sgk2 abrogated the inhibition effect of Nedd4-2 on hOAT4 transport activity. However, in cells transfected with an ubiquitin ligase-dead mutant of Nedd4-2 (Nedd4-2/C821A), sgk2 was unable to enhance hOAT4 activity. Similar results were also observed in cells

transfected with Nedd4-2-specific siRNA to knock down the endogenous Nedd4-2 (Fig. 2-9). As shown in Fig. 2-9a, Nedd4-2-specific siRNA effectively reduced the expression of endogenous Nedd4-2 without interference with the expression of the house-keeping protein β-actin was (Fig. 2-9b). Under such condition, sgk2 failed to significantly stimulate hOAT4-mediated transport activity in cells transfected with Nedd4-2-specific siRNA as compared to that in cells transfected with scramble siRNA (Fig. 2-9c).

Figure 2-8. Effects of Nedd4-2 ligase activity on sgk2 regulation of hOAT4 transport function. COS-7 cells were transfected with hOAT4, CA-sgk2 and control vector, or with hOAT4, CA-sgk2 and Nedd4-2, or with hOAT4, CA-sgk2 and ubiquitin ligase-dead Nedd4-2 mutant (Nedd4-2/C821A). Transfected cells were then measured for the uptake of [^{3}H]-estrone sulfate (3-min uptake and 0.1 μM estrone sulfate). The data represent uptake into hOAT4-transfected cells minus uptake into mock cells (parental COS-7 cells). Values are mean ± S.E. (n = 3). *P<0.05, NS: statistically not significant.

Figure 2-8

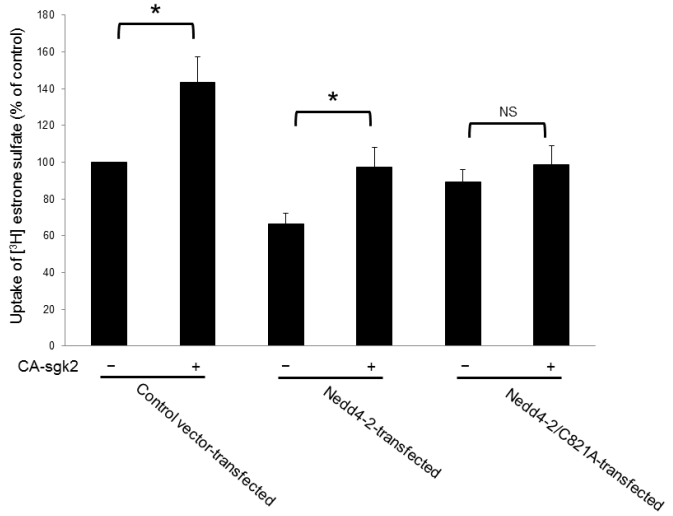

Figure 2-9. Effect of Nedd4-2-specifc siRNA-knock down of endogenous Nedd4-2 on sgk2 regulation of hOAT4 transport activity (a) COS-7 cells were co-transfected with hOAT4 and scrambled control siRNA or with hOAT4 and Nedd4-2-specific siRNA. The effectiveness of Nedd4-2-specific siRNA was tested by probing the lysis sample with anti-Nedd4-2 antibody. (b) COS-7 cells were co-transfected with hOAT4 and scrambled control siRNA or with hOAT4 and Nedd4-2-specific siRNA. The expression of the house-keeping protein β-actin was determined by probing the lysis sample with anti-actin antibody. (c) COS-7 cells were co-transfected with hOAT4 and scrambled control siRNA or with hOAT4 and Nedd4-2-specific siRNA. Transfected cells were then measured for the uptake of [^{3}H]-estrone sulfate (3-min uptake and 0.1 μM estrone sulfate). The data represent uptake into hOAT4-transfected cells minus uptake into mock cells

(parental COS-7 cells). Values are mean ± S.E. (n = 3). *P<0.05, NS: statistically not significant.

Figure 2-9

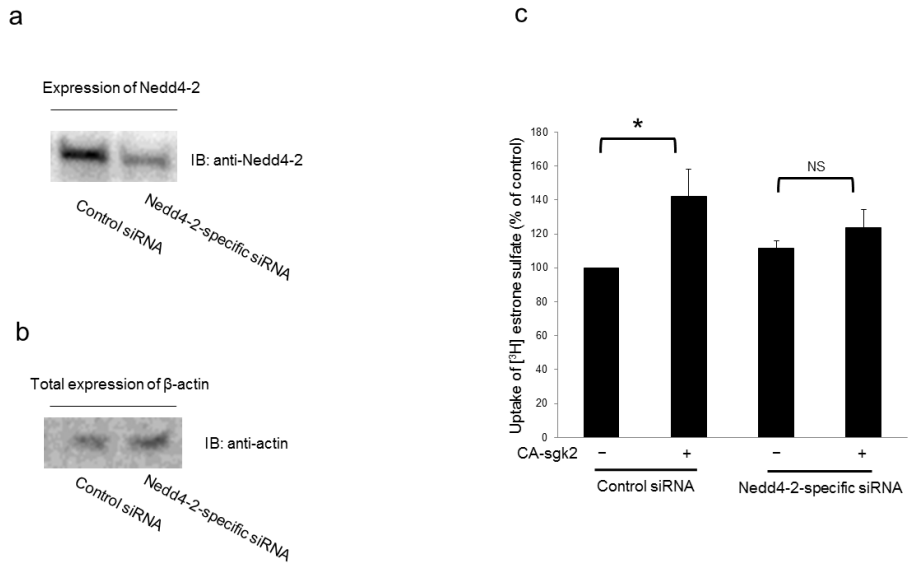

3. Discussion

Organic anion transporters (OATs) is a major deciding factor of the effects of therapeutics and toxic chemicals. Thus, delineating the regulation of OATs at the molecular and cellular levels is clinically and pharmacologically important. The present study revealed a new regulatory mechanism for hOAT4-mediated organic anion/drug transport, namely, sgk2 regulated hOAT4 transport activity through modulating the inhibition of the transporter by Nedd4-2.

Our present studies were performed in a heterologous cell system – COS-7 cells, which have been proven to be an excellent model system for investigation of the cloned organic anion transporter (41, 42, 69). First, these cells are originated from the kidney. Examinations in such system have revealed other renal transport processes. Secondly, this cell line does not endogenously express OATs. Thus, expression of hOAT4 in these cells will permit us to characterize this transporter without the difficulty of being interfered by other organic anion transporters. Thirdly, the many signaling pathways are intact in these cells, providing a good exploratory model system for understanding the regulation of many transport processes. Lastly, the previous work revealed that the transport properties of OATs in these cells were consistent with those displayed in other systems. Our investigation in COS-7 cells will pave the path for the next stage of work concentrating on evaluating whether the similar mechanisms are operational in native epithelia.

In our current study, we first established that sgk2 stimulated hOAT4-mediated estrone sulfate uptake (Fig. 2-1) as a result of an enhanced maximum transport velocity (V_{max}) (Fig. 2-2), an increased hOAT4 expression (Fig. 2-3), and a decreased degradation rate (Fig.2- 4).

One of the mechanisms in which sgk kinases modulate their targets is by interaction with cytosolic mediators. Among these mediators is the ubiquitin ligase Nedd4-2, which has been shown to play a key role in the regulation of many membrane proteins such as epithelial sodium

channel ENaC, potassium channel hERG, and the human excitatory amino acid transporter EAAT2 (65, 66, 70). Nedd4-2 catalyzes the conjugation of ubiquitin molecules to its target membrane proteins, which leads to the internalization of these membrane proteins from cell surface and subsequent degradation. As a result, the amount of these membrane proteins at the cell surface is reduced and their function is decreased. Our current studies identified Nedd4-2 as an important regulator for hOAT4. Nedd4-2 enhanced hOAT4 ubiquitination (Figs. 2-5a and 5c), and inhibited hOAT4 transport activity (Fig. 2-5d).

The results from our current studies also revealed that the inhibitory effect of Nedd4-2 on hOAT4 occurs through a direct association between these two proteins as co-immunoprecipitation assay detected a binding between them (Fig. 2-6). Our finding that Nedd4-2 was a crucial mediator for sgk2 regulation of hOAT4 expression and transport activity was supported by several lines of evidence: first, our coimmunoprecipitation experiments showed that sgk2 weakened the interaction between Nedd4-2 and hOAT4 (Fig. 2-6). Secondly, sgk2 abrogated inhibition effect of Nedd4-2 on hOAT4 cell surface expression. However, sgk2 was without any influence on hOAT4 expression in the presence of an ubiquitin ligase-dead Nedd4-2 mutant (Nedd4-2/C821A) (Fig. 2-7). Thirdly, sgk2 abolished inhibition effect of Nedd4-2 on hOAT4 transport activity. However, sgk2 was without any influence on hOAT4 activity in cells transfected with an ubiquitin ligase-dead Nedd4-2 mutant (Nedd4-2/C821A) (Fig. 2-8) or in cells transfected with Nedd4-2-specific siRNA to knock down the endogenous Nedd4-2 (Fig. 2-9).

Sgks, like other protein kinases, exert their effects through phosphorylating their target substrates. The hOAT4 sequence does not bear any putative sgk phosphorylation consensus sites. Therefore, sgk2 may modulate hOAT4 expression and function by phosphorylating an unconventional site(s) in hOAT4 sequence. On the other hand, it has been reported that several transporters and channels are modulated by sgk1, an isoform of sgk2, not directly through phosphorylating the transporters themselves but rather indirectly through phosphorylating the

ubiquitin ligase Nedd4-2 (66, 70, 71). The work aiming at identifying the sgk2-specific phosphorylation sites on hOAT4 and/or Nedd4-2 is currently being carried out in our lab.

In conclusion, this is the first demonstration of a new regulatory mechanism of hOAT4 transport activity: sgk2 stimulates hOAT4 transport activity by abrogating the inhibition effect of Nedd4-2 on the transporter.

Chapter 3

SGK1/Nedd4-2 signaling pathway regulates the activity of Human Organic Anion Transporters 3

Majority of the work presented in this chapter has been published in the following article:

Haoxun Wang and Guofeng You.

SGK1/Nedd4-2 signaling pathway regulates the activity of human organic anion transporters 3. Biopharm Drug Dispos. 2017 Nov;38(8):449-457. doi: 10.1002/bdd.2085.

1. Introduction

Organic anion transporter 3 (OAT3) is localized at the basolateral membrane of the renal proximal tubule cells and facilitates the renal secretion of numerous clinical drugs, including anti-HIV therapeutics, anti-tumor drugs, antibiotics, antihypertension drugs, and anti-inflammatories (10-15). In Chapter 2, we showed that sgk2 is an important regulator for OAT4 expression and activity. In this Chapter, we investigated the role of sgk1, another sgk family member, in the regulation of OAT3.

2. Results

2.1 Sgk1 stimulates hOAT3 transport activity

The role of sgk1 in hOAT3 function was explored. COS-7 cells-expressing hOAT3 were transfected with wild type sgk1 (WT-sgk1), constitutive active form of sgk1 (CA-sgk1), or inactive sgk1 (IN-sgk1), followed by the measurement of hOAT3-mediated uptake of [^{3}H] estrone sulfate. As shown in Fig. 3-1, WT-sgk1 enhanced the uptake by ~ 40% as compared to that in control cells (hOAT3-expressing cells without WT-sgk1), and CA-sgk1 further amplified the effect of WT-sgk1, whereas the inactive sgk1 (IN-sgk1) resulted in a slight decrease in the uptake, possibly through suppressing the activity of endogenous sgk1. In a separate experiment, we treated hOAT3-expressing cells with a sgk-selective inhibitor GSK650394, followed by the measurement of hOAT3-mediated uptake of [^{3}H] estrone sulfate. GSK650394 induced a concentration-dependent inhibition with 40% and 85% inhibition at concentrations of 100 nM and 1 μM separately (Fig. 3-2). The influence of sgk1 on the kinetic characteristics of hOAT3-mediated [^{3}H] estrone sulfate uptake was then determined at different substrate concentrations. An Eadie-Hofstee analysis (Fig. 3-3) showed that there was an increase in the maximal transport velocity Vmax of hOAT3 in CA-sgk1-transfected cells as compared to that in cells transfected with control vector (154.0 ± 13.0 pmol·mg−1·3min−1 with control cells and 219.6 ± 9.7 pmol·mg−1·3min−1 with cells transfected with CA-sgk1), whereas there was no significant difference in the substrate-binding affinity Km of the transporter in both control and CA-sgk1-transfected cells (5.46 ± 0.32 μM with control cells and 5.94 ± 0.19 μM with cells transfected with CA-sgk1).

Figure 3-1. Sgk1 stimulates hOAT3 transport activity. COS-7 cells were co-transfected with hOAT3 and control vector, with hOAT3 and wild type sgk1 (WT-sgk1), with hOAT3 and constitutive active form of sgk1 (CA-sgk1), or with hOAT3 and inactive sgk1 (IN-sgk1). 3-min

uptake of [^{3}H]-estrone sulfate (0.3 μM) was then determined. The data represented uptake into hOAT3-transfected cells minus uptake into mock cells (parental COS-7 cells). Uptake activity was expressed as a percentage of the uptake measured in control cells. Values are mean ± S.E. (n = 3).

Figure 3-1

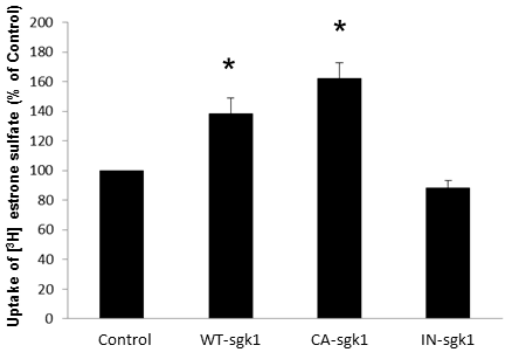

Figure 3-2. Sgk-specific inhibitor decreases hOAT3 transport activity. COS-7 cells were co-transfected with hOAT3 and CA-sgk1. Transfected cells were incubated with sgk-specific inhibitor GSK650394 for 30 min at indicated concentrations. 3-min uptake of [^{3}H]-estrone sulfate (0.3 μM) was then determined. The data represented uptake into hOAT3-transfected cells minus uptake into mock cells (parental COS-7 cells). Uptake activity was expressed as a percentage of the uptake measured in control cells. Values are mean ± S.E. (n = 3).

Figure 3-2

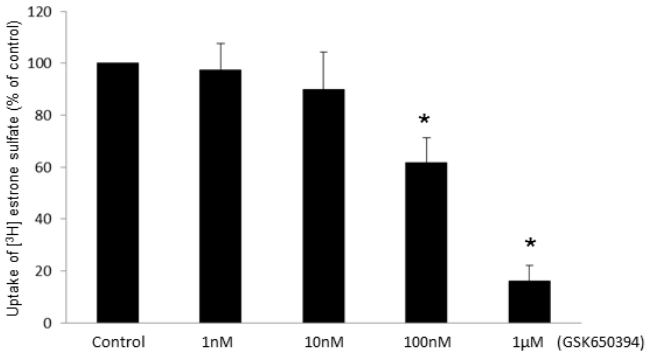

Figure 3-3. Effect of sgk1 on the kinetics of hOAT3-mediated estrone sulfate transport. COS-7 cells were co-transfected with hOAT3 and control vector or with hOAT3 and the constitutive active form of sgk1 (CA-sgk1). 3-min uptake of [^{3}H] estrone sulfate was then determined at the concentrations of 0.1–10 μM. The data represented uptake into hOAT3-transfected cells minus uptake into mock cells (parental COS-7 cells). Values are means ± S.E. (n = 3). V, velocity; S, substrate concentration.

Figure 3-3

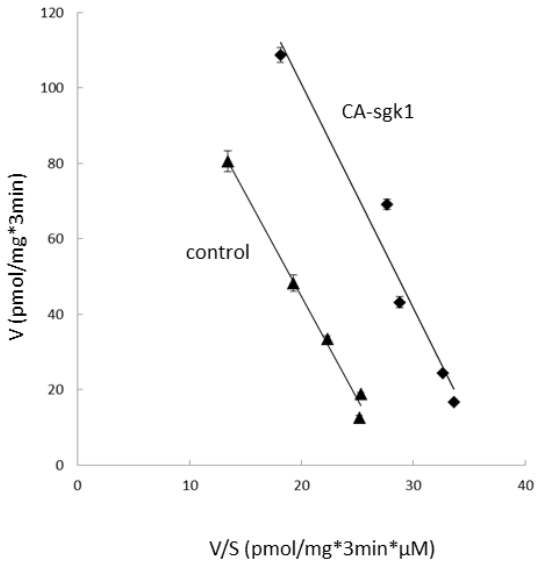

2.2 Sgk1 enhances hOAT3 Expression

Sgk1-induced increase in the maximal transport velocity Vmax of hOAT3 shown above (Fig. 3-3) could either reflect an increased number of the transporter at the plasma membrane or an increased transporter turnover rate. To differentiate between these possibilities, we examined the transporter expression both at the plasma membrane and in total cell lysates. Our results revealed that hOAT3 expressions at the cell surface (Fig. 3-4a, top panel) and in total cell lysate (Fig. 3-4c, top panel) were both increased in cells transfected with CA-sgk1 as compared to that in control cells. The increase in hOAT3 expression was specific as there was no significant changes in the expression of cell surface protein marker E-cadherin (Fig. 3-4a, bottom panel) and cellular protein marker β-actin (Fig. 3-4c, bottom panel).

Figure 3-4. Sgk1 enhances hOAT3 expression. a. Top panel: hOAT3 expression at the cell surface. COS-7 cells were co-transfected with hOAT3 and control vector or with hOAT3 and the constitutive active form of sgk1 (CA-sgk1). Cell surface proteins were labeled with biotin, separated with streptavidin beads, followed by immunoblotting (IB) with an anti-myc antibody (epitope myc was tagged to hOAT3 for immune-detection). Bottom panel: The expression of cell surface protein marker E-cadherin. The same blot from the Top panel was re-probed with anti- E-cadherin antibody. b. Densitometry plot of results from Fig. 3-4a, Top panel as well as from other experiments. c. Top Panel: Total cell expression of hOAT3. COS-7 cells were co-transfected with hOAT3 and control vector or with hOAT3 and CA-sgk1. Transfected cells were lysed, followed by immunoblotting (IB) with an anti-myc antibody. Bottom panel: Total cell expression of cellular protein marker β-actin. The same blot from Top panel was re-probed with anti-β-actin antibody. (d). Densitometry plot of results from Fig. 3-4c, Top panel as well as from other experiments. The values are mean ± S.E. (n = 3).

Figure 3-4

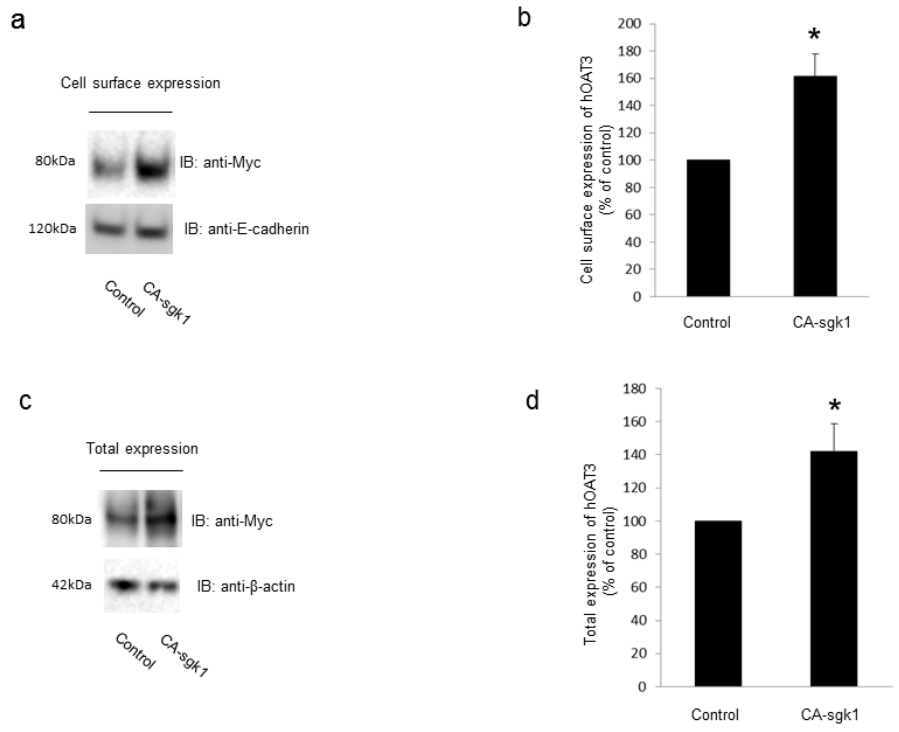

2.3 Sgk1 stabilizes hOAT3

An increased expression of hOAT3 at the cell surface observed above (Fig. 3-4a, top panel) may result from an enhanced insertion of the transporter into the plasma membrane or a decreased removal of the transporter from the plasma membrane. We used a reagent brefeldin A (BFA) to distinguish between these two mechanisms. BFA inhibits secretory mechanisms by blocking the transition of the transporters from endoplasmic reticulum (ER) to Golgi, and preventing formation of vesicles at the Golgi apparatus. As a result, insertion of the transporters into the plasma membrane is inhibited (72). As shown in Fig. 3-5a, top panel, after a 6-hr treatment with BFA, the decrease of hOAT3 expression at the plasma membrane was less dramatic in cells transfected with CA-sgk1 (65%) as compared to that in control cells (80%). We also examined

the effect of BFA on the total expression of hOAT3 (Fig. 3-5c, top panel). Under BFA treatment, hOAT3 displayed two bands at molecular sizes of 60 kDa and 80 kDa. Our lab previously demonstrated (38, 39) that OAT undergoes a maturation process when transiting from ER to Golgi. The ER form is a non-glycosylated form of 60 kDa, which matures in Golgi to a glycosylated form of 80 kDa. Only the glycosylated form (80 kDa) can target to plasma membrane. BFA blocked the transition of hOAT3 from ER to Golgi, which led to the appearance of a 60 kDa band after BFA treatment. Therefore, the total expression of hOAT3 is the combination of the band at 60 kDa and the band at 80 kDa. It is important to note that even when we combined the two bands (60 kDa + 80 kDa) together, the intensity was still slightly lower than that without BFA treatment. The possible explanation is that BFA blocked the insertion of hOAT3 into the plasma membrane but did not blocked hOAT3 degradation. After 6-hour period, part of hOAT3 was removed from the plasma membrane and was degraded. The degradation in the presence of sgk1 is slower than that without sgk1. Similarly, the decrease of hOAT3 transport activity was ~61% in cells transfected with CA-sgk1 as compared to a more significant decline of ~74% in control cells (Fig. 3-5d). These data suggest that sgk1 plays a significant role in stabilizing hOAT3 both at the plasma membrane and in total expression.

Figure 3-5. Sgk1 stabilizes hOAT3. a. Top panel: hOAT3 expression at the cell surface. COS-7 cells were co-transfected with hOAT3 and control vector or with hOAT3 and constitutive active form of sgk1 (CA-sgk1). The transfected cells were treated with brefeldin A (BFA, 0.1 μg/ml) for 6 hrs., followed by the determination of hOAT3 expression at the cell surface through a biotinylation approach and immunoblotting with anti-myc antibody (epitope myc was tagged to hOAT3 for immune-detection). Bottom panel: The expression of cell surface marker protein E-cadherin. The same blot from Fig. 3-5a, Top panel was re-probed with anti- E-cadherin antibody. b. Densitometry plot of results from Fig. 3-5a, Top panel as well as from other experiments. The amount of cell surface hOAT3 was expressed as % of total initial cell surface

hOAT3 pool (at 0 hr. of BFA treatment). Values are mean ± S.E. (n = 3). c. Top Panel: Total cell expression of hOAT3. COS-7 cells were co-transfected with hOAT3 and control vector or with hOAT3 and constitutive active form of sgk1 (CA-sgk1). The transfected cells were treated with brefeldin A (BFA, 0.1 μg/ml) for 6 hrs. Treated cells were lysed, followed by immunoblotting (IB) with an anti-myc antibody. Bottom panel: Total cell expression of β-actin, a cellular protein marker. The same blot from Fig. 3-5c, Top panel was re-probed with anti-β-actin antibody. d. COS-7 cells were co-transfected with hOAT3 and control vector, or with hOAT3 and CA-sgk1. The transfected cells were treated with brefeldin A (BFA, 0.1 μg/ml) for 6 hrs. [^{3}H] estrone sulfate uptake (3min, 0.3 μM) was then measured. Uptake activity was expressed as % of the uptake value measured at 0 hr. of BFA treatment.

Figure 3-5

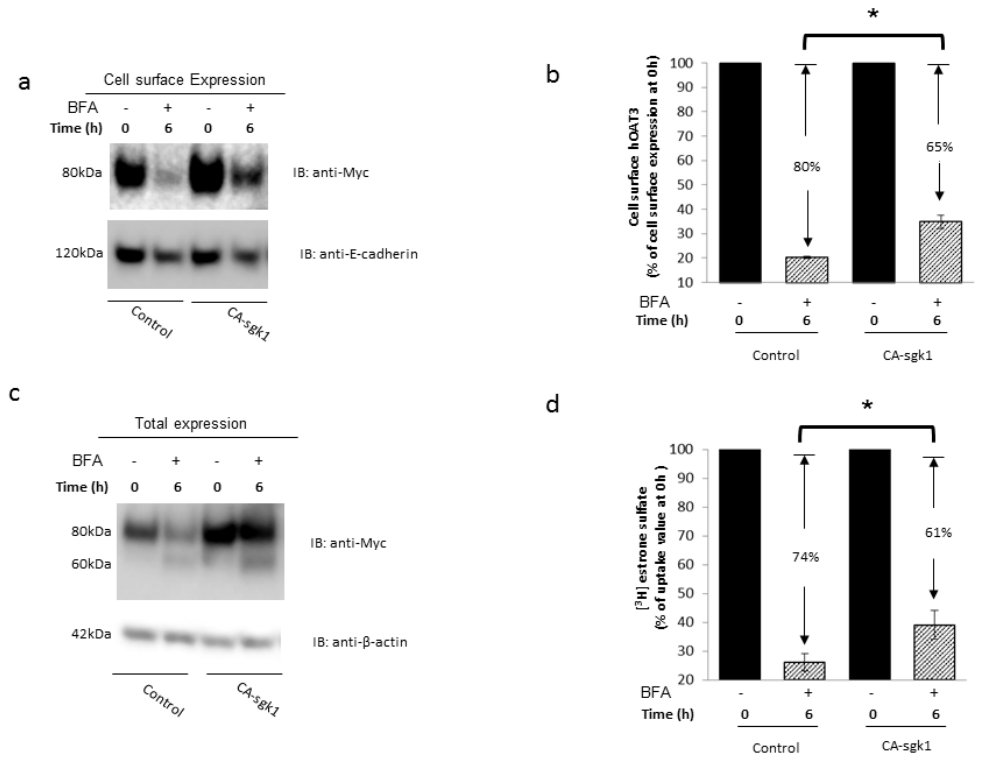

2.4 Sgk1 phosphorylates Nedd4-2 in COS-7 cells

Previous investigations (73) in other systems reported that sgk1 regulates its substrates, at least in part, by phosphorylating Nedd4-2 at serine residue 327 (Ser 327). In the current experiment, we examined whether sgk1 also phosphorylated Nedd4-2 in our system. COS-7 cells were co-transfected with Nedd4-2 and control vector or with Nedd4-2 and CA-sgk1. Phospho-Nedd4-2 was examined by immunoblotting with phosphor-Nedd4-2 (Ser327)-specific antibody. As shown in Fig. 3-6a, the phospho-Nedd4-2-specific antibody recognized a band around the size of Nedd4-2 in control cells, indicating that Nedd4-2 was indeed phosphorylated at Ser327. The phosphorylation signal was increased by 37% in cells transfected with CA-sgk1. The total expression of Nedd4-2 was not affected by CA-sgk1 (Fig. 3-6c). Therefore, sgk1 enhanced Nedd4-2 phosphorylation in COS-7 cells.

Figure 3-6. Sgk1 phosphorylates Nedd4-2. a. COS-7 cells were transfected with Nedd4-2 and control vector or with Nedd4-2 and CA-sgk1. Transfected cells were lysed and immunoblotted with anti-phospho-Nedd4-2(Ser327)-specific antibody. b. Densitometry plot of results from Fig. 3-6a, as well as from other experiments. The values are mean ± S.E. (n = 3). c. The same blot from Fig. 6a was re-probed with anti-Nedd4-2. d. Densitometry plot of results from Fig. 3-6c as well as from other experiments. The values are mean ± S.E. (n = 3). e. The same blot from Fig. 3-6a, was re-probed with anti-β actin antibody. β actin is a cellular protein marker.

Figure 3-6

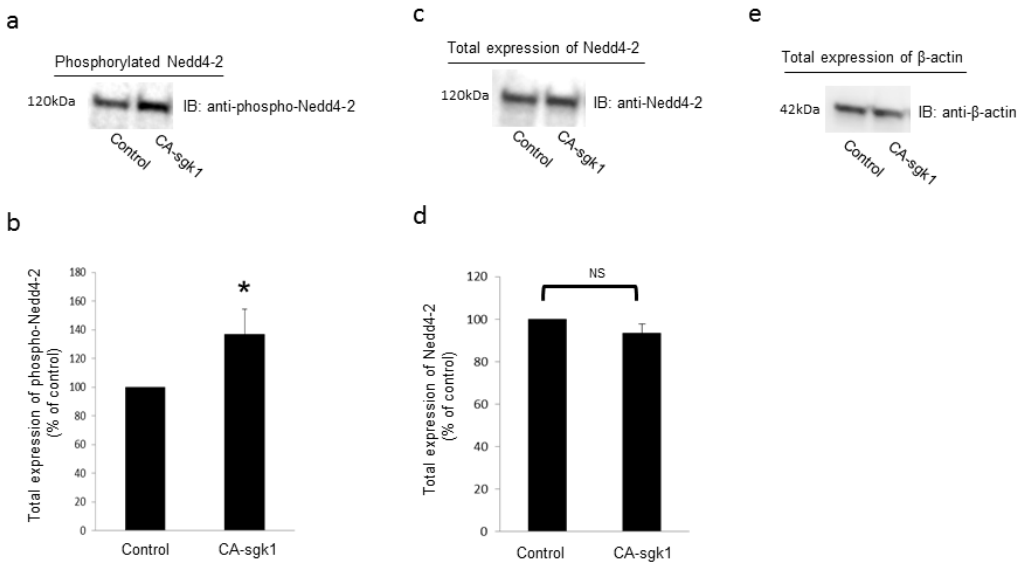

2.5 Sgk1 interferes with the interaction between Nedd4-2 and hOAT3

Our lab recently demonstrated (45, 46) that Nedd4-2, an ubiquitin ligase, binds to OAT and inhibits OAT transport activity by promoting the conjugation of ubiquitin to OAT, which leads to OAT internalization from the plasma membrane and subsequent degradation (45-47). Next we studied the relationship among sgk1, Nedd4-2 and hOAT3 using a co-immunoprecipitation strategy. As shown in Fig. 3-7a, top panel, significant amount of Nedd4-2 was pulled down in hOAT3 immunoprecipitates (lane 1) in cells transfected with Nedd4-2, indicating a binding association between these two proteins. However, in cells transfected with Nedd4-2 and sgk1, much less amount of Nedd4-2 was detected in hOAT3 immunoprecipitates (lane 2). The difference in the amount of Nedd4-2 detected in hOAT3 immunoprecipitates was not due to the

difference in the amount of hOAT3 immunoprecipitated as similar amount of hOAT3 was pulled down in both samples (Fig. 3-7a, bottom panel). These results suggest that sgk1 interfered with the association between hOAT3 and Nedd4-2.

Figure 3-7. Sgk1 weakens the interaction between Nedd4-2 and hOAT3. a. Top panel: hOAT3-expressing COS-7 cells were transfected with Nedd4-2 and control vector or with Nedd4-2 and CA-sgk1. Transfected cells were lysed and hOAT3 was immunoprecipitated by anti-myc antibody (epitope myc was tagged to hOAT3), followed by immunoblotting with anti-Nedd4-2 antibody. Bottom panel: The same immunoblot from Fig. 3-7a, Top panel was reprobed by anti-myc antibody. b. Densitometry plot of results from Fig. 3-7a, Top panel as well as from other experiments. The values are mean ± S.E. (n = 3).

Figure 3-7

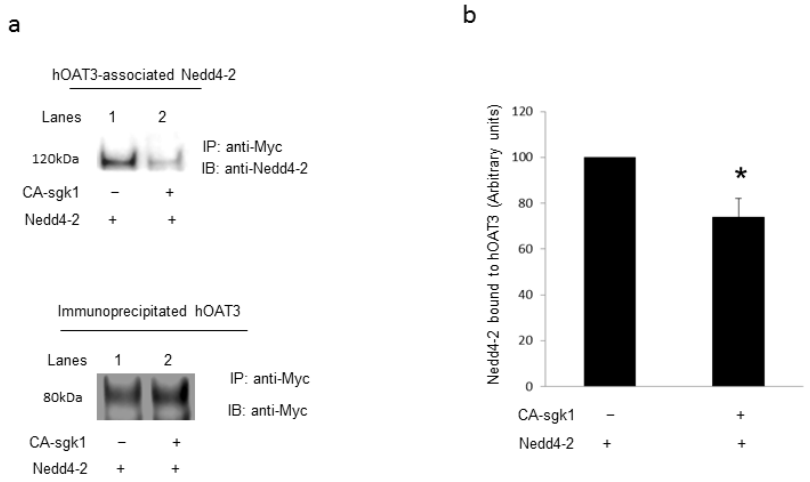

2.6 Sgk1 inhibits hOAT3 ubiquitination

The effect of sgk1 on hOAT3 ubiquitination was then examined (Fig. 3-8). In cells transfected with Nedd4-2 alone, hOAT3 was heavily ubiquitinated. However, the ubiquitination of hOAT3 was significantly decreased in cells transfected with both Nedd4-2 and sgk1 (Fig. 3-8a, top panel). The difference in the amount of ubiquitinated OAT3 was not due to the difference in the amount of OAT3 immunoprecipitated as similar amount of OAT3 was pulled down in both samples (Fig. 3-8a, bottom panel). These results suggest that sgk1 inhibits Nedd4-2-mediated OAT3 ubiquitination.

Figure 3-8. The effect of Sgk1 on OAT3 ubiquitination. a. Top panel: COS-7 cells were transfected with hOAT3, Nedd4-2 and control vector or with hOAT3, Nedd4-2 and CA-sgk1. Transfected cells were treated with the PKC activator PMA (1 μM) for 30 min to enhance hOAT3 ubiquitination. Treated cells were then lysed and hOAT3 was immunoprecipitated by anti-myc antibody (epitope myc was tagged to hOAT3), followed by immunoblotting with anti-ubiquitin antibody. Bottom panel: The same immunoblot from Fig. 3-8a, Top panelwas reprobed by anti-myc antibody. b. Densitometry plot of results from Fig. 3-8a, top panel as well as from other experiments. The values are mean ± S.E. (n = 3).

Figure 3-8

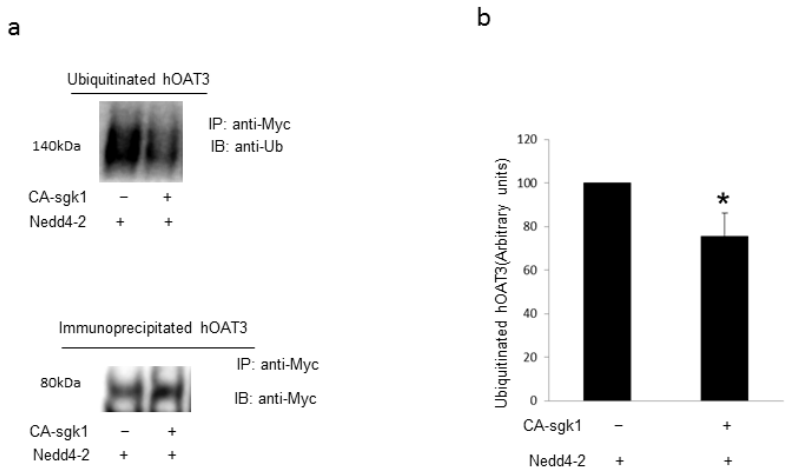

2.7 Nedd4-2 ligase-dead mutant attenuates sgk1-induced stimulation of hOAT3 transport activity

Our result obtained above demonstrated that sgk1 phosphorylated hOAT3 (Fig. 3-6), interfered with the binding of Nedd4-2 to hOAT3 (Fig. 3-7), and inhibited hOAT3 ubiquitination (Fig. 3-8). The functional consequence due to such action was then assessed. hOAT3-expressing COS-7 cells were transfected with CA-sgk1 and control vector or with CA-sgk1 and a ligase-dead mutant of Nedd4-2 (Nedd4-2/C821A). This mutant is incapable of ubiquitinating OATs. As shown in Fig. 3-9, sgk1 stimulated hOAT3 transport activity by 38% in control cells, presumably through interfering with the inhibitory effect of the endogenous Nedd4-2 on hOAT3. However, in cells

transfected with a ligase-dead mutant of Nedd4-2 (Nedd4-2/C821A), the stimulatory effect of sgk1 on hOAT3 was attenuated.

Figure 3-9. Nedd4-2 ligase-dead mutant attenuates the stimulatory effect of CA-sgk1 on hOAT3 transport activity. hOAT3-expressing COS-7 cells were transfected with sgk1 and control vector or with sgk1 and a ligase-dead mutant of Nedd4-2 (Nedd4-2/C821A). 3-min uptake of [^{3}H]-estrone sulfate (0.3 μM) was then determined. Uptake activity was expressed as a percentage of the uptake measured in cells without the transfection of sgk1. Values are mean ± S.E. (n = 3).

Figure 3-9

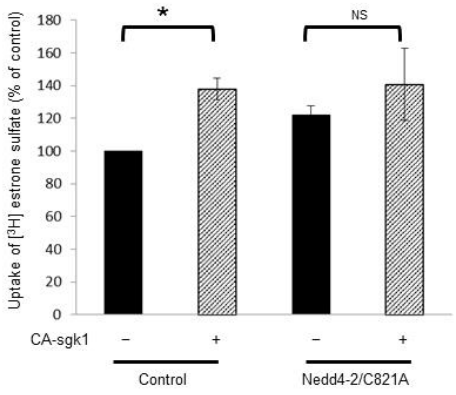

3. Discussion

From our study, we acquired several pieces of crucial information. First, sgk1 has a significant regulatory role in hOAT3 function. Overexpression of sgk1 resulted in a stimulation of hOAT3-mediated estrone sulfate uptake (Fig. 3-1). Treatment of the cells with a sgk-specific inhibitor has an opposite effect (Fig. 3-2), although we cannot exclude the possibility that the effect of GSK650394 may result from the inhibition of sgk1 as well as other Sgk1-related kinases. The stimulation of hOAT3 activity by sgk1 was due to an enhanced maximum transport velocity (Vmax) without changing the binding affinity (Km) of the transporter for its substrates, as revealed by our kinetic analysis (Fig. 3-3). The enhanced Vmax correlated with an increased amount of the transporter at the plasma membrane (Fig. 3-4), which resulted, at least in part, from the role of sgk1 in stabilizing hOAT3 at the cell surface (Fig. 3-5).

Secondly, sgk1 regulates hOAT3 function via ubiquitin ligase Nedd4-2. Sgk kinases were previously shown to modulate their targets by interacting with cytosolic components, one of which is the ubiquitin ligase Nedd4-2. Nedd4-2 is a key regulator of a variety of membrane proteins, including sodium channel ENaC, potassium channel hERG, and the amino acid transporter EAAT2 (70, 71, 73). Our lab recently demonstrated that Nedd4-2 directly binds to OATs and catalyzes the attachment of ubiquitin molecules to these transporters, which leads to the endocytosis/internalization of OATs from plasma membrane to intracellular endosomes and subsequent degradation. Consequently, both the amount of cell surface OATs and their transport activity are decreased (45-47). In exploring the relationship among sgk1, Nedd4-2 and hOAT3, we found that sgk1 phosphorylated Nedd4-2 (Fig. 3-6), weakened the binding between Nedd4-2 and hOAT3 (Fig. 3-7), and decreased hOAT3 ubiquitination (Fig. 3-8). The sgk1-induced phosphorylation of Nedd4-2 may cause a conformational change of the ubiquitin ligase, hinder its binding to hOAT3 and attenuate its inhibition of hOAT3 transport activity. Therefore, the

stimulatory effect of sgk1 on hOAT3 transport activity is due, in part, to the ability of sgk1 to interfere with the inhibitory effect of Nedd4-2 on hOAT3.

OATs are under the control of several protein kinases including protein kinase C (40) and sgk1 as demonstrated in our current study. These protein kinases exert their roles through phosphorylating their substrates. Our lab previously demonstrated that PKC regulates OAT activity by altering the trafficking kinetics of OATs without direct phosphorylation of the transporter itself (40, 42). It is possible that PKC regulates OAT by phosphorylating an OAT-interacting partner. In our current study, we showed that sgk1 phosphorylated Nedd-4-2 (Fig. 3-6). Whether sgk1 directly phosphorylates hOAT3 is an interesting topic for future investigation.

In summary, our current study demonstrated that hOAT3 activity is regulated through sgk1/Nedd4-2 signaling pathway. Sgk1 stimulated hOAT3 transport activity by interfering with the inhibitory effect of Nedd4-2 on the transporter. Sgk is the downstream signaling molecule for many physiological hormones such as glucocorticoids and mineralocorticoids (74, 75). Therefore, our current study provides important insights into how hOAT3-mediated drug elimination is regulated in vivo.

Chapter 4

The activity of organic anion transporter-3: Role of dexamethasone.

Majority of the work presented in this chapter has been published in the following article:

Haoxun Wang, Chenchang Liu, and Guofeng You.

The activity of organic anion transporter-3: Role of dexamethasone.

J Pharmacol Sci. 2018 Feb;136(2):79-85. doi: 10.1016/j.jphs.2017.12.011.

1. Introduction

In Chapter 2 and Chapter 3, we demonstrated that sgk1 and sgk2 stimulate OAT activity by weakening the association of OAT with an ubiquitin ligase Nedd4-2, which leads to a deceleration of ubiquitin-dependent OAT internalization from the plasma membrane to intracellular compartments. As a result, the amount of OAT at the cell surface is enhanced and OAT transport activity is increased (76, 77).

Glucocorticoids are hormones that regulate numerous physiological activities related with metabolic, cardiovascular, and inflammatory processes (78). Excess of glucocorticoids contribute to obesity, hyperlipidemia, hypertension, and glucose intolerance (79). Glucocorticoids have been used for the treatment of diarrhea related to inflammatory bowel diseases and nontropical sprue (80). Several studies have shown that one of the signaling molecule downstream glucocorticoids is sgk (81-83). In the current study, we studied the role of dexamethasone, a synthetic glucocorticoid, in OAT3 expression and transport activity.

2. Results

2.1 Cis-inhibition of hOAT3-mediated estrone sulfate (ES) uptake by dexamethasone - Cis-inhibition studies were performed in hOAT3-expressing HEK293 cells. The 4-min uptake of [^{3}H]-ES (300 nM) in the presence of dexamethasone (100 μM) or probenecid (100 μM) were measured. Probenecid is a known competitive inhibitor for OATs. As shown in Fig. 4-1, dexamethasone exhibited ~80% inhibition of ES uptake, similar to the inhibitory potency of probenecid.

Figure 4-1. Cis-inhibition of hOAT3-mediated [^{3}H]-ES uptake by dexamethasone. 4-min uptake of 300 nM [^{3}H]-ES in the presence of dexamethasone (100 μM) or probenecid (100 μM) was measured. Each data point represented only carrier-mediated transport after subtraction of values from parental cells. Uptake activity was expressed as percentage of uptake measured in control cells from three independent experiments. Results shown are means ± S.E. of three separate experiments. *$P<0.05$

Figure 4-1

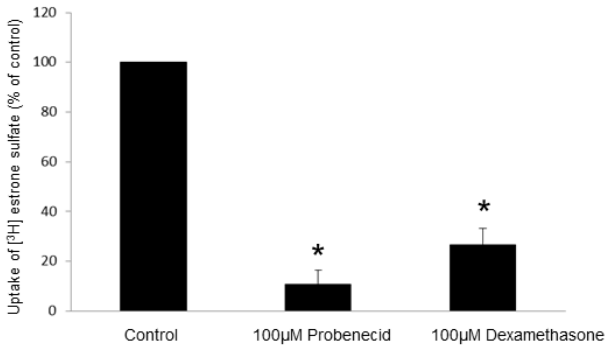

2.2 Dose-dependent effects of dexamethaosne on hOAT3-mediated transport - Dose response curve was then constructed to evaluate the effectiveness of dexamethasone as an inhibitor of hOAT3 uptake. 4-min uptake of [^{3}H]-ES (300 nM) was measured in the presence of 0.1-1000 μM dexamethasone. Our result showed that dexamethasone inhibited hOAT3-mediated ES uptake in a concentration-dependent manner with IC_{50} values of 49.91 μM (Fig. 4-2). IC_{50} value is the concentrations at which 50% inhibition is achieved.

Figure 4-2. Concentration dependence of dexamethasone inhibition on hOAT3-mediated uptake. hOAT3-expressing cells were incubated for 4 min with 300 nM [^{3}H]-ES in the presence of various concentrations of dexamethasone. Each data point represented only carrier-mediated transport after subtraction of values from parental cells. Uptake activity was expressed as

percentage of uptake measured in control cells from three independent experiments. Results shown are means ± S.E. of three separate experiments. *P<0.05. The line represents a best fit of data using nonlinear regression analysis.

Figure 4-2

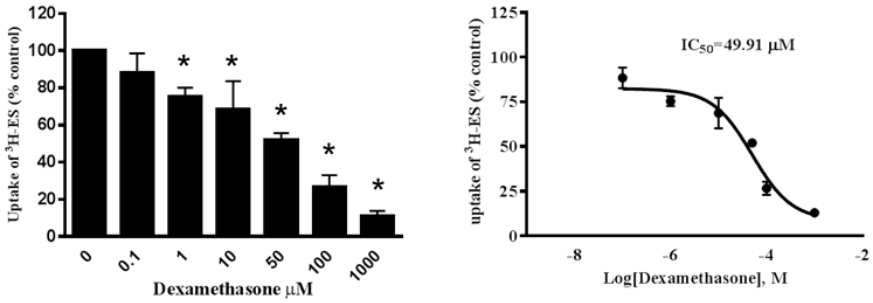

2.3 Dixon plot analysis – We further characterized the mechanism of dexamethasone-induced inhibition on hOAT3 transport activity by measuring the hOAT3-mediated [^{3}H]-ES uptake in the presence and absence of dexamethasone, followed by analysis via Dixon plot (Fig. 4-3). Dexamethasone demonstrated a competitive mechanism of inhibition of [^{3}H]-ES uptake by hOAT3 (as the lines for substrate concentrations converge above the x axis). Then, the constant Ki (inhibition constant) value was calculated by fitting the data to a competitive inhibition model (described by eq. 1). The K_m values of OAT3 for ES was 5μM, the inhibition constant (K_i) of dexamethasone was then estimated as 47.08 μM.

Figure 4-3. Dixon plot analysis of the inhibitory effects of dexamethasone on hOAT3-mediated transport. [^{3}H]-ES uptake (1.2 μM and 2.4 μM) was determined at 4 min in the presence of varying concentrations of dexamethasone. Each data point represented only carrier-mediated transport after subtraction of values from parental cells. Results shown are means ± SE percentage of uptake measured in control cells. The data were fitted by linear regression and K_i was calculated.

Figure 4-3

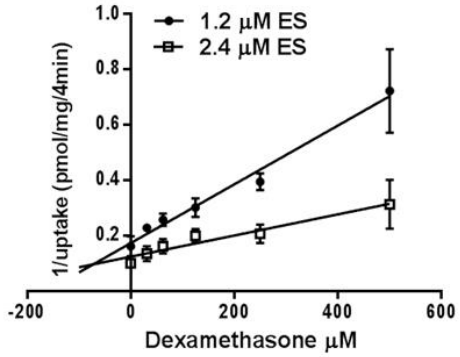

2.4 Long-term treatment of hOAT3-expressing cells with dexamethasone stimulates hOAT3 transport activity – The above studies (Figs. 4-1-4-3) were designed by measuring the 4-min uptake of [^{3}H]-ES (300 nM) in the presence of dexamethasone (100 μM). However, the long-term effect of dexamethasone on hOAT3 is not known. In the current experiment, we pretreated hOAT3-expressing cells with dexamethasone for 0 – 6 hrs., followed by measuring [^{3}H]-ES

uptake. Our results showed that long-term treatment of hOAT3-expressing cells with dexamethasone resulted in a stimulation of hOAT3-mediated [^{3}H]-ES uptake with 40% stimulation after 6 hrs. pretreatment (Fig. 4-4a). Dexamethasone also induced a dose-dependent stimulation of hOAT3 mediated transport with 6 hrs. pretreatment (Fig. 4-4b). In order to investigate the mechanism of dexamethasone-induced stimulation on hOAT3 transport activity, we measured hOAT3-mediated [^{3}H]-ES uptake at various substrate (ES) concentrations. An Eadie-Hofstee analysis of the measured data (Fig. 4-5) revealed that treatment of hOAT3-expressing cells with dexamethasone resulted in an increased maximal transport velocity V_{max} of hOAT3 (330 ± 24 pmol·mg^{-1}·4min^{-1} with control cells and 387 ± 29 pmol·mg^{-1}·4min^{-1} with cells transfected with dexamethasone). However, the substrate-binding affinity K_m of the transporter was not significantly changed (5.07 ± 0.49 μM with control cells and 5.08 ± 0.51 μM with cells transfected with dexamethasone).

Figure 4-4. Long-term treatment of hOAT3-expressing cells with dexamethasone stimulates hOAT3 transport activity. (a). Time dependence. hOAT3-expressing cells were pretreated with dexamethasone (10nM) for 2, 4 and 6 hrs. 4-min uptake of [^{3}H]-ES (300 nM) was then measured. Uptake activity was expressed as a percentage of the uptake measured in control cells. The data represent uptake into hOAT3-expressing cells minus uptake into mock cells (parental cells). Values are mean ± S.E. (n = 3). *P<0.05. (b). Dose dependence. hOAT3-expressing cells were pretreated for 6 hrs. with dexamethasone at varies doses. 4-min uptake of [^{3}H]-ES (300 nM) was then measured. Uptake activity was expressed as a percentage of the uptake measured in control cells. The data represent uptake into hOAT3-expressing cells minus uptake into control cells (parental cells). Values are mean ± S.E. (n = 3). *P<0.05.

Figure 4-4

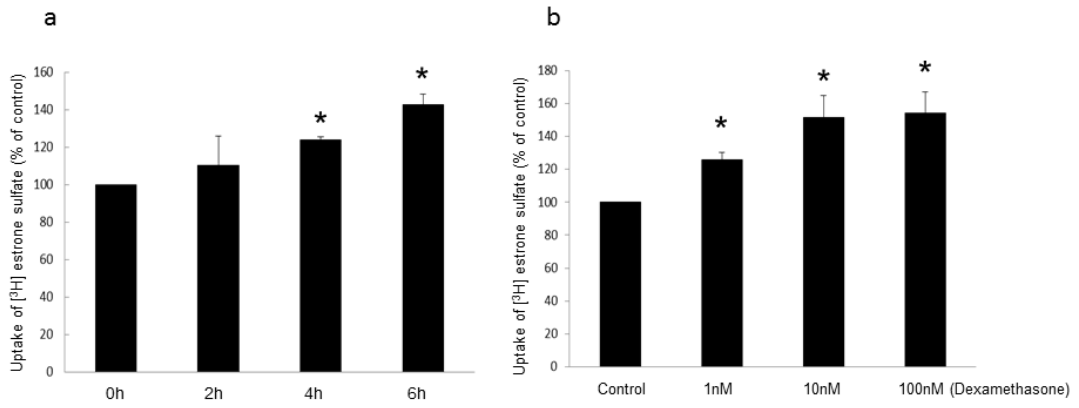

Figure 4-5. Kinetic analysis of hOAT3-mediated ES transport. Kinetic characteristics were determined at substrate concentration ranging from 0.05 to 10 μM (ES, 4-min uptake) after pretreatment of dexamethasone for 6 hrs. (10 nM). The data represent uptake into hOAT3-expressing cells minus uptake into control cells (parental cells). Values are mean ± S.E. (n = 3). Transport kinetic values were calculated using the Eadie–Hofstee transformation.

Figure 4-5

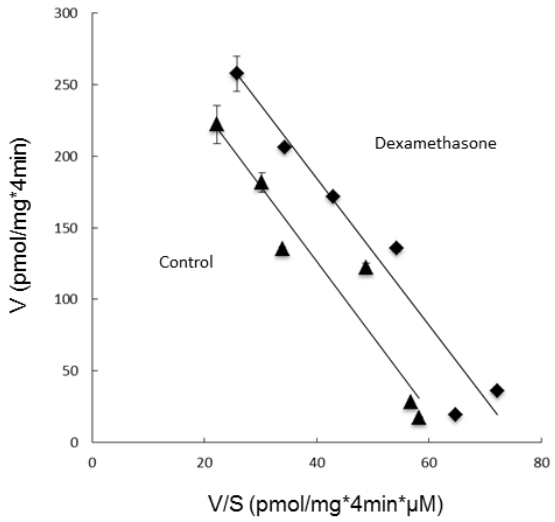

2.5 Effect of dexamethasone on hOAT3 expression – Either an enhanced number of the transporter at the plasma membrane or an enhanced transporter turnover rate could contribute to an increased Vmax (Fig. 4-5). Therefore, we conducted biotinylation assay to differentiate between these two possibilities by measuring transporter expression both at the plasma membrane and in the total cell lysates. Our results indicated that dexamethasone treatment enhanced hOAT3 expression at the plasma membrane without altering the total cell expression of hOAT3 (Fig. 4-6).

Figure 4-6. Effect of dexamethasone on hOAT3 expression. (a). *Top panel:* Cell surface expression of hOAT3. hOAT3-expressing cells were pretreated with the dexamethasone (10nM, 6 hrs.). Cells were labeled with biotin. Biotinylated cell surface proteins were separated with streptavidin beads, followed by immunoblotting (IB) with an anti-myc antibody (hOAT3 was

tagged with epitope myc for immunodetection). *Bottom panel:* The expression of cell surface protein marker E-cadherin. The same blot from the top panel was re-probed with anti- E-cadherin antibody. (b). Densitometry plot of results from Fig. 4-6a, top panel as well as from other experiments. The values are mean ± S.E. (n = 3). *P<0.05. (c). *Top panel:* Total cell expression of hOAT3. hOAT3-expressing cells were pretreated with the Dexamethasone (10nM, 6 hrs.). Cells were lysed, followed by immunoblotting (IB) with an anti-myc antibody. *Bottom panel:* Total cell expression of cellular protein marker β-actin. The same blot from top panel was re-probed with anti-β-actin antibody. (d). Densitometry plot of results from Fig. 4-6c, top panel as well as from other experiments. The values are mean ± S.E. (n = 3). *P<0.05.

Figure 4-6

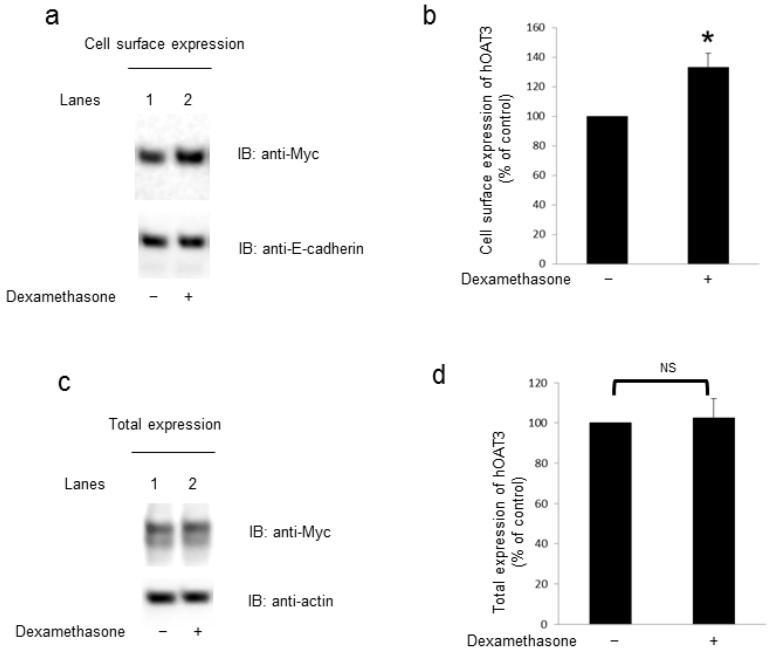

2.6 Sgk inhibitor GSK650394 abrogates the stimulatory effect of dexamethasone on hOAT3 transport activity – Several studies have shown that one of the signaling molecule downstream glucocorticoids is the serum- and glucocorticoid-inducible kinases (sgk). In this experiment, we

examined whether sgk mediates the effect of dexamethasone on hOAT3. We treated hOAT3-expressing cells with dexamethasone with or without a sgk-selective inhibitor GSK650394, followed by the measurement of hOAT3-mediated uptake of [^{3}H]-ES. As shown in Fig. 4-7, dexamethasone stimulated hOAT3-mediated transport ~40% in control cells, whereas such stimulation was blocked in the presence of GSK650394.

Figure 4-7. Sgk inhibitor GSK650394 abrogates the stimulatory effect of dexamethasone on hOAT3 transport activity. hOAT3-expressing cells were incubated for 6 hrs. with 10 nM dexamethasone in the presence and absence of sgk inhibitor GSK650394 (100 nM). After washing the cells, 4-min uptake of [^{3}H]-ES (300 nM) was measured. Uptake activity was expressed as a percentage of the uptake measured in control cells. The data represent uptake into hOAT3-expressing cells minus uptake into mock cells (parental HEK293 cells). The values are mean ± S.E. (n = 3). *P<0.05.

Figure 4-7

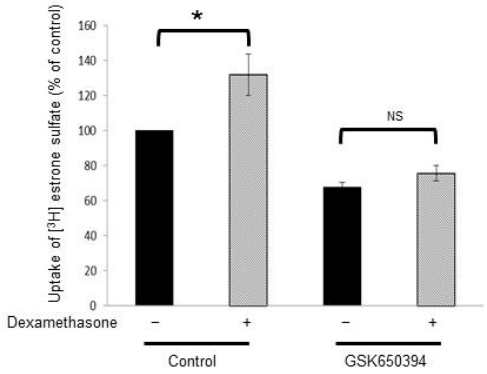

2.7 Dexamethsaone enhanced sgk1 phosphorylation – Previous investigations (83-85) reported that activation of sgk1 is dependent upon the phosphorylation of this kinase, at least in part, by phosphorylating sgk1 at serine residue 422 (Ser 422). Thus, we examined the effect of dexamethasone on the phosphorylation levels of sgk1. hOAT3-expressing cells were pretreated with dexamethasone for 6 hrs. (10nM). Treated cells were then lysed, followed by immunoblotting (IB) with anti-phospho-sgk1-specific antibody. Our results showed that dexamethasone significantly enhanced the level of sgk1 phosphorylation as compared to that of the control (Fig. 4-8a) without change in the total expression of sgk1 (Fig. 4-8c). The expression level of cellular protein marker β-actin was also not changed.

Figure 4-8. Dexamethasone phosphorylates sgk1. (a) Total cell expression of phospho-sgk1. hOAT3-expressing cells were pretreated with dexamethasone (10nM, 6 hrs.). Cells were lysed, followed by immunoblotting (IB) with anti-phospho-sgk1(Ser422)-specific antibody. (b) Densitometry plot of results from Fig. 8a, as well as from other experiments. The values are mean ± SE (n = 3). (c) The same blot from Fig. 4-8a was re-probed with anti-sgk1. (d) Densitometry plot of results from Fig. 4-8c as well as from other experiments. The values are mean ± SE (n = 3). (e) The same blot from Fig. 4-8a was re-probed with anti-β-actin antibody. β-actin is a cellular protein marker.

Figure 4-8

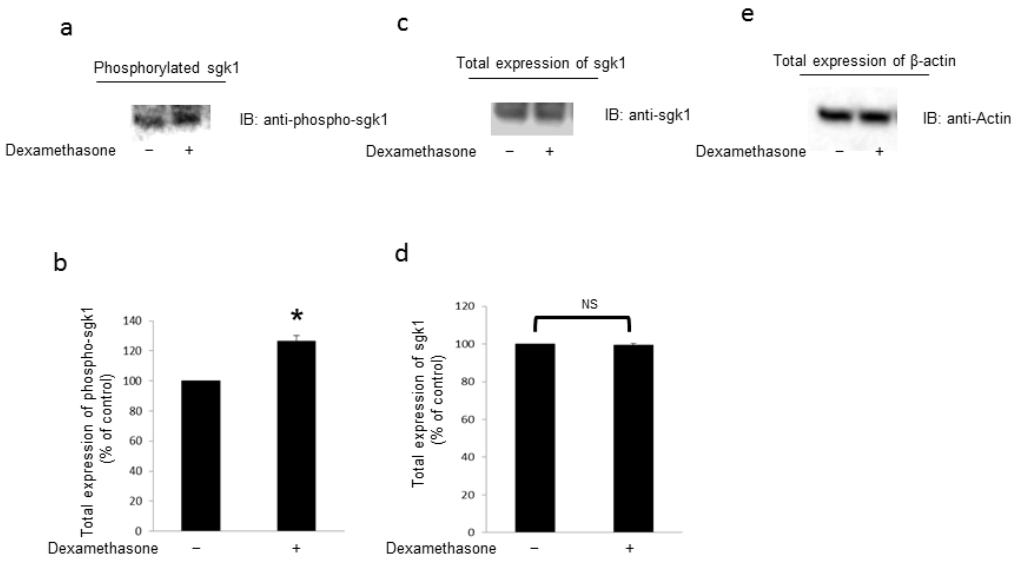
a
Phosphorylated sgk1
IB: anti-phospho-sgk1
Dexamethasone – +
c
Total expression of sgk1
IB: anti-sgk1
Dexamethasone – +
e
Total expression of β-actin
IB: anti-Actin
Dexamethasone – +
b
Total expression of phospho-sgk1 (% of control)
140
120
100
80
60
40
20
0
*
Dexamethasone – +
d
Total expression of sgk1 (% of control)
120
100
80
60
40
20
0
NS
Dexamethasone – +

3. Discussion

The current investigation revealed that dexamethasone, a synthetic glucocorticoid, has a significant role in modulating hOAT3 expression and transport activity.

Glucocorticoids are known to affect a variety of renal functions. Glucocorticoid excess can lead to metabolic alkalosis and potassium depletion (86). In addition, glucocorticoids such as dexamethsone have been shown to specifically regulate, through glucocorticoid receptors, a set of transporters/exchangers (e.g. Na^+:HCO_3^- cotransporter, Na^+/H^+ exchanger) in renal proximal tubules, where OATs are expressed (82, 87, 88).

We chose to perform our investigation in human kidney HEK293 cells, a widely-used cell model for answering mechanistic questions of many renal transport processes (89-92). Therefore, our studies in these cells will provide insights into the future investigation in evaluating whether similar regulation is working *in vivo*.

From our investigation, we gained several pieces of valuable information. Dexamethasone has dual effects on hOAT3 transport activity. First, when co-present with hOAT3 substrate for a brief period of time (4 min), dexamethasone acts as an inhibitor for hOAT3-mediated transport (Fig. 4-1). Further characterization of the inhibition mechanism by Dixon plot revealed that the dexamethasone is a competitive inhibitor (Fig. 4-3). Such mode of inhibition is that the binding of the inhibitor to the active site on the transporter excludes the binding of the substrate and *vice versa.* The IC_{50} value of dexamethasone for hOAT3 determined in the present study is 49.91 µM (Fig. 4-2). This is the concentrations at which 50% inhibition was achieved. The maximum plasma concentration (C_{max}) of dexamethasone is 0.16 µM (64.4µg/L), as suggested by spoorenberg et al. (93). Corrected by unbound fraction value of 0.272 (94), the unbound maximum plasma concentration ($C_{u,max}$) of dexamethasone is ~0.045 µM. A $C_{u,max}/IC_{50}$ value greater than 0.1 would suggest a potential for drug-drug interaction (2). The $C_{u,max}/IC_{50}$ value of

dexamethasone for hOAT3 was < 0.1. Therefore, the propensity for dexamethasone to cause drug-drug interaction through inhibition of hOAT3 is low.

Interestingly, long-term treatment of hOAT3-expressing cells at the clinically relevant concentration of dexamethasone (10nM), displayed an opposite effect of dexamethasone on hOAT3 transport activity. Instead of an inhibitory role, pretreatment of hOAT3-expressing cells with dexamethasone for 6 hrs. resulted in a 40% stimulation of hOAT3 activity (Fig. 4-4). The stimulation of hOAT3 transport activity by dexamethasone correlated with an enhanced hOAT3 expression at the cell surface. One of the signaling pathways downstream of dexamethasone is the serum- and glucocorticoid-inducible kinases (sgk) pathway. Our lab previously demonstrated that sgk stimulates OAT expression and activity by weakening the interaction of OAT with an ubiquitin ligase Nedd4-2 and therefore preventing Nedd4-2-dependent OAT internalization from the cell surface (76, 77, 95). To examine the role of sgk in the effect of dexamethasone on hOAT3, we pretreated hOAT3-expressing cells with dexamethasone in the presence or absence of sgk-specific inhibitor GSK650394. We showed that GSK650394 abrogated stimulatory effect of dexamethasone on hOAT3 transport activity, suggesting that dexamethasone exerts its effect on hOAT3 through the activation of sgk (Fig. 4-7). This conclusion was further reinforced by our results showing that dexamethasone enhanced sgk phosphorylation (Fig. 4-8). Phosphorylation of sgk was previously reported to be a prerequisite for the activation of this kinase (83, 85). Based on previously published work, dexamethasone diffuses passively into cells (96), stimulates PI3K signaling pathway through binding to glucocorticoid receptor (82), which leads to the phosphorylation of SGK1 and enhancement of SGK1 activity.

Dexamethasone is a synthetic glucocorticoid. Because of its potent anti-inflammatory and immunosuppressant effect, it has been widely used to treat inflammatory and autoimmune conditions, such as rheumatic problems, and severe allergies (97). What is more, it is often used with chemotherapy in cancer patient to counteract certain side effects of their antitumor

treatments (98). Our *in vitro* study showed that at a clinical relevant concentration (10nM), long-term treatment with dexamethasone stimulated hOAT3 transport activity, suggesting that hOAT3-mediated drug elimination might be affected if a hOAT3 substrate/drug is taken with dexamethasone simultaneously. The *in vivo* study aiming at identifying the effect of dexamethasone on hOAT3 activity is currently being carried out in our lab.

In summary, current study uncovered dual roles of dexamethasone in hOAT3 transport activity: dexamethasone can act as a competitive inhibitor for hOAT3-mediated transport. Interestingly, once entering the cells, dexamethasone activates sgk1, which leads to an enhanced hOAT3 expression at the cell surface and an enhanced hOAT3 transport activity.

Chapter 5

The Mechanistic Links between Insulin and Human Organic Anion Transporter 4

Majority of the work presented in this chapter has been published in the following article:

Haoxun Wang, Jinghui Zhang, and Guofeng You.

The Mechanistic Links between Insulin and Human Organic Anion Transporter 4.

Int J Pharm. 2019 Jan 30;555:165-174. doi: 10.1016/j.ijpharm.2018.11.040.

1. Introduction

In Chapter 2, we have demonstrated that sgk stimulated OAT transport activity by abrogating the inhibitory effect of Nedd4-2 on the transporter (77, 99).

Insulin has been shown to regulate the cellular processes through multiple signaling pathways (100-102). One of the mediators for insulin is sgk (103). Therefore, in the current study, we investigated the effect of insulin on hOAT4. Interestingly, we discovered that insulin regulates hOAT4 by competing with sgk rather than through sgk.

2. Results

2.1 Effect of insulin on hOAT4 transport activity – To examine the role of insulin in hOAT4 function, we treated hOAT4-expressing COS-7 cells with insulin, followed by the measurement of hOAT4-mediated uptake of [^{3}H]-estrone sulfate (ES), a prototypical substrate for hOAT4. As shown in Fig. 5-1, insulin induced a dose-, and time-dependent rise in the uptake in compared with that in control cells with a ~ 180% stimulation at insulin concentration of 100 nM for 12 hr. treatment. To investigate the mechanism of insulin-induced stimulation of hOAT4 activity, we measured hOAT4-mediated uptake of [^{3}H]-estrone sulfate at various substrate concentrations. Using an Eadie-Hofstee analysis (Fig. 5-2), we showed that treatment with insulin caused an increased maximal transport velocity V_{max} of hOAT4 (129.77 ± 19.82 pmol·mg^{-1}·3min^{-1} with control cells and 230.07 ± 22.21 pmol·mg^{-1}·3min^{-1} with cells treated with insulin) without notable alteration in the substrate-binding affinity K_m of the transporter (3.27 ± 0.30 μM with control cells and 3.45 ± 0.26 μM with cells treated with insulin).

Figure 5-1. Effect of insulin on hOAT4 transport activity. (a) Time-dependent stimulation of hOAT4 transport activity. hOAT4-expressing COS-7 cells were treated with insulin (100nM) for 2h, 4h, 6h and 12h. 3-min uptake of [^{3}H]-estrone sulfate (0.3 μM) was then measured. Uptake activity was expressed as a percentage of the uptake measured in control cells. The data represent uptake into hOAT4-expressing cells minus uptake into mock cells (parental COS-7 cells). Values are mean ± SD (n = 3). *P<0.05. (b) Dose-dependent stimulation of hOAT4 transport activity. hOAT4-expressing COS-7 cells were treated with insulin at varies doses in 12h-treatment. 3-min uptake of [^{3}H]-estrone sulfate (0.3 μM) was then measured. Uptake activity was expressed as a percentage of the uptake measured in control cells. The data represent uptake into hOAT4-expressing cells minus uptake into mock cells (parental COS-7 cells). Values are mean ± SD (n = 3). *P<0.05.

Figure 5-1

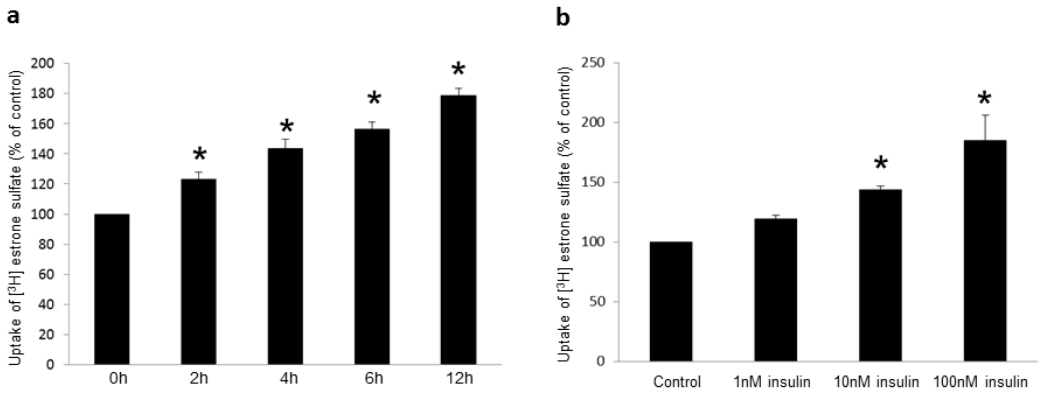

Figure 5-2. Effect of insulin on the kinetics of hOAT4-mediated estrone sulfate transport. COS-7 cells expressing hOAT4 were treated with the insulin (100nM, 12h), and initial uptake (3 min) of [^{3}H]-estrone sulfate was measured at the concentration of 0.1–10 μM. The data represent uptake into hOAT4-transfected cells minus uptake into mock cells (parental COS-7 cells). Values are means ± SD (n = 3). V, velocity; S, substrate concentration.

Figure 5-2

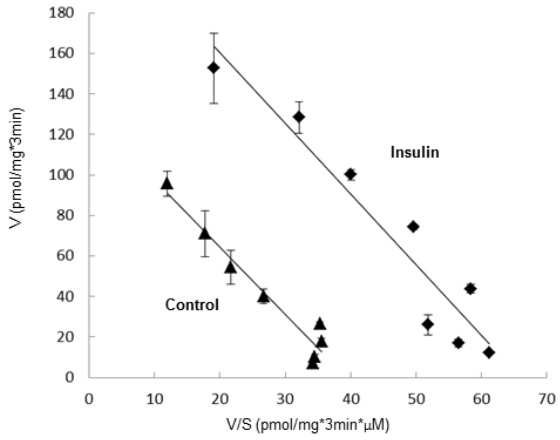

2.2 Effect of insulin on hOAT4 Expression – Two possibilities could be responsible for a rise in the maximal transport velocity V_{max} of hOAT4 shown in Fig. 5-2: either the number of the transporter at the plasma membrane could be increased or the transporter turnover rate could be enhanced. We carried out experiments that dissect these likelihoods by examining transporter expression both at the plasma membrane and in the total cell lysates. We showed that treatment with insulin led to an increase of hOAT4 expression at the plasma membrane (Fig. 5-3a), and in total cell lysates (Fig. 5-3c, top panel). Such a change in hOAT4 expression was not because of the overall perturbation of the cellular proteins since the expression of cellular protein marker β-actin was not affected under these situations (Fig. 5-3c, bottom panel).

Figure 5-3. Effect of insulin on hOAT4 expression. (a). Cell surface expression of hOAT4.

hOAT4-expressing COS-7 cells were treated with the insulin (100nM, 12h). Cells were labeled with biotin. Biotinylated/cell surface proteins were separated with streptavidin beads, followed by immunoblotting (IB) with an anti-Myc antibody. Epitope Myc was tagged to hOAT4 for immune-detection. (b). Densitometry plot of results from Fig. 5-3a, as well as from other experiments. The values are mean ± SD (n = 3). *P<0.05. (c). Top panel: Total expression of hOAT4. hOAT4-expressing COS-7 cells were treated with the insulin (100nM, 12h). Cells were lysed, followed by immunoblotting (IB) with an anti-Myc antibody. Epitope Myc was tagged to hOAT4 for immune-detection. Bottom panel: the same blot from Fig. 5-3c was re-probed with anti β-actin antibody. β-actin is a cellular protein marker. (d). Densitometry plot of results from Fig. 5-3c, top panel as well as from other experiments. The values are mean ± SD (n = 3). *P<0.05.

Figure 5-3

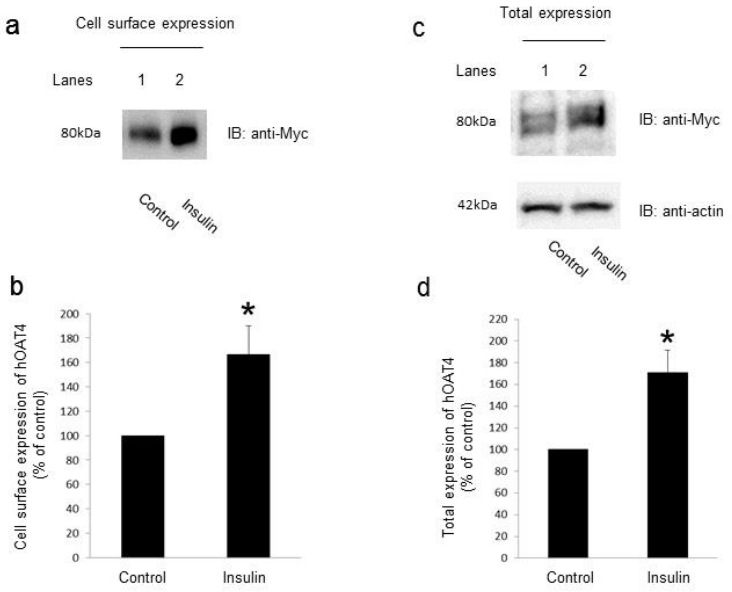

2.3 Relationship between insulin and sgk2 on hOAT4 transport activity – One of the downstream mediators for insulin is sgk. We therefore investigated the relationship between insulin and sgk2 on hOAT4 transport activity. We transfected hOAT4-expressing cells with control vector, inactive form of sgk2 (IN-sgk2), wild-type of sgk2 (WT-sgk2), or the constitutive active form of sgk2 (CA-sgk2). Transfected cells were then treated with or without insulin (100nM, 12h), followed by [^{3}H]-estrone sulfate uptake (3min, 0.3 μM). As shown in Fig. 5-4a, in the absence of insulin, hOAT4-mediated uptake was not significantly changed in IN-sgk2-transfected cells, was moderate in WT-sgk2-transfected cells, and was highest in CA-sgk2-transfected cells as compared to that in control cells, consistent with activity of the sgk2. However, when these cells were treated with insulin (Fig. 5-4b), we observed a maximum stimulation of hOAT4-mediated uptake in control or in IN-sgk2-transfected cells, suggesting that overexpression of IN-sgk2 failed to block insulin's stimulatory effect. However, in cells transfected with WT-sgk2, the stimulatory effect of insulin became smaller as compared to that in cells transfected with IN-sgk2. In cells transfected with CA-sgk2, the stimulatory effect of insulin became diminished as compared to that in cells transfected with IN-sgk2. Similar results were observed in the cells overexpressing Nedd4-2 (Fig. 5-4c). These results indicate that the sgk2-stimulated hOAT4 uptake and insulin-stimulated uptake were not additive. When cells expressed highest level of sgk2 activity (CA-sgk2), insulin was unable to further stimulate hOAT4 transport activity.

Figure 5-4. Relationship between insulin and sgk2 on hOAT4 transport activity. (a) The effect of sgk2 on hOAT4 transport activity. COS-7 cells were transfected with hOAT4 and control vector, or with hOAT4 and the inactive form of sgk2 (IN-sgk2), or with hOAT4 and the wild-type of sgk2 (WT-sgk2), or with hOAT4 and the constitutive active form of sgk2 (CA-sgk2). After 48h transfection, cells were starved for 12h. [^{3}H]-estrone sulfate uptake was then measured (3min, 0.3 μM). Uptake activity was expressed as a percentage of the uptake measured

in control cells. The data represent uptake into hOAT4-expressing cells minus uptake into mock cells (parental COS-7 cells). Values are mean ± SD (n = 3). *P<0.05. (b) Relationship between insulin and sgk2 on hOAT4 transport activity. COS-7 cells were transfected with hOAT4 and control vector, or with hOAT4 and the inactive form of sgk2 (IN-sgk2), or with hOAT4 and the wild-type of sgk2 (WT-sgk2), or with hOAT4 and the constitutive active form of sgk2 (CA-sgk2). Transfected cells were then treated with or without insulin (100nM, 12h), followed by the measurement of [^{3}H]-estrone sulfate uptake (3min, 0.3 μM). Uptake activity was expressed as a percentage of the uptake measured in control cells. The data represent uptake into hOAT4-expressing cells minus uptake into mock cells (parental COS-7 cells). Values are mean ± SD (n = 3). *P<0.05. NS: statistically not significant. (c) Relationship between insulin and sgk2 on hOAT4 transport activity in the cells overexpressing Nedd4-2. COS-7 cells were transfected with Nedd4-2, hOAT4 and the inactive form of sgk2 (IN-sgk2), or with Nedd4-2, hOAT4 and the constitutive active form of sgk2 (CA-sgk2). Transfected cells were then treated with or without insulin (100nM, 12h), followed by the measurement of [^{3}H]-estrone sulfate uptake (3min, 0.3 μM). Uptake activity was expressed as a percentage of the uptake measured in control cells. The data represent uptake into hOAT4-expressing cells minus uptake into mock cells (parental COS-7 cells). Values are mean ± SD (n = 3). *P<0.05. NS: statistically not significant.

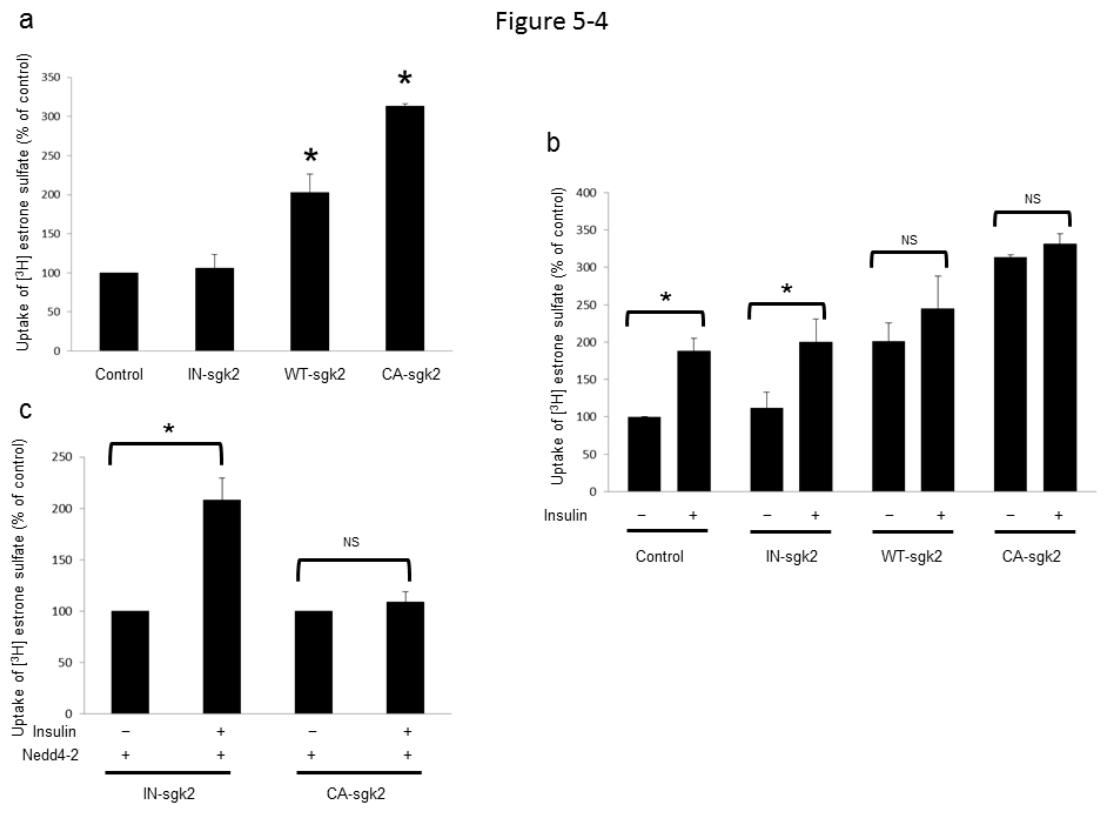

2.4 Effect of Nedd4-2 on insulin-stimulated hOAT4 expression – We previously demonstrated that the ubiquitination of OAT catalyzed by ubiquitin ligase Nedd4-2 leads to the internalization of the transporter from cell surface and subsequent degradation. In this experiment, we investigated the role of Nedd4-2 in insulin-stimulated hOAT4 expression (Fig. 5-5). In control cells, insulin significantly enhanced hOAT4 expression at the plasma membrane (Fig. 5-5a), whereas in cells transfected with Nedd4-2-specific siRNA to knock down the expression of endogenous Nedd4-2, insulin was unable to enhance hOAT4 expression at the plasma membrane (Fig. 5-5c). These results suggest that insulin stimulated hOAT4 expression through Nedd4-2.

Figure 5-5. Role of Nedd4-2 in insulin-stimulated hOAT4 expression. (a) COS-7 cells were co-transfected with hOAT4 and scrambled control siRNA. Transfected cells were treated with or

without insulin (100nM) for 12h and then were labeled with biotin. Biotinylated/cell surface proteins were separated with streptavidin beads, followed by immunoblotting (IB) with an anti-Myc antibody. Epitope Myc was tagged to hOAT4 for immune-detection. (b). Densitometry plot of results from Fig. 4-5a, as well as from other experiments. The values are mean ± SD (n = 3). *P<0.05, (c) COS-7 cells were co-transfected with hOAT4 and Nedd4-2-specific siRNA. Transfected cells were treated with or without insulin (100nM) for 12h and then were labeled with biotin. Biotinylated/cell surface proteins were separated with streptavidin beads, followed by immunoblotting (IB) with an anti-Myc antibody. Epitope Myc was tagged to hOAT4 for immune-detection. (d). Densitometry plot of results from Fig. 4-5c, as well as from other experiments. The values are mean ± SD (n = 3). NS: statistically not significant.

Figure 5-5

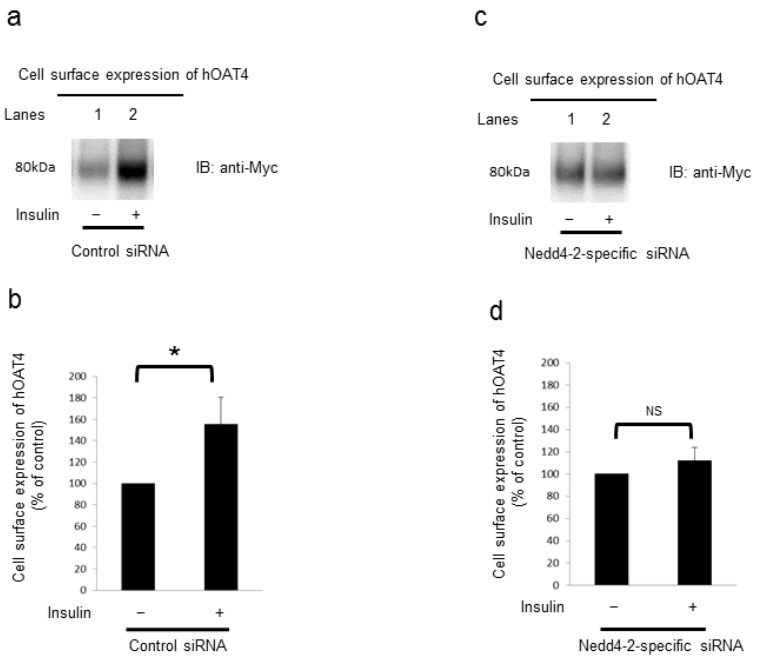

2.5 Effect of Nedd4-2 on insulin-stimulated hOAT4 transport activity – We next investigated the role of Nedd4-2 in insulin-stimulated hOAT4 transport activity (Fig. 5-6). In control cells (Fig. 5-6a) and cells transfected with Nedd4-2 (Fig. 5-6b), insulin significantly enhanced hOAT4-mediated uptake of [^{3}H]-estrone sulfate, whereas in cells transfected with Nedd4-2-specific siRNA to knock down the expression of endogenous Nedd4-2, insulin was unable to enhance hOAT4 transport activity (Fig. 5-6c), demonstrating that insulin stimulated hOAT4 transport activity through Nedd4-2.

Figure 5-6. Role of Nedd4-2 in insulin-stimulated hOAT4 transport activity. (a) COS-7 cells were co-transfected with hOAT4 and scrambled control siRNA. Transfected cells were treated with or without insulin (100nM) for 12h and then measured for the uptake of [^{3}H]-estrone sulfate (3-min uptake and 0.3 μM estrone sulfate). The data represent uptake into hOAT4-transfected cells minus uptake into mock cells (parental COS-7 cells). Values are mean ± SD (n = 3). *P<0.05 (b) COS-7 cells were triple-transfected with hOAT4, Nedd4-2 and scrambled control siRNA. Transfected cells were treated with or without insulin (100nM) for 12h and then measured for the uptake of [^{3}H]-estrone sulfate (3-min uptake and 0.3 μM estrone sulfate). The data represent uptake into hOAT4-transfected cells minus uptake into mock cells (parental COS-7 cells). Values are mean ± SD (n = 3). *P<0.05. (c) COS-7 cells were co-transfected with hOAT4 and Nedd4-2-specific siRNA. Transfected cells were treated with or without insulin (100nM) for 12h and then measured for the uptake of [^{3}H]-estrone sulfate (3-min uptake and 0.3 μM estrone sulfate). The data represent uptake into hOAT4-transfected cells minus uptake into mock cells (parental COS-7 cells). Values are mean ± SD (n = 3). NS: statistically not significant.

Figure 5-6

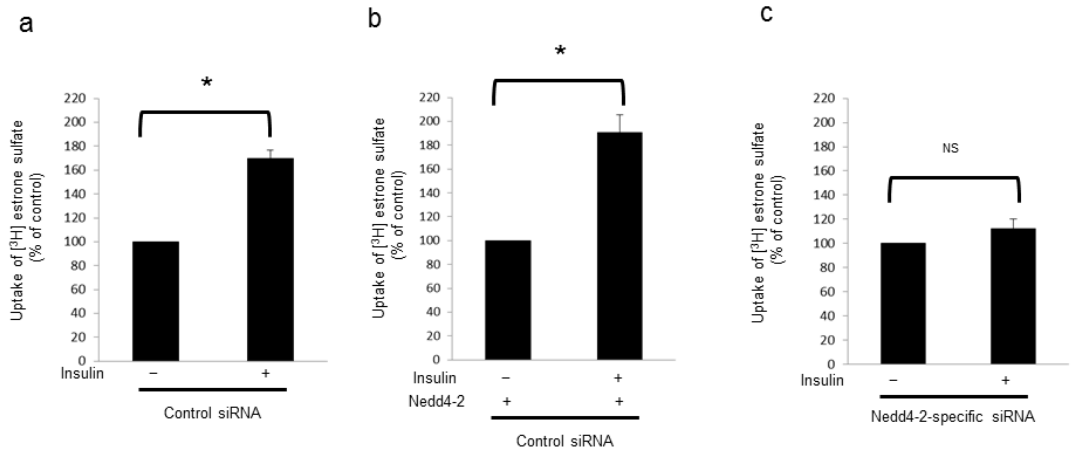

2.6 Effect of insulin on the interaction of Nedd4-2 with hOAT4 – Nedd4-2 regulates OAT ubiquitination by directly interacting with the transporter. We assessed the effect of insulin on the interaction of Nedd4-2 with hOAT4 through co-immunoprecipitation assay. hOAT4-expressing cells were transfected with Nedd4-2. Transfected cells were incubated with or without insulin. hOAT4 was then immunoprecipitated, followed by immunoblotting with anti-Nedd4-2 antibody to detect hOAT4-associated Nedd4-2. As shown in Fig. 5-7a top panel, in the absence of insulin, a significant quantity of Nedd4-2 was found in hOAT4 immunoprecipitates (lane 1), indicating a direct association between these two proteins. Yet, in cells treated with insulin (lane 2), the quantity of Nedd4-2 found in hOAT4 immunoprecipitates was much reduced. These data suggest that insulin hindered the interaction between hOAT4 and Nedd4-2. The difference in the amount of Nedd4-2 associated with hOAT4 was not due to the difference in the amount of hOAT4 pulled

down because the same quantity of hOAT4 was immunoprecipitated under these conditions (Fig. 5-7a bottom panel). Similar results were obtained using a reciprocal approach, where Nedd4-2 was pulled down first, followed by immunoblotting with anti-Myc antibody (epitope Myc was tagged to hOAT4) to detect Nedd4-2-associated hOAT4 (Fig. 5-7c, top panel).

Figure 5-7. Role of insulin in the interaction between Nedd4-2 and hOAT4. (a) COS-7 cells were transfected with hOAT4 and Nedd4-2. *Top panel:* Transfected cells were treated with or without insulin (100nM, 12h) and then lysed, and hOAT4 was immunoprecipitated (IP) with anti-Myc antibody, followed by immunoblotting (IB) with the anti-Nedd4-2 antibody. Epitope Myc was tagged to hOAT4 for immune-detection. *Bottom panel:* The same immunoblot from Fig. 5-7a top panel was reprobed by anti-Myc antibody to detect the total amount of hOAT4 pulled down. (b) Densitometry plot of results from Fig. 5-7a as well as from other experiments. The values are mean ± SD (n = 3). *P<0.05. (c) *Top panel:* Transfected cells were treated with or without insulin (100nM, 12h) and then lysed, and Nedd4-2 (tagged with epitope Flag for immunodetection) was immunoprecipitated (IP) with anti-Flag M2 affinity gel, followed by immunoblotting (IB) with the anti-Myc antibody. Bottom panel: The same immunoblot from Fig. 5-7c top panel was reprobed by anti-Flag antibody to detect the total amount of Nedd4-2 pulled down. (d) Densitometry plot of results from Fig. 5-7c as well as from other experiments. The values are mean ± SD (n = 3). *P<0.05. (Fig. 5-7c provided by Jinghui Zhang)

Figure 5-7

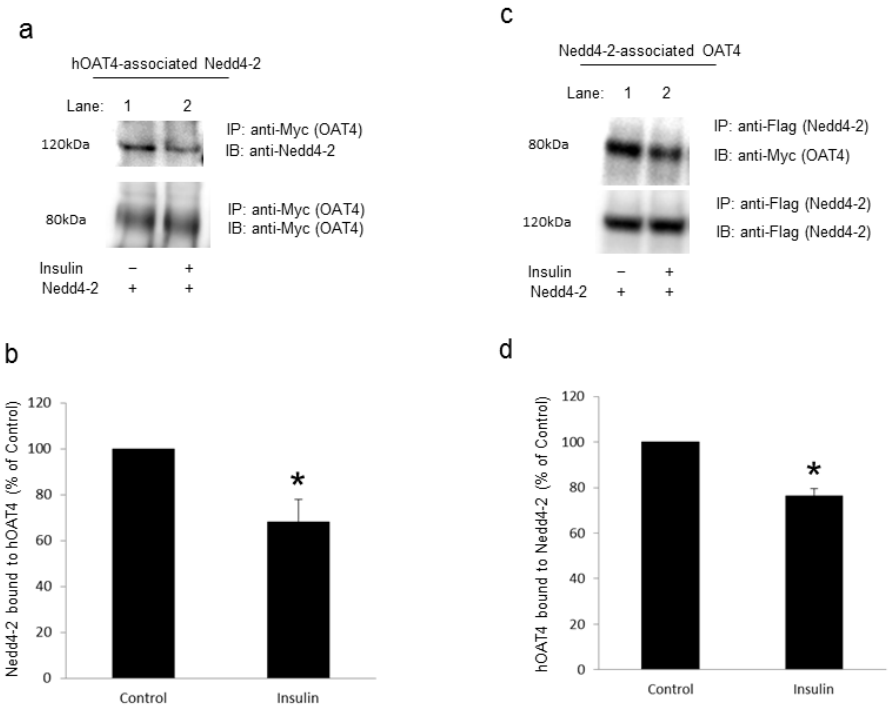

2.7 Effect of insulin on Nedd4-2 phosphorylation – We previously showed that sgk stimulates OAT activity by phosphorylating the amino acid residue serine 327 on Nedd4-2 (99). In this experiment, we examined whether insulin stimulates hOAT4 activity by phosphorylating Nedd4-2 at the same site. We transfected Nedd4-2 into hOAT4-expressing cells. The transfected cells were treated with or without insulin, followed by immunoblotting with phosphor-Nedd4-2 (Ser327)-specific antibody. As shown in Fig 8a, top panel, the phosphor-Nedd4-2-specific antibody detected a band at the size of Nedd4-2 in control cells, suggesting that Nedd4-2 was certainly phosphorylated at Ser327. The phosphorylation signal was enhanced by 70% in cells treated with insulin. The total expression of Nedd4-2 was not affected by insulin (Fig 5-8a, middle panel). Furthermore, the difference in the amount of Nedd4-2 phosphorylated was not due to an overall change in cellular proteins as the amount of cellular protein marker β-actin was not

affected under this condition (Fig. 5-8a, bottom panel). Therefore, insulin enhanced the phosphorylation of Nedd4-2 at serine 327.

Figure 5-8. Effect of insulin on Nedd4-2 phosphorylation. (a) COS-7 cells were co-transfected with hOAT4 and Nedd4-2. Transfected cells were treated with or without insulin (100nM) and then lysed, followed by immunoblotting with the anti-Phospho-Nedd4-2 antibody (Top panel), anti-Nedd4-2 antibody (middle panel), or anti-β-actin antibody (bottom panel) respectively. β-actin is a cellular protein marker. (b). Densitometry plot of results from Fig. 5-8a, the top panel as well as from other experiments. The values are mean ± SD (n = 3). *P<0.05.

Figure 5-8

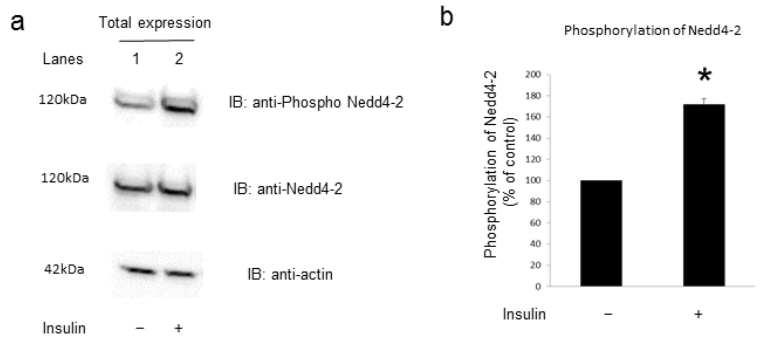

2.8 Effects of PI3K inhibitors on insulin-stimulated hOAT4-mediated estrone sulfate uptakes –PI3K has been shown to be the key regulator in insulin pathway (104-106) and PI3K inhibitors have been utilized to block insulin-mediated effect (107, 108). To examine the effects of PI3K inhibitors on insulin-stimulated hOAT4-mediated estrone sulfate uptakes, we employed

two selective PI3K inhibitors wortmannin and buparsilib. As shown in Fig. 5-9, both inhibitors significantly blocked the stimulatory effect of insulin on hOAT4 transport activity (wortmmanin or buparsilib alone did not show non-specific cytotoxicity). Together these results provide evidence that PI3K plays an essential role in the regulation of insulin stimulated hOAT4 activity.

Figure 5-9. The effects of wortmannin and buparlisib on insulin stimulation of hOAT4-mediated transport. hOAT4-expressing cells were treated with insulin (100nM, 12h) with or without PI3K inhibitors (wortmannin (100nM, 12h) or buparlisib (250nM, 12h)) or PI3K inhibitors alone, followed by measuring the uptake [^{3}H] estrone sulfate (ES, 3min, 0.3 μM). Uptake activity was expressed as a percentage of the uptake determined in control cells. The data represent uptake into hOAT4-expressing cells minus uptake into mock cells. Values are mean ± SD (n = 3). *P<0.05.

Figure 5-9

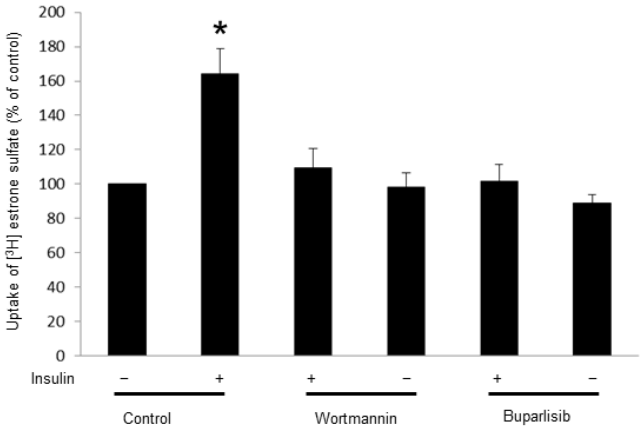

3. Discussion

Nedd4-2 is under the control of many protein kinases (65, 73, 99, 102, 109). It is possible that differential regulations of OAT by various protein kinases are exerted through the dynamic phosphorylation at different sites on Nedd4-2, in doing so, bringing about diverse conformational change in Nedd4-2 and altering its binding to OAT, which results in a change in OAT ubiquitination, trafficking and transport activity (73, 99, 102). Our lab has recently demonstrated that the serum- and glucocorticoid-inducible kinases (sgks) stimulated OAT transport activity by selectively phosphorylating serine residue 327 on Nedd4-2 (99), which weakens the binding of Nedd4-2 to OAT, leading to a reduced ubiquitin-triggered OAT internalization and degradation (77, 99). Here our results further indicate that insulin increases hOAT4 expression and activity by inducing phosphorylation of the same serine on Nedd4-2.

Insulin is a peptide hormone that regulates the activity of many membrane proteins (e.g. epithelial sodium channel (ENaC), Glucose Transporter type 4 (Glut4) and Na+/H+ exchanger 3) (102, 110, 111). The regulation of insulin in cellular processes could be through multiple signaling pathways. Several lines of evidence indicate that insulin was an upstream activator of sgks (102, 112, 113). In the current study, we showed that insulin stimulated hOAT4 expression and transport activity (Figs. 5-1-5-3). We further showed that regulation of hOAT4 activity by insulin was mediated by ubiquitin ligase Nedd4-2. Knocking down endogenous Nedd4-2 by Nedd4-2-specific siRNA abolished the effect of insulin on hOAT4 (Figs. 5-5 and 5-6). The effect of insulin on hOAT4 expression and activity was paralleled with the phosphorylation of serine 327 on Nedd4-2 and a weakened association of Nedd4-2 to hOAT4 (Figs. 5-7 and 5-8). However, interestingly, the effect of insulin on hOAT4 was diminished in cells overexpressing sgk2 (Fig. 5-4), suggesting that the effect of insulin and sgk2 were not additive, and that insulin competes with sgk2, rather than acting through sgk2, in the regulation of hOAT4. PI3K has been shown to be the key regulator in insulin pathway (104-106). In our current study, we observed that two selective PI3K inhibitors wortmannin and buparlisib significantly blocked the stimulatory effect of insulin

on hOAT4 transport activity (Fig. 5-9). PI3K has been reported to be a target for anti-tumor therapeutics. Wortmannin is a widely used model inhibitor for PI3K in both in vitro and in vivo studies (107, 108, 114). Buparlisib is currently under late-stage clinical development. Multiple clinical trials have been initiated to investigate the anti-tumor effect of Buparlisib in the patients with a variety of cancers (115).

In addition to its role in the kidney, OAT4, specifically expressed in higher primates, is localized to the basolateral membrane of syncytiotrophoblast of the placenta and responsible for the elimination of steroid sulfates, xenobiotics, and clinically important drugs from the fetal compartment and therefore reducing the toxicity for the developing fetus. Gestational diabetes mellitus (GDM) is a condition in which a pregnant woman develops any degrees of glucose intolerance due to the lack of insulin. GDM has already become a major health concern with a growing prevalence. Further studies investigating the activity and expression of OAT4 in GDM placenta would be particularly interesting.

In conclusion, our current study demonstrated that insulin stimulates hOAT4 expression and transport activity through modulating the ubiquitin ligase Nedd4-2. Interestingly, the action of insulin is in competition with that of sgk2 rather than through sgk2 (Fig. 5-10).

Figure 5-10. The Mechanistic Links between Insulin, sgk, and hOAT4. U: ubiquitin. P: phosphorylation

Figure 5-10

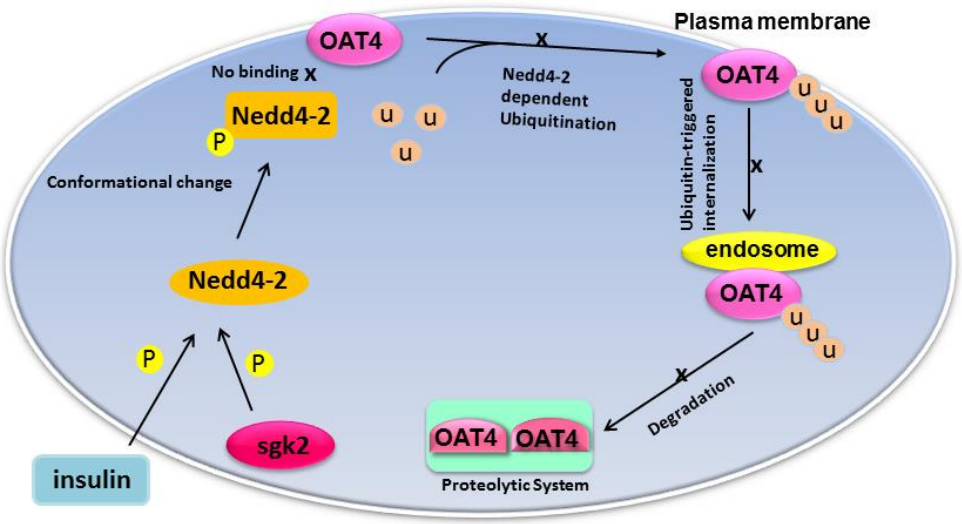
Plasma membrane
OAT4
No binding X
X
Nedd4-2
dependent
Ubiquitination
OAT4
u u u
Nedd4-2
P
u u
u
Ubiquitin-triggered
internalization
X
Conformational change
endosome
Nedd4-2
OAT4
u u u
P
P
X
Degradation
sgk2
OAT4 OAT4
Proteolytic System
insulin

Chapter 6

Activation of Protein Kinase A stimulates SUMOylation, expression, and transport activity of Organic Anion Transporter 3

Majority of the work presented in this chapter has been published in the following article:

Haoxun Wang, Jinghui Zhang, and Guofeng You.

Activation of Protein Kinase A stimulates SUMOylation, expression, and transport activity of Organic Anion Transporter 3

AAPS J (2019) 21: 30. https://doi.org/10.1208/s12248-019-0303-4.

1. Introduction

In Chapter 2 and Chapter 3, we mentioned that post-translational modification of OAT by ubiquitination is a major mechanism that governs PKC-regulated OAT trafficking and transport activity. Another important ubiquitin-like modifier is the small ubiquitin-related modifier SUMO (48, 116). SUMO family consists of three functional isoforms SUMO1-3. All three are polypeptides of ~12 kDa, and are broadly detected in many tissues, including brain, liver, and kidney. SUMO2 and SUMO3 are regularly mentioned as SUMO2/3 as they have 97% identity. In contrast, SUMO2/3 is only ~50% identical in the sequence with SUMO-1. Consistent with such sequence differences, SUMO1 and SUMO2/3 modify different substrates in vivo (48, 116). The modification of substrate proteins by SUMOylation involves the consecutive steps of the E1 SUMO-activating enzymes and the E2 SUMO-conjugating enzyme 9 (Ubc9). This process leads to the formation of an isopeptide bond between the carboxy-terminal glycine of SUMO and lysine residues of specific target proteins. Although chemically stable, modification by SUMO is reversible by specific isopeptidases that break the bond between SUMO and the lysine residue(s) of target substrate. SUMOylation was initially identified as a major regulatory mechanism of protein function on nuclear proteins (117). Within the last decade, more and more membrane proteins such as channels and receptors were identified as SUMO substrates (118-124). And the roles of SUMOylation in the regulation of these membrane proteins have been investigated. Recently, it has become obvious that ubiquitin and SUMO, although performing different biological functions, frequently communicate, and cooperatively affect the properties of shared substrate proteins, in certain cases by modifying the same site in a competitive manner (125, 126). Whether OAT is subject to the regulation by SUMOylation is currently unknown.

Contrary to the inhibitory effect of PKC on OATs, protein kinase A (PKA) has been shown to stimulate OAT activity (52, 100, 127). However, its mechanism of action is not well

understood. A thorough understanding of PKA-regulated OAT activity is of high significance because various physiological stimuli such as insulin-like growth factor exert its biological effect through the activation of PKA (128). In the present study, we examined the mechanism of PKA action on OAT3. We demonstrated that PKA stimulated OAT3 expression and transport activity by altering the trafficking kinetics of the transporter possibly through the crosstalk between ubiquitination and SUMOylation.

2. Results

2.1 Effect of PKA on hOAT3 transport activity – To examine the role of PKA in hOAT3 function, we treated hOAT3-expressing COS-7 cells with PKA activator Bt2-cAMP, followed by the measurement of hOAT3-mediated uptake of [^{3}H] estrone sulfate (ES), a prototypical substrate for hOAT3. As shown in Fig. 6-1a, Bt2-cAMP induced a dose-dependent rise in the uptake in compared with that in control cells with a ~ 40% stimulation at Bt2-cAMP concentration of 10 μM. Such Bt2-cAMP-induced increase in hOAT3 transport activity was abrogated in the presence of a PKA inhibitor H-89 (H-89 alone did not show non-specific cytotoxicity) (Fig. 6-1b), confirming the specific regulation of hOAT3 by PKA. To investigate the mechanism underlying PKA-induced increase in hOAT3 activity, we measured hOAT3-mediated uptake of [^{3}H] ES at various substrate concentrations. An Eadie-Hofstee analysis (Fig. 6-2) revealed that activation of PKA by Bt2-cAMP caused an augmented maximal transport velocity V_{max} of hOAT3 (147.33 ± 18.72 pmol·mg^{-1}·4min^{-1} with control cells and 230.18 ± 16.46 pmol·mg^{-1}·4min^{-1} with cells treated with Bt2-cAMP) without notable alteration in the substrate-binding affinity K_m of the transporter (6.08 ± 0.65 μM with control cells and 5.84 ± 0.56 μM with cells treated with Bt2-cAMP).

Figure 6-1. Effect of PKA activator Bt2-cAMP on hOAT3 transport activity. (a) hOAT3-expressing cells were treated with Bt2-cAMP at **various** doses for 30 min. 4-min uptake of [^{3}H]-estrone sulfate (ES, 0.3 μM) was then determined. Transport activity was expressed as % of the uptake in control cells (mock cells). The data correspond to the uptake into hOAT3-expressing cells minus uptake into mock cells and was normalized to protein concentration. Values are mean ± S.D. (n = 3). *P<0.05. **(b) Selectivity of PKA on hOAT3 transport activity.** hOAT3-expressing cells were pretreated with or without a PKA inhibitor H-89 (4μM, 10min). After that, the cells were treated with PKA activator Bt2-cAMP (10μM, 30min) with or without PKA inhibitor H-89 (4μM, 30min), or H-89 alone, followed by measuring the uptake of [^{3}H] estrone

sulfate (ES, 4min, 0.3 μM). Transport activity was expressed as % of the uptake in control cells. The data correspond to the uptake into hOAT3-expressing cells minus uptake into mock cells and was normalized to protein concentration. Values are mean ± S.D. (n = 3). *P<0.05.

Figure 6-1

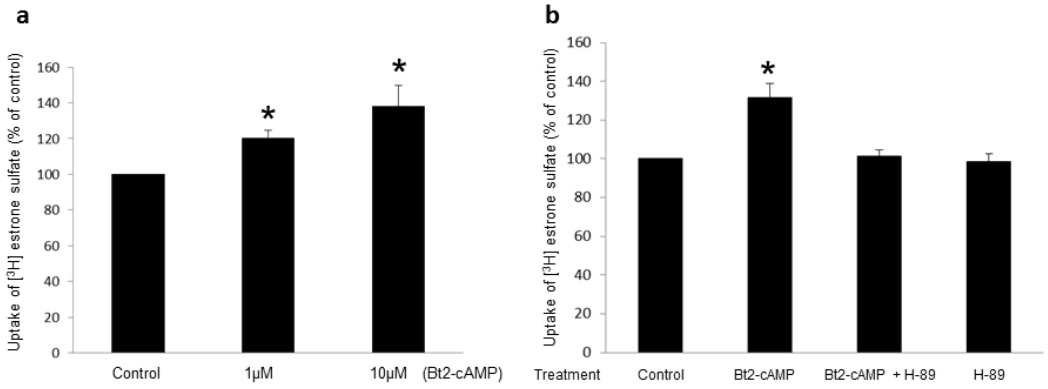

Figure 6-2. Effect of PKA activator Bt2-cAMP on the kinetics of hOAT3-mediated transport of estrone sulfate. hOAT3-expressing cells were treated with the Bt2-cAMP (10μM, 30min), and initial uptake (4 min) of [^{3}H] estrone sulfate was determined at the concentration of 0.1–10 μM. The data correspond to uptake into hOAT3-expressing cells minus uptake into mock cells. Values are means ± S.D. (*n* = 3). *V*, velocity; S, substrate concentration.

Figure 6-2

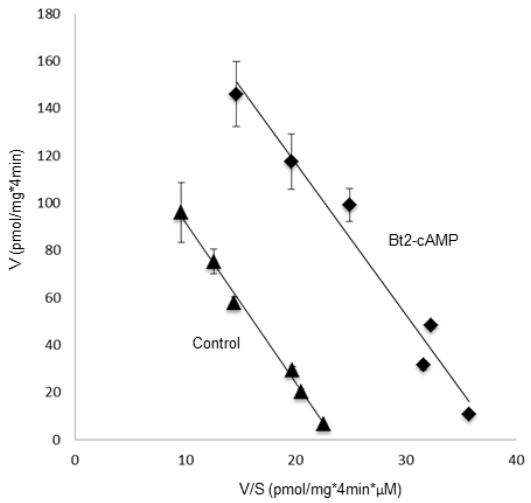

2.2 Effect of PKA on hOAT3 Expression – Two possibilities could be responsible for a rise in the maximal transport velocity V_{max} of hOAT3 shown in Fig. 6-2: either the quantity of the transporter at the plasma membrane could be increased or the transporter turnover rate could be enhanced. We conducted analyses that differentiate between these likelihoods by looking at the expression of the transporter both at the plasma membrane and in the total cell extracts. We revealed that PKA activation by Bt2-cAMP led to an increase of hOAT3 expression at the cell surface (Fig. 6-3a, top panel), without altering its total expression (Fig. 6-3d). Such a change in hOAT3 expression at the plasma membrane was not because of the overall disturbance of membrane proteins since the expression of plasma membrane protein marker E-cadherin was not affected under these situations (Fig. 6-3a, bottom panel & Fig. 6-3c).

Figure 6-3. Effect of PKA activator Bt2-cAMP on hOAT3 expression. (a). Cell surface expression of hOAT3. Top panel: hOAT3-expressing cells were pretreated with or without H-89 (4μM, 10min). After that, cells were treated with Bt2-cAMP (10μM, 30min) in the presence and absence of PKA inhibitor H-89 (4μM, 30min). Biotinylation of treated cells was then performed, as described in the section of "Materials and Methods" followed by immunoblotting (IB) with an anti-Myc antibody (hOAT3 was tagged with the Myc epitope to facilitate the immunodetection). Bottom panel: The identical blot as the top panel was re-probed with anti-E-cadherin antibody. E-cadherin is a cell membrane marker protein. (b). Densitometry analyses of results from Fig. 6-3a, Top panel, along with other experiments. The values are mean ± S.D. (n = 3). *P<0.05. (c) Densitometry analyses of results from Fig. 6-3a, Bottom panel, along with other experiments. The values are mean ± S.D. (n = 3). (d). Total expression of hOAT3. hOAT3-expressing cells were pretreated with or without H-89 (4μM, 10min). After that, cells were treated with the Bt2-cAMP (10μM, 30min) in the presence and absence of PKA inhibitor H-89 (4μM, 30min). Cells were immunoblotted (IB) with an anti-Myc antibody. (e). Densitometry analyses of results from Fig. 6-3d, Top panel, along with other experiments. The values are mean ± S.D. (n = 3). (f) Densitometry analyses of results from Fig. 6-3d, Bottom panel, along with other experiments. The values are mean ± S.D. (n = 3).

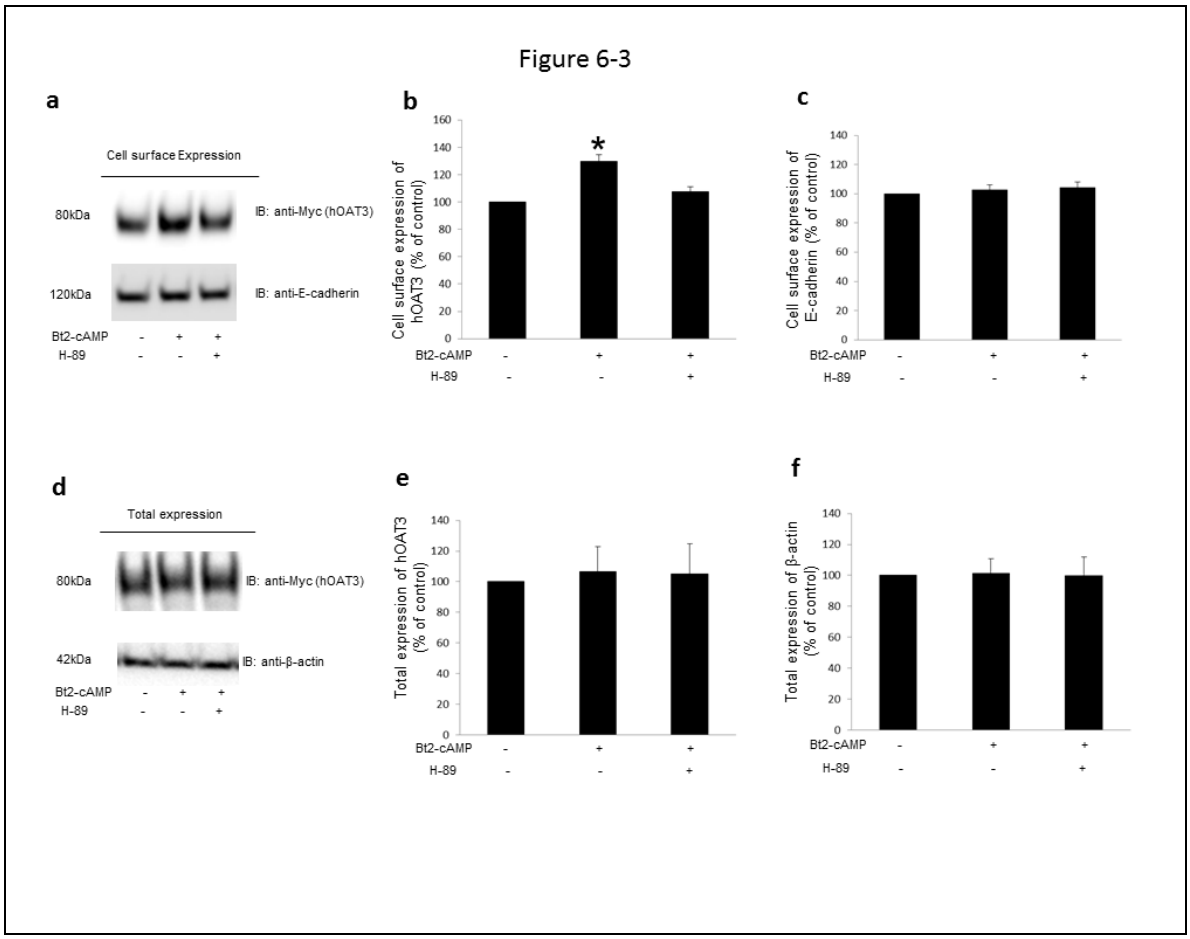

2.3 Effect of PKA hOAT3 Trafficking – We earlier demonstrated that the members of OAT family naturally internalize from and recycle back to the plasma membrane. In the current experiment, we assessed whether PKA-induced increase of OAT expression at the cell surface could result from altered trafficking kinetics. First, we examined whether PKA activation alters the rate of hOAT3 recycling. We observed that the quantity of surface-labeled hOAT3 recycled to the cell surface in the presence of PKA activator Bt2-cAMP was higher than that in the absence of Bt2-cAMP (Fig. 6-4a, Top panel), while the amount**s** of membrane protein marker E-cadherin were comparable between Bt2-cAMP treated group and non-treated group at indicated time points (Fig. 46-a, Bottom panel), suggesting that PKA activation enhanced the rate of hOAT3 recycling. We next examined whether PKA activation alters the rate of hOAT3 internalization. We observed that the quantity of surface-labeled hOAT3 internalized with the PKA activator Bt2-

cAMP present was similar as that in the absence of Bt2-cAMP (Fig. 6-5), indicating that PKA activation does not affect the rate of hOAT3 internalization.

Figure 6-4. Biotinylation analysis of Bt2-cAMP-modulated hOAT3 recycling. (a). Top panel: hOAT3 recycling (5 min and 10 min) was analyzed as described in the section of "Materials and Methods" in the presence and the absence of Bt2-cAMP (10μM), in conjunction with immunoblotting (IB) using anti-Myc antibody (1:100). hOAT3 was tagged with the Myc epitope to facilitate the immunodecetion. Bottom panel: The identical blot as the top panel was re-probed with anti-E-cadherin antibody. E-cadherin is a cell membrane marker protein. (b) Densitometry analyses of results from Fig. 6-4a, Top panel along with other experiments. Total biotin-labeled hOAT3 was expressed as % of OAT3 biotinylated at 4 °C. Values are mean ± S.D. (n = 3). *P<0.05.

Figure 6-4

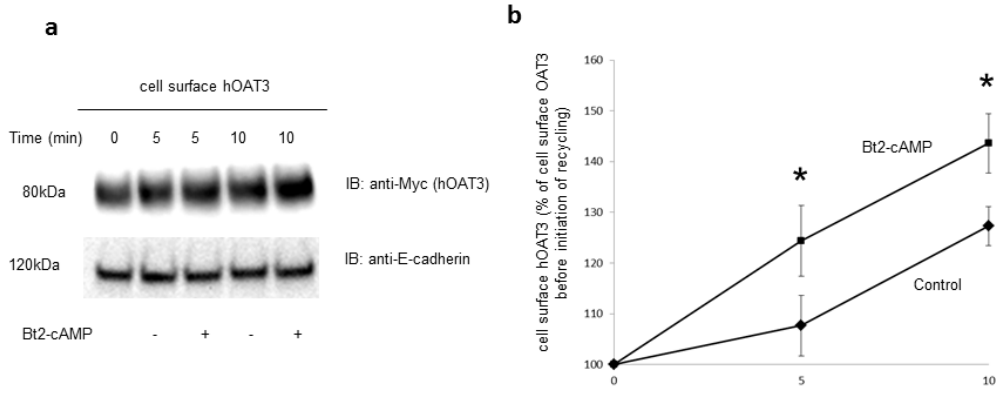

Figure 6-5. Biotinylation analysis of hOAT3 internalization. (a). hOAT3 internalization was examined as described in the section of "Materials and Methods", in the presence and the absence of Bt2-cAMP (10μM), in conjunction with immunoblotting (IB) using anti-Myc antibody (1:100). (b). Densitometry analyses of results from Fig. 6-5a along with other experiments. Internalized hOAT3 was expressed as % of total initial cell surface hOAT3 pool. Values are mean ± S.D. (n = 3). NS: statistically not significant.

Figure 6-5

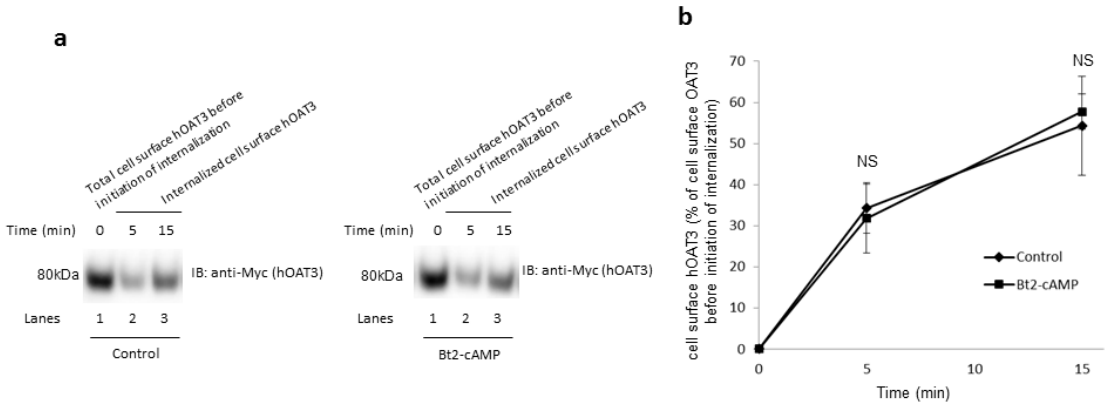

2.4 Effect of Long-Term PKA Activation on hOAT3 Stability – The above experiments were carried out with a short-term PKA activation (with 30-min Bt2-cAMP treatment). The effect of long-term activation of PKA (Bt2-cAMP treament for 3-hrs & 6-hrs) on cell surface hOAT3 was next evaluated using a biotinylation approach. Our results (Fig. 6-6) showed that there was significantly less amount of hOAT3 degraded after 3 hrs and 6 hrs of treatment with PKA

activator Bt2-cAMP as compared to that of control (Fig. 6-6a, Top panel), while the amounts of membrane protein marker E-cadherin were comparable between Bt2-cAMP treated group and non-treated group at indicated time points (Fig. 6-6a, Bottom panel), indicating that PKA activation slowed down the degradation rate of hOAT3.

Figure 6-6 Effect of Bt2-cAMP on the degradation of cell surface hOAT3. (a) Top panel: COS-7 cells expressing hOAT3 were treated with the Bt2-cAMP (10μM). Cell surface hOAT3 degradation was then examined as described in the section of "Materials and Methods", in conjunction with immunoblotting (IB) using anti-Myc antibody. Bottom panel: The identical blot as the top panel was re-probed with anti-E-cadherin antibody. E-cadherin is a cell membrane marker protein. (b) Densitometry analyses of results from Fig. 6-6a top panel along with other experiments. The amount of undegraded cell surface hOAT3 was expressed as % of total initial cell surface hOAT3 pool. Values are mean ± S.D. (n = 3). *P<0.05.

Figure 6-6

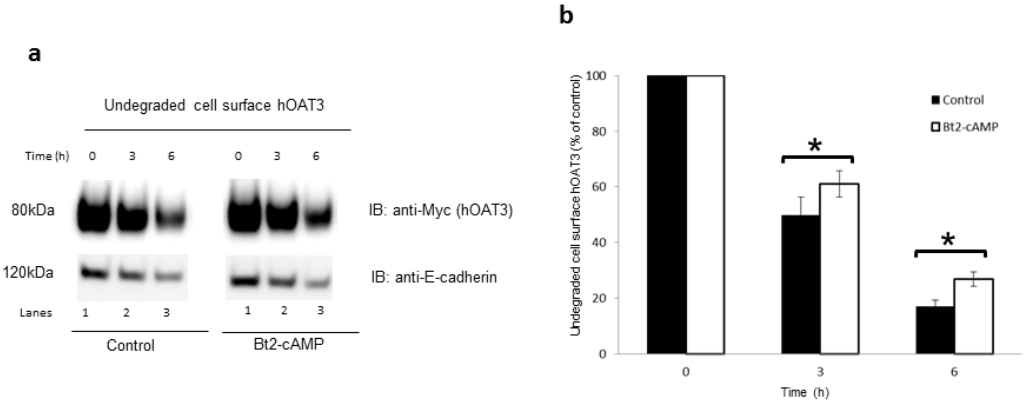

2.5 Effect of PKA on hOAT3 SUMOylation – SUMO family consists of three functional isoforms SUMO1-3. To examine whether hOAT3 is a substrate for SUMOylation, we transfected hOAT3-expressing cells with epitope HA-tagged SUMO-1, SUMO-2, or SUMO-3 together with Ubc9, an enzyme catalyzing the conjugation of SUMO to its protein substrate. Transfected cells were then lysed and hOAT3 was immunoprecipitated with anti-Myc antibody (hOAT3 was tagged with the Myc epitope), followed by immunoblotting (IB) with anti-HA antibody to detect SUMOylated hOAT3. As shown in Fig. 6-7a, top panel, hOAT3 was SUMOylated by SUMO-2 and SUMO-3 but not by SUMO-1. hOAT3 SUMOylation depended on the amount of Ubc9 transfected with the maximum SUMOylation at 2.4 μg of Ubc9 (Fig. 6-7b, top panel). When cells were treated with PKA activator Bt2-cAMP, hOAT3 SUMOylation by SUMO-2 conjugation was significantly enhanced in comparison to that in control cells (Fig. 6-7c, top panel). Moreover, Bt2-cAMP-enhanced hOAT3 SUMOylation was abrogated in the presence of PKA inhibitor H-89 (Fig. 6-7c, top panel), suggesting that hOAT3 SUMOylation is PKA-dependent. The difference in the hOAT3 SUMOylation was not due to the variance in the amount of hOAT3 immunoprecipitated because similar quantity of hOAT3 was pulled down in all samples (bottom panels of Fig. 6-7a, Fig. 6-7b, and Fig. 6-7c).

Figure 6-7. The effect of PKA on hOAT3. (a) Effects of SUMO1, SUMO2, SUMO3 and Ubc9 on hOAT3 SUMOylation. Top panel: cDNAs for HA-tagged SUMO1, SUMO2, or SUMO3 were transfected into COS-7 cells separately with Ubc9, a SUMO-conjugating enzyme. 48 hrs after transfection, hOAT3 was pulled down by anti-Myc antibody (hOAT3 was tagged with the Myc epitope), with subsequent immunoblotting (IB) using anti-HA antibody. Bottom panel: The same blot from the top panel was re-probed with anti-Myc antibody to detect the amount of hOAT3 pulled down. **(b) Effects of Ubc9 on hOAT3 SUMOylation.** Top panel: cDNAs for HA-tagged SUMO2 was transfected into COS-7 cells with different amount of Ubc9 for 48 hrs. After transfection, hOAT3 was pulled down by anti-Myc antibody (hOAT3 was

tagged with the Myc epitope), with subsequent immunoblotting (IB) using anti-HA antibody. Bottom panel: The same blot from the top panel was re-probed with anti-Myc antibody to detect the amount of hOAT3 pulled down. **(c) PKA Specificity on hOAT3 SUMOylation.** Top panel: hOAT3-expressing cells were transfected with HA-SUMO2 and Ubc9 for 48h, then pretreated with or without H-89 (4μM, 10min). After that, cells were treated with the Bt2-cAMP (10μM, 30min) in the presence and absence of PKA inhibitor H-89 (4μM, 30min). hOAT3 was pulled down by anti-Myc antibody, with subsequent immunoblotting (IB) using anti-HA antibody. Bottom panel: The identical blot from the top panel was re-probed with anti-Myc antibody. (d) Densitometry analyses of results from Fig. 6-7c. Values are mean ± S.D. (n = 3). *P<0.05.

Figure 6-7

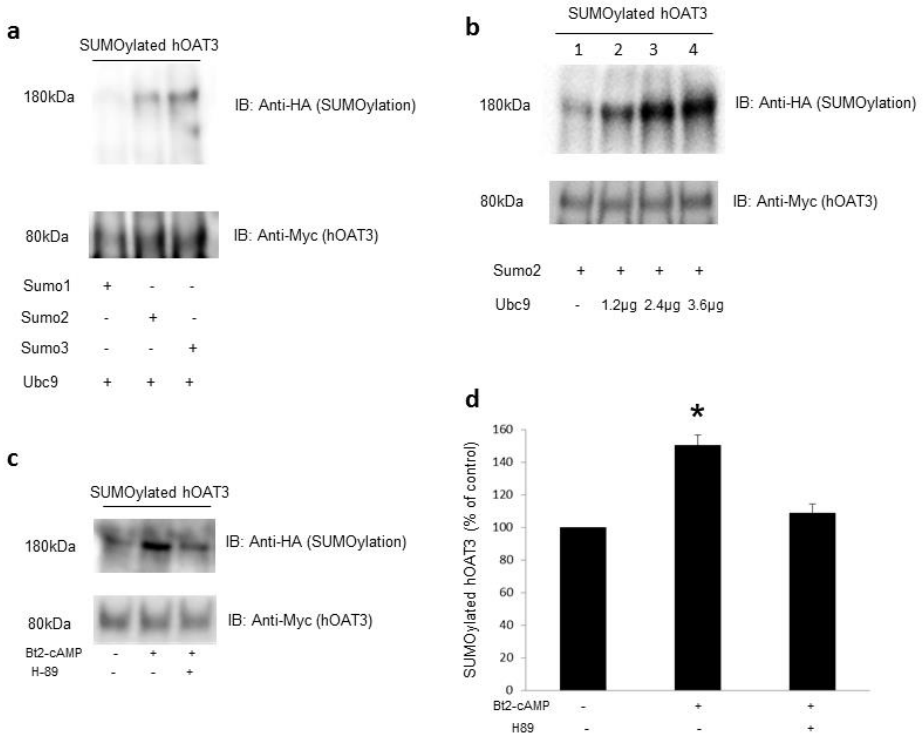

2.6 Effect of PKA on hOAT3 ubiquitination – We earlier demonstrated that protein kinase C (PKC) down regulates hOAT3 activity by enhancing ubiquitin conjugation to the transporter. In contrast to the inhibitory effect of PKC on hOAT3, PKA activation stimulated hOAT3 activity.

We, therefore, examined the effect of PKA on hOAT3 ubiquitination. hOAT3-expressing cells were incubated with PKA activator Bt2-cAMP. hOAT3 was then immunoprecipitated with anti-Myc antibody, followed by immunoblotting (IB) with anti-ubiquitin antibody to detect ubiquitinated hOAT3. As revealed in Fig. 6-8a, top panel, Bt2-cAMP suppressed hOAT3 ubiquitination in a dose-dependent manner as compared to that in control cells. The difference in hOAT3 ubiqitination was not due to the variance in the amount of hOAT3 pulled down because the same amount of hOAT3 was immunoprecipitated in all the samples (Fig. 6-8a, bottom panel).

Figure 6-8. The effect of PKA activator Bt2-cAMP on OAT3 ubiquitination. (a). Top panel: hOAT3-expressing cells were treated with the Bt2-cAMP (1μM or 10μM, 30min). Cells were then treated with the PKC activator PMA (1 μM) for 30 min to enhance hOAT3 ubiquitination. hOAT3 was pulled down by anti-Myc antibody (hOAT3 was tagged with the Myc epitope), with subsequent immunoblotting (IB) using anti-ubiquitin antibody. Bottom panel: The identical immunoblot from Fig. 6-8a, Top panel was reprobed by anti-Myc antibody. (b). Densitometry analyses of results from Fig. 6-8a. The values are mean ± S.D. (n = 3). *P<0.05.

Figure 6-8

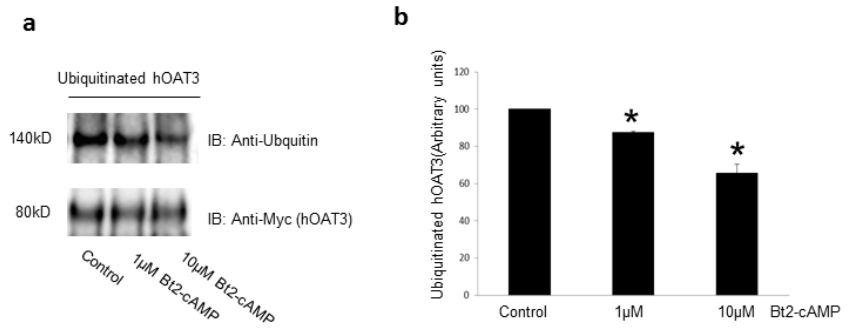

2.7 Effect of Insulin like growth factor (IGF-1) on hOAT3 transport activity and SUMOylation – cAMP signaling pathway has been shown to be an important mediator for many physiological hormones such as IGF-1. Therefore we investigated the effect of IGF-1 on hOAT3 transport activity and SUMOylation. As shown in Fig. 6-9a, IGF-1 (100nM and 3h treatment) significantly increased hOAT3-mediated uptake of estrone sulfate (ES). This stimulatory effect was blocked by the PKA inhibitor H-89, indicating that IGF-1 regulates hOAT3 transport activity through PKA pathway. Moreover, IGF-1 greatly stimulated hOAT3 SUMOylation by SUMO2 conjugation (Fig. 6-9b).

Figure 6-9. The effect of IGF-1 on OAT3 transport activity and SUMOylation. (a) The effect of IGF-1 on hOAT3 transport activity. hOAT3-expressing cells were pretreated with or

without a PKA inhibitor H-89 (20μM, 10min). After that, the cells were treated with IGF-1 (100nM, 3hrs) in the presence and absence of PKA inhibitor H-89 (20μM, 3hrs), or H-89 alone, followed by [^{3}H] estrone sulfate uptake (4min, 0.3 μM). Uptake activity was expressed as % of the uptake in control cells. The data correspond to the uptake into hOAT3-expressing cells minus uptake into mock cells and was normalized to protein concentration. Values are mean ± S.D. (n = 3). *P<0.05. (b) The effect of IGF-1 on OAT3 SUMOylation. hOAT3-expressing cells were transfected with HA-SUMO2 and Ubc9 for 48hrs, then treated with the IGF-1 (100nM, 3hrs). hOAT3 was pulled down by anti-Myc antibody, in conjunction with immunoblotting (IB) using anti-HA antibody. (c) Densitometry analyses of results from Fig. 6-9b. Values are mean ± S.D. (n = 3). *P<0.05. (Figure 6-9 was generated by Jinghui Zhang and Haoxun Wang together)

Figure 6-9

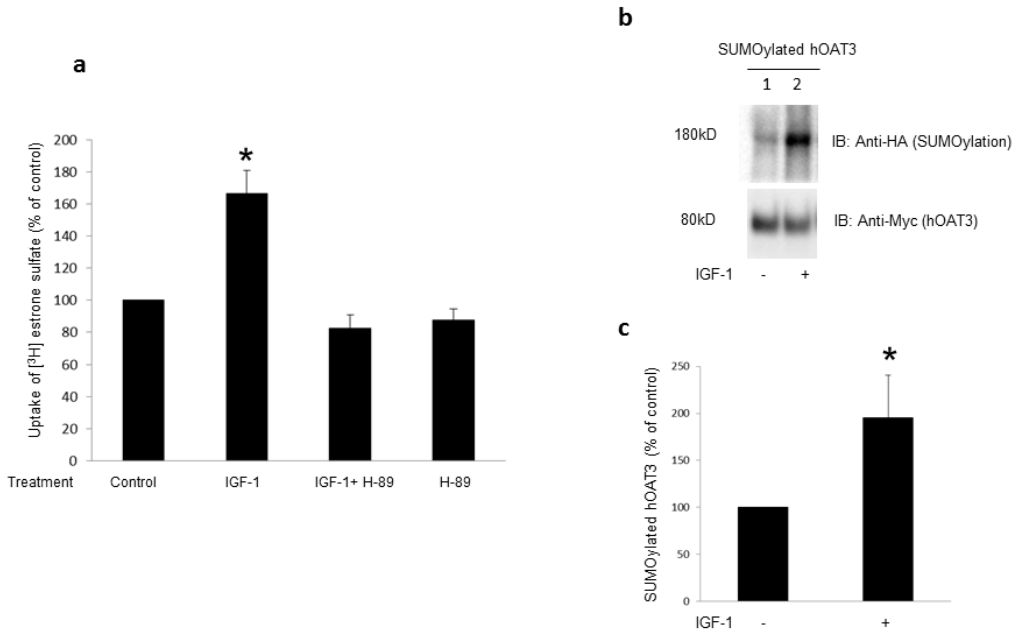

3. Discussion

Our current study showed that PKA stimulated hOAT3 activity which is opposite to the action of PKC. In contrast to the action of PKC, we showed that PKA stimulated hOAT3 expression and transport activity (Figs. 6-1-6-3) by accelerating the rate of hOAT3 recycling (Fig. 6-4) without affecting the internalization rate of the transporter (Fig. 6-5). Prolonged activation of PKA slowed down hOAT3 degradation (Fig. 6-6). We further showed that hOAT3 was SUMOylated by SUMO2 and SUMO3 but not by SUMO1 (Fig. 6-7a). SUMO2 and SUMO3 contain internal consensus motifs for SUMO conjugation, and therefore are capable of forming polySUMO chains. Yet, SUMO1 does not share such property. The molecular size for SUMOylated hOAT3 was ~ 180 kDa, 100 kDa larger than the size of hOAT3 (~ 80 kDa). Given that SUMO is a 12 kDa polypeptide, hOAT3 is most likely multi- or poly-SUMOylated. (Fig. 6-7a).

Our results also revealed that the activation of PKA promoted an enhancement in hOAT3 SUMOylation (Fig. 6-7b). Interestingly, the enhanced SUMOylation of hOAT3 by PKA activation is correlated with a reduced hOAT3 ubiquitination (Fig. 6-8a), indicating that there may be a communication between SUMOylation and ubiquitination. It has been suggested that SUMOylation and ubiquitination may crosstalk and mutually influence each other in a competitive manner (125, 126). In this context, SUMO and ubiquitin may modify the identical lysine residue(s). Alternatively, attachment of SUMO may potentially mask a nearby ubiquitination site. An increasing number of proteins have been reported to serve as substrates for both SUMOylation and ubiquitination. The two modifiers, often viewed as antagonists, enforce an opposite fate on their shared target and cooperatively exert regulatory control over a biological process. Therefore, it seems likely that the PKA-regulated and SUMOylation-dependent stimulation of hOAT3 expression and transport activity counters the PKC-regulated and ubiquitination-dependent inhibition of hOAT3 expression and transport activity. The work

aiming at further identifying the relationship between SUMOylation and ubiquitination on hOAT3 is currently being pursued in our laboratory.

Most SUMO substrates bear the consensus motif, Ψ-K-x-D/E (where ψ is a hydrophobic residue, K is the lysine conjugated to SUMO, x is any amino acid, E is a glutamic acid and D is an aspartic acid) (48). Based on the computer modeling, there are ten intracellular lysine residues on hOAT3, two of which, K285 and K518, lie within the SUMO-modification consensus motif: indicating that these lysine residues could be the potential SUMO-conjugation sites. Additionally, several online programs are capable of predicting SUMOylation sites. A program called SUMOplot™ Analysis Program (http://www.abgent.com/sumoplot.html) predicts K69, K285, K286, K515, K518 to be the potential SUMOylation sites. However, it should be noted that SUMOylation can also occur at lysine residues outside conventional motifs and the presence of conventional motifs do not guarantee the SUMOylation. The mapping of SUMO-conjugation sites on hOAT3 is currently underway in our laboratory.

PKA, like other protein kinases, regulates the target protein substrates by either directly phosphorylating the target protein or phosphorylating a protein that is associated with the target protein (129). Whether PKA directly phosphorylates OATs or phosphorylates an OAT-interacting protein would be an interesting topic for future investigation. In addition, protein phosphorylation has been revealed to play a role in regulating SUMOylation in some proteins, where it could stimulate or inhibit substrate SUMOylation depending on what the substrate is (120, 130-132). Therefore, if hOAT3 is a substrate of PKA phosphorylation, a co-regulation between phosphorylation and SUMOylation may also exist.

IGF-1 plays significantly roles in growth, development, and metabolism (133, 134). The abnormalities in the IGF-1 have been reported to be related to the development of several diseases, such as Laron syndrome and Acromegaly (135, 136). And a synthetic analog of IGF-1, Mecasermin, has been approved by the both U S Food and Drug Administration (FDA) and European Medicines Agency (EMA) for the treatment of growth failure (137). In our current

work, IGF-1 significantly enhanced OAT3 transport activity through PKA pathway (Fig. 6-9a) as well as OAT3 SUMOylation (Fig. 6-9b). Renal cortical slices from normal rats and diabetic rats have been utilized as tools for the studies involving the roles of PKA signaling pathway induced by hormones in OAT3. (32, 100). However, none of these studies illustrated the relationship between PKA stimulated SUMOlyation and OAT3 function in vivo. Therefore the in vivo investigations about SUMOlyation and OAT3 activity will be established in the future. As mentioned above, the abnormalities in the IGF-1 have been linked to the development of Laron syndrome. Further studies investigating the activity, expression and SUMOylatin of OAT3 in kidney from Laron mouse model would be particularly interesting.

In addition, our findings about the IGF-1 regulation on OAT3 through PKA signaling are consistent with a remote sensing and signaling model for transporters (138). Based on such a model, transporters in networks are regulated by hormones and growth factors, and effectively communicate among one another. In doing so, these transporters coordinately maintain the solute balance between multiple organs and therefore system homeostasis. Hormones/growth factors, released from one organ under the influence of the stimuli/environmental changes, enter the blood stream, and then reach to the target organs and exert their regulatory functions on transporters through cell signaling. Consistent with this general model, our data support that IGF-1, which is produced primarily by the liver under the stimuli, arrives at the kidney through blood stream, and then binds to its receptors and up-regulates OAT3 through PKA signaling.

Our study clearly illustrates PKA signaling on OAT3 regulation. By comparing our in vitro results with the metabolomics analyses of the Oat3 Knockout mice (139, 140) , we observe an interesting connection here. In OAT3 knockout mice, many metabolites accumulated, including gentisate and bile acids which are capable of activating G-protein-coupled receptors (GPCRs). Following the activation of GPCRs, the secondary messenger cAMP level maybe elevated leading to the activation of PKA signaling pathway. Based on our data, PKA activation increased OAT3 surface expression and transporter activity. Therefore, the interesting connection

is that metabolite variations contributed by the OAT3 reduction form a negative feedback loop to up-regulate OAT3 expression and function through PKA signaling.

Conclusion: We provided the first demonstration that PKA stimulated hOAT3 expression and transport activity by altering the trafficking kinetics of hOAT3 possibly through the crosstalk between SUMOylation and ubiquitination (Fig. 10).

Figure 6-10. The role of PKA in OAT3 transport activity, trafficking and SUMOylation. S: SUMO, IGF-1: insulin-like growth factor 1

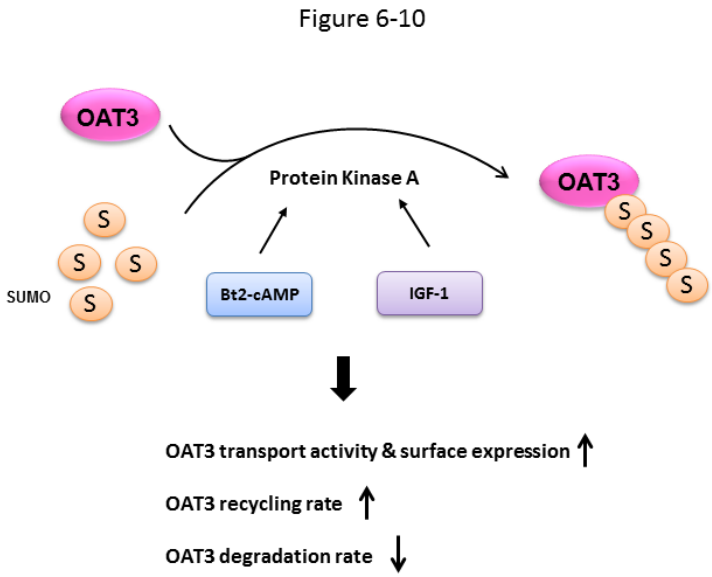

Chapter 7

Future direction

Portions of the information presented in this chapter have been published in the following article:

Haoxun Wang, Jinghui Zhang, and Guofeng You.

Activation of Protein Kinase A stimulates SUMOylation, expression, and transport activity of Organic Anion Transporter 3

AAPS J (2019) 21: 30. https://doi.org/10.1208/s12248-019-0303-4.

Portions of the information presented in this chapter are currently in preparation for the following article:

Haoxun Wang, Jinghui Zhang, Yunzhou Fan and Guofeng You.

Post-translational Regulation of Organic Anion Transporters - An Update

Our published work showed that both protein kinase sgk (sgk1 and sgk2) and endogenous hormone insulin regulated OATs expression and transport activity through phosphorylating an ubiquitin ligase Nedd4-2 with decreasing the association between Nedd4-2 and OATs, and eventually blocking the inhibitory effect of Nedd4-2 on OATs (76, 77, 141). Our unpublished work suggested that on the contrary to the up-regulation of sgk and insulin on OATs, PKC down-regulated OATs also through phosphorylating Nedd4-2, but leading to an enhanced binding between OATs and Nedd4-2. It is likely that differential regulations of OAT through different protein kinases are due to the dynamic phosphorylation at different sites on Nedd4-2, therefore resulting in diverse conformational changes in Nedd4-2 and altering its interaction to OATs, which further results in a change in OATs ubiquitination, trafficking and transport activity (73, 76, 102, 141). Our findings on the protein kinase-Nedd4-2 signaling network in the regulation of OATs will provide important insights into the understanding of how those hormones and protein kinases regulate OATs in vivo.

SUMOylation is now regarded as one of the major post-translational regulations in eukaryotic cells (48, 116). Our published work showed that hOAT3 was identified as a SUMOylation substrate, and a cross-talk may exist between SUMOylation and ubiquitination (142). Theoretically, SUMOylation may regulate OAT3 activity in an ubiquitination-independent manner. On the other hand, the two modification systems may crosstalk and mutually influence each other in a competitive manner (48). In this context, SUMO and ubiquitin may modify the identical lysine residue(s). Alternatively, attachment of SUMO may potentially mask a nearby ubiquitination site. Therefore, it is possible that the PKA up-regulated hOAT3 SUMOylation through competing hOAT3 ubiquitination. Our lab is currently identifying the relationship between SUMOylation and ubiquitination on hOAT3. In addition, the mapping of SUMO-conjugation sites on hOAT3 is currently underway in our laboratory.

SUMOylation is a dynamic and reversible event, and SUMO-specific proteases including members of Ulp (in yeast) and SENP family (in mammals) remove the SUMO moiety (deSUMOylation) from their substrates (143). Till now, six human Senp proteins have been cloned and identified with the ability to de-conjugate SUMO (144). In addition to the deSUMOylation enzymes, SUMO E3 ligases including members of Siz (in yeast) and PIAS family (in mammals) facilitate SUMO conjugation onto the substrates (48). Identification of the specific de-SUMOylation enzymes and SUMO E3 ligases would be particularly interesting.

PKA, like other protein kinases, regulates the target protein substrates by either directly phosphorylating the target protein or phosphorylating a protein that is associated with the target protein (129). Whether PKA directly phosphorylates OATs or phosphorylates an OAT-interacting protein would be an interesting topic for future investigation. In addition, protein phosphorylation has been revealed to play a role in regulating SUMOylation in some proteins, where it could stimulate or inhibit substrate SUMOylation depending on what the substrate is (120, 130-132). Therefore, if hOAT3 is a substrate of PKA phosphorylation, a co-regulation between phosphorylation and SUMOylation may also exist. Other than phosphorylation and ubiquitination, acetylation, which is another important post-translational modification, has been reported to cross-talk with SUMOylation (48). Whether hOAT3 is acetylation substrate and whether hOAT3 acetylation would cross-talk with hOAT3 SUMOylation will be an interesting research area to purse.

In summary, by illustrating the post-translational modifications of OATs would greatly contribute to the understanding of regulation of OAT-mediated drug transport in a variety of physiological and clinical conditions.

Chapter 8

Materials and Methods

Portions of the information presented in this chapter have been published in the following articles:

Haoxun Wang, Jinghui Zhang, and Guofeng You.

Activation of Protein Kinase A stimulates SUMOylation, expression, and transport activity of Organic Anion Transporter 3

AAPS J (2019) 21: 30. https://doi.org/10.1208/s12248-019-0303-4.

Haoxun Wang, Jinghui Zhang, and Guofeng You.

The Mechanistic Links between Insulin and Human Organic Anion Transporter 4.

Int J Pharm. 2019 Jan 30;555:165-174. doi: 10.1016/j.ijpharm.2018.11.040.

Haoxun Wang, Chenchang Liu, and Guofeng You.

The activity of organic anion transporter-3: Role of dexamethasone.

J Pharmacol Sci. 2018 Feb;136(2):79-85. doi: 10.1016/j.jphs.2017.12.011.

Haoxun Wang, Da Xu, May Fern Toh, Alan C. Pao, and Guofeng You.

Serum- and Glucocorticoid-Inducible Kinase SGK2 Regulates Human Organic Anion Transporters 4 via Ubiquitin Ligase Nedd4-2.

Biochemical Pharmacology, 2016, 102, pp 120-129. doi: 10.1016/j.bcp.2015.11.024.

1. Materials – COS-7 cells and HEK293 cells were obtained from ATCC (Manassas, VA). [3H]-labeled estrone sulfate (ES) was obtained from PerkinElmer (Waltham, MA). We ordered membrane-impermeable biotinylation reagent NHS-SS-biotin (Catalog number: 21331), streptavidin-agarose (Catalog number: 20349) and protein G-agarose (Catalog number: 20399) from Thermo Fisher Scientific (Waltham, MA). cDNAs for mouse sgk2 (wild-type sgk2 and constitutive active sgk2 (CA-sgk2)) and cDNA for mouse Flag-tagged sgk1 were generously provided by Dr. Alan C. Pao from Department of Medicine, Stanford University (Stanford, CA). cDNA for human Nedd4-2 was generously provided by Dr. Peter M. Snyder of the College of Medicine, University of Iowa (Iowa City, IA).cDNAs for HA-tagged SUMO-1, SUMO-2, SUMO-3, and Ubc9 were kindly provided by Dr. Jorge A Iñiguez-Lluhí from University of Michigan Medical School. Mouse anti-Myc antibody (9E10) was obtained from Roche (Indianapolis, IN). Rabbit anti-sgk2 antibody and rabbit anti-P-Nedd4-2 were purchased from Cell signaling (Danvers, MA). Rabbit anti-HA antibody, Rabbit anti-Nedd4-2 antibody and mouse anti-E-Cadherin antibody were obtained from abcam (Cambridge, MA). Mouse anti-ubiquitin antibody and mouse anti-β-actin were obtained from Santa Cruz (Santa Cruz, CA). Nedd4-2-specific siRNA oligonucleotides (Silencer® Select, identification number s23570) and negative control siRNA oligonucleotides (Silencer® Select, catalog number 4390843) were acquired from Ambion (Grand Island, NY). Dexamethasone, Dibutyryl cyclic-AMP sodium salt (Bt2-cAMP), H-89 dihydrochloride hydrate (H-89), Insulin-like Growth Factor-I human (IGF-1), insulin and all other reagents were acquired from Sigma-Aldrich (St. Louis, MO).

2. Experimental Procedures

2.1 Culturing of the cells and cDNA transfection

Parental COS-7 cells or parental HEK293 cells were grown in Dulbecco's modified Eagle's medium (DMEM) (Invitrogen, Carlsbad, CA) supplemented with 10% fetal bovine serum at 37 °C in 5% CO2. Transfection of cDNAs using Lipofectamine 2000 (Invitrogen, Carlsbad, CA) was performed for 48 h, following the manufacturer's instructions. Cells stably expressing hOATs (hOAT3 or hOAT4) were kept in DMEM medium supplemented with 0.2 mg/ml G418 (Invitrogen, Carlsbad, CA), 10% fetal bovine serum (43, 52).

2.2. Transport Measurements

Uptake of [^{3}H]-estrone sulfate (100 nM) was carried out, following standard protocol previously established in our lab (38, 43, 77). Uptake solution (phosphate-buffered saline with 1 mM $CaCl_2$ and 1 mM $MgCl_2$, pH 7.4 and 0.3μM [^{3}H]-estrone sulfate) was added to 48-well plates in which cells were plated. The uptake process was terminated by removing the uptake solution and washing the cells with ice-cold PBS twice at indicated time points. 0.2 N NaOH was used for cell lysis and then 0.2 N HCl was used for neutralization. Liquid scintillation counter (Beckman LSC LS6500) was used for detection of [^{3}H]-estrone sulfate. The transporter uptake activity was described as a percentage of the uptake measured in control cells. Data were corrected for nonspecific background measured in mock cells (parental cells).

2.3 Cell Surface Biotinylation

The measurement of the expression level of hOAT at the plasma membrane was performed using a biotinylation strategy, following the standard protocol previously established in our lab (43, 77). Sulfo-NHS-SS-biotin (0.5 mg/ml in phosphate-buffered saline with 1 mM $CaCl_2$ and 1 mM $MgCl_2$, pH 8.0) was added to 6-well plates in which cells were plated. After biotinylation and quenching of the unreacted sulfo-NHS-SS-biotin by rinsing with 100 mM glycine in PBS/CM, the cells were lysed on ice for 30 min. After 20 min centrifugation at 16000g at 4 °C, each sample supernatant of cell lysates was added to 40 μl of streptavidin-agarose beads to purify the cell

membrane proteins. Then we obtained hOAT (tagged with Myc at its carboxyl terminus) expression at plasma membrane by SDS-PAGE and eventually immunoblotted with an anti-Myc antibody (9E10).

2.4 Recycling Assay

We carried out the recycling assay by following the procedure previously established in our group (42). hOAT3-expressing cells were biotinylated with sulfo-NHS-SS-biotin at 4 ℃ to label hOAT3 at the plasma membrane. Then, one set of cells was unceasingly biotinylated at 4 ℃. The duplicate set of cells were warmed to 37 ℃ and unceasingly biotinylated at 37 ℃. At the indicated time points, biotinylation was ended and biotin-labeled hOAT3 was examined by SDS-PAGE and immunoblotting as described above. Recycled hOAT3 was calculated as the difference between hOAT3 biotin-labeled at 37 ℃ and hOAT3 biotin-labeled at 4 ℃.

2.5 Internalization Assay

We carried out the internalization assay by following the procedure established in our group (42, 43) by using a biotinylation approach in conjunction with immunoblotting. Relative hOAT3 internalized from the plasma membrane was described as % of the total initial cell surface hOAT3 pool.

2.6 Degradation Assay

We carried out the Degradation assay by following the procedure established in our group (43, 77). hOAT-expressing cells were subjected to biotinylation with 0.5 mg/ml sulfo-NHS-SS-biotin at 4 ℃. After biotinylation, followed by quenching of the unreacted NHS-SS-biotin with 2ml PBS containing 100mM glycine. For the Bt2-cAMP treatment study, the biotin-labeled cells were incubated in DMEM containing Bt2-cAMP at 37℃. For the sgk2 transfected study, the biotin-labeled cells were incubated in DMEM at 37℃. Then the cells were collected at indicated time points and lysed in lysis buffer with protease inhibitor cocktail, and centrifugated at 16,000 × g at 4 ℃. After that, supernatant was incubated with 40 μl of streptavidin agarose to isolate plasma membrane proteins, and eventually immunoblotting with anti-Myc antibody.

2.7 Immunoprecipitation

We carried out the immunoprecipitation assay by following the procedure previously established in our group (41, 77, 145). Cells were lysed with lysis buffer, containing 1% of proteinase inhibitor cocktail. For the experiment in which anti-Myc was used to pull-down hOAT, the lyzed cells were precleared with protein G-agarose beads (20-30 μl). Anti-Myc antibody (1:100) was incubated with protein G-agarose beads (20-30 μl) at 4 °C for 1.5 hours. The precleared cell lysates were then mixed with antibody-bound protein G-agarose beads with rotating at 4 °C overnight. For the experiment in which Anti-Flag M2 affinity gel (Sigma–Aldrich, St. Louis, MO) was used to pull-down Nedd4-2, the precleared cell lysates were mixed with Anti-Flag M2 affinity gel with rotating at 4 °C overnight. Proteins bound to the protein G-agarose beads or Anti-Flag M2 affinity gel were eluted with Urea buffer containing β-mecaptoethanol and examined by immunoblotting with appropriate antibodies.

2.8 Electrophoresis and Immunoblotting

We carried out the experiments by following the procedure previously established in our group (41, 77). We separated Protein samples on 7.5% SDS-PAGE minigels (Bio-Rad, Hercules, CA) and electro-transferred on to PVDF membranes (Invitrogen, Carlsbad, CA). After electro-transfer, we incubated the blots with 5% nonfat dry milk for 1h in PBS-0.05% Tween 20 at room temperature, washed, and incubated with appropriate primary antibodies at 4 °C overnight. Then the blots were incubated with horseradish peroxidase-conjugated secondary antibodies for 1 h at room temperature, followed by detection with SuperSignal West Dura Extended Duration Substrate kit (Pierce, Rockford, IL). The scanning densitometry with the FluorChem 8000 imaging system (Alpha Innotech Corp., San Leandro, CA) was used to quantify the nonsaturating, immunoreactive protein bands.

2.9 Concentration-dependent inhibition studies

We carried out the inhibition assay by following the procedure established in our group (146, 147). Inhibition studies were performed at varying concentrations of Dexamethasone. hOAT3

specific uptake was calculated by subtracting [^{3}H]-ES uptake into parental cells from the uptake into hOAT3-expressing cells. The IC_{50} (concentration of the drugs required to inhibit 50% of ES uptake) was determined by nonlinear regression using GraphPad Prism.

2.10 Dixon plot

We carried out the Dixon plot analysis by following the procedure established in our group (146, 147). The mechanism of inhibition was determined by linear regression analysis of reciprocal saturable uptake (1/v) for different substrate concentrations (1.2 μM or 2.4 μM ES) as a function of inhibitor concentration. hOAT3 mediated [^{3}H]-ES uptake was accessed at 4 min in both the absence and presence of different concentrations of dexamethasone. The specific uptake was calculated by subtracting [^{3}H]-ES uptake into mock cells from the uptake into hOAT3-expressing cells. The linear regression analysis was utilized to analyze the data with GraphPad Prism. The constant Ki (inhibition constant) value was calculated by fitting the data to a competitive inhibition model (148-150), where C represents the concentration of substrates (μM) and K_m represents the Michaelis constant (μM).

$$K_i = \frac{IC_{50}}{1+{}^{C}/_{K_m}} \quad (1)$$

2.11 Data Analysis

We repeated each experiment a minimum of three times, and multiple experiments were used for statistical analysis. Statistical analysis was performed using Student's paired t-tests between two groups or GraphPad Prism software (GraphPad Software Inc., San Diego, CA), one-way ANOVA, multiple comparisons among multiple treatments. A p-value of <0.05 was considered significant.

REFERENCE

1. You GF, Morris ME. DRUG TRANSPORTERS : Molecular Characterization and Role in Drug Disposition, 2nd Edition Wiley Ser Drug Disc. 2014. doi: Book_Doi 10.1002/9781118705308.

2. International Transporter C, Giacomini KM, Huang SM, Tweedie DJ, Benet LZ, Brouwer KL, et al. Membrane transporters in drug development. Nat Rev Drug Discov. 2010;9(3):215-36. doi: 10.1038/nrd3028.

3. Hillgren KM, Keppler D, Zur AA, Giacomini KM, Stieger B, Cass CE, et al. Emerging transporters of clinical importance: an update from the International Transporter Consortium. Clin Pharmacol Ther. 2013;94(1):52-63. doi: 10.1038/clpt.2013.74.

4. Guidance for Industry (Draft): Drug Interaction Studies- Study Design, Data Analysis, Implications for Dosing, and Labeling Recommendations <http://www.fda.gov/Drugs/GuidanceComplianceRegulatoryInformation/Guidances/ucm064982.htm>. Accessed 18 February 2012.

5. Guidance for Industry (Draft): In Vitro Metabolismand Transporter Mediated Drug-Drug Interaction Studies<https://www.fda.gov/downloads/Drugs/Guidances/UCM581965.pdf>. Accessed 24 October 2017.

6. Yin J, Wang J. Renal drug transporters and their significance in drug-drug interactions. Acta Pharm Sin B. 2016;6(5):363-73. doi: 10.1016/j.apsb.2016.07.013.

7. Chu X, Bleasby K, Chan GH, Nunes I, Evers R. The Complexities of Interpreting Reversible Elevated Serum Creatinine Levels in Drug Development: Does a Correlation with Inhibition of Renal Transporters Exist? Drug Metab Dispos. 2016;44(9):1498-509. doi: 10.1124/dmd.115.067694.

8. Krajcsi P. Drug-transporter interaction testing in drug discovery and development. World J Pharmacol. 2013;2(1):35-46. doi: 10.5497/wjp.v2.i1.35.

9. Yang X, Ma Z, Zhou S, Weng Y, Lei H, Zeng S, et al. Multiple Drug Transporters Are Involved in Renal Secretion of Entecavir. Antimicrob Agents Chemother. 2016;60(10):6260-70. doi: 10.1128/AAC.00986-16.

10. Ahn SY, Nigam SK. Toward a systems level understanding of organic anion and other multispecific drug transporters: a remote sensing and signaling hypothesis. Mol Pharmacol. 2009;76(3):481-90. doi: 10.1124/mol.109.056564.

11. Dantzler WH, Wright SH. The molecular and cellular physiology of basolateral organic anion transport in mammalian renal tubules. Biochim Biophys Acta. 2003;1618(2):185-93.

12. Srimaroeng C, Perry JL, Pritchard JB. Physiology, structure, and regulation of the cloned organic anion transporters. Xenobiotica. 2008;38(7-8):889-935. doi: 10.1080/00498250801927435.

13. VanWert AL, Gionfriddo MR, Sweet DH. Organic anion transporters: discovery, pharmacology, regulation and roles in pathophysiology. Biopharm Drug Dispos. 2010;31(1):1-71. doi: 10.1002/bdd.693.

14. You G. Structure, function, and regulation of renal organic anion transporters. Med Res Rev. 2002;22(6):602-16. doi: 10.1002/med.10019.

15. Terada T, Inui K. Gene expression and regulation of drug transporters in the intestine and kidney. Biochem Pharmacol. 2007;73(3):440-9. doi: 10.1016/j.bcp.2006.10.010.

16. Vallon V, Eraly SA, Wikoff WR, Rieg T, Kaler G, Truong DM, et al. Organic anion transporter 3 contributes to the regulation of blood pressure. J Am Soc Nephrol. 2008;19(9):1732-40. doi: 10.1681/ASN.2008020180.

17. Alebouyeh M, Takeda M, Onozato ML, Tojo A, Noshiro R, Hasannejad H, et al. Expression of human organic anion transporters in the choroid plexus and their interactions with neurotransmitter metabolites. J Pharmacol Sci. 2003;93(4):430-6.

18. Pritchard JB. Rat renal cortical slices demonstrate p-aminohippurate/glutarate exchange and sodium/glutarate coupled p-aminohippurate transport. J Pharmacol Exp Ther. 1990;255(3):969-75.

19. Taki K, Nakamura S, Miglinas M, Enomoto A, Niwa T. Accumulation of indoxyl sulfate in OAT1/3-positive tubular cells in kidneys of patients with chronic renal failure. J Ren Nutr. 2006;16(3):199-203. doi: 10.1053/j.jrn.2006.04.020.

20. Cha SH, Sekine T, Kusuhara H, Yu E, Kim JY, Kim DK, et al. Molecular cloning and characterization of multispecific organic anion transporter 4 expressed in the placenta. J Biol Chem. 2000;275(6):4507-12.

21. Xu D, Wang H, You G. Posttranslational Regulation of Organic Anion Transporters by Ubiquitination: Known and Novel. Med Res Rev. 2016;36(5):964-79. doi: 10.1002/med.21397.

22. Shimada H, Moewes B, Burckhardt G. Indirect coupling to Na+ of p-aminohippuric acid uptake into rat renal basolateral membrane vesicles. Am J Physiol. 1987;253(5 Pt 2):F795-801. doi: 10.1152/ajprenal.1987.253.5.F795.

23. Pritchard JB. Coupled transport of p-aminohippurate by rat kidney basolateral membrane vesicles. Am J Physiol. 1988;255(4 Pt 2):F597-604. doi: 10.1152/ajprenal.1988.255.4.F597.

24. Pritchard JB, Miller DS. Mechanisms mediating renal secretion of organic anions and cations. Physiol Rev. 1993;73(4):765-96. doi: 10.1152/physrev.1993.73.4.765.

25. Saito H. Pathophysiological regulation of renal SLC22A organic ion transporters in acute kidney injury: pharmacological and toxicological implications. Pharmacol Ther. 2010;125(1):79-91. doi: 10.1016/j.pharmthera.2009.09.008.

26. Sun H, Frassetto L, Benet LZ. Effects of renal failure on drug transport and metabolism. Pharmacol Ther. 2006;109(1-2):1-11. doi: 10.1016/j.pharmthera.2005.05.010.

27. Monica Torres A, Mac Laughlin M, Muller A, Brandoni A, Anzai N, Endou H. Altered renal elimination of organic anions in rats with chronic renal failure. Biochim Biophys Acta. 2005;1740(1):29-37. doi: 10.1016/j.bbadis.2005.03.002.

28. Naud J, Michaud J, Beauchemin S, Hebert MJ, Roger M, Lefrancois S, et al. Effects of chronic renal failure on kidney drug transporters and cytochrome P450 in rats. Drug Metab Dispos. 2011;39(8):1363-9. doi: 10.1124/dmd.111.039115.

29. Matsuzaki T, Watanabe H, Yoshitome K, Morisaki T, Hamada A, Nonoguchi H, et al. Downregulation of organic anion transporters in rat kidney under ischemia/reperfusion-induced acute [corrected] renal failure. Kidney Int. 2007;71(6):539-47. doi: 10.1038/sj.ki.5002104.

30. Schneider R, Sauvant C, Betz B, Otremba M, Fischer D, Holzinger H, et al. Downregulation of organic anion transporters OAT1 and OAT3 correlates with impaired secretion of para-aminohippurate after ischemic acute renal failure in rats. Am J Physiol Renal Physiol. 2007;292(5):F1599-605. doi: 10.1152/ajprenal.00473.2006.

31. Villar SR, Brandoni A, Anzai N, Endou H, Torres AM. Altered expression of rat renal cortical OAT1 and OAT3 in response to bilateral ureteral obstruction. Kidney Int. 2005;68(6):2704-13. doi: 10.1111/j.1523-1755.2005.00741.x.

32. Phatchawan A, Chutima S, Varanuj C, Anusorn L. Decreased renal organic anion transporter 3 expression in type 1 diabetic rats. Am J Med Sci. 2014;347(3):221-7. doi: 10.1097/MAJ.0b013e3182831740.

33. Xu C, Zhu L, Chan T, Lu X, Shen W, Gillies MC, et al. The altered renal and hepatic expression of solute carrier transporters (SLCs) in type 1 diabetic mice. PLoS One. 2015;10(3):e0120760. doi: 10.1371/journal.pone.0120760.

34. Cheng Q, Aleksunes LM, Manautou JE, Cherrington NJ, Scheffer GL, Yamasaki H, et al. Drug-metabolizing enzyme and transporter expression in a mouse model of diabetes and obesity. Mol Pharm. 2008;5(1):77-91. doi: 10.1021/mp700114j.

35. More VR, Wen X, Thomas PE, Aleksunes LM, Slitt AL. Severe diabetes and leptin resistance cause differential hepatic and renal transporter expression in mice. Comp Hepatol. 2012;11(1):1. doi: 10.1186/1476-5926-11-1.

36. Nowicki MT, Aleksunes LM, Sawant SP, Dnyanmote AV, Mehendale HM, Manautou JE. Renal and hepatic transporter expression in type 2 diabetic rats. Drug Metab Lett. 2008;2(1):11-7.

37. Liu T, Guo X, Meng Q, Wang C, Liu Q, Sun H, et al. Effect of JBP485 on obstructive jaundice is related to regulation of renal Oat1, Oat3 and Mrp2 expression in ANIT-treated rats. Peptides. 2012;36(1):78-85. doi: 10.1016/j.peptides.2012.04.003.

38. Zhou F, Xu W, Hong M, Pan Z, Sinko PJ, Ma J, et al. The role of N-linked glycosylation in protein folding, membrane targeting, and substrate binding of human organic anion transporter hOAT4. Mol Pharmacol. 2005;67(3):868-76. doi: 10.1124/mol.104.007583.

39. Tanaka K, Xu W, Zhou F, You G. Role of glycosylation in the organic anion transporter OAT1. J Biol Chem. 2004;279(15):14961-6. doi: 10.1074/jbc.M400197200.

40. You G, Kuze K, Kohanski RA, Amsler K, Henderson S. Regulation of mOAT-mediated organic anion transport by okadaic acid and protein kinase C in LLC-PK(1) cells. J Biol Chem. 2000;275(14):10278-84.

41. Zhang Q, Li S, Patterson C, You G. Lysine 48-linked polyubiquitination of organic anion transporter-1 is essential for its protein kinase C-regulated endocytosis. Mol Pharmacol. 2013;83(1):217-24. doi: 10.1124/mol.112.082065.

42. Zhang Q, Hong M, Duan P, Pan Z, Ma J, You G. Organic anion transporter OAT1 undergoes constitutive and protein kinase C-regulated trafficking through a dynamin- and clathrin-dependent pathway. J Biol Chem. 2008;283(47):32570-9. doi: 10.1074/jbc.M800298200.

43. Zhang Q, Suh W, Pan Z, You G. Short-term and long-term effects of protein kinase C on the trafficking and stability of human organic anion transporter 3. Int J Biochem Mol Biol. 2012;3(2):242-9.

44. Li S, Zhang Q, You G. Three ubiquitination sites of organic anion transporter-1 synergistically mediate protein kinase C-dependent endocytosis of the transporter. Mol Pharmacol. 2013;84(1):139-46. doi: 10.1124/mol.113.086769.

45. Xu D, Wang H, You G. An Essential Role of Nedd4-2 in the Ubiquitination, Expression, and Function of Organic Anion Transporter-3. Mol Pharm. 2016;13(2):621-30. doi: 10.1021/acs.molpharmaceut.5b00839.

46. Xu D, Wang H, Zhang Q, You G. Nedd4-2 but not Nedd4-1 is critical for protein kinase C-regulated ubiquitination, expression, and transport activity of human organic anion transporter 1. Am J Physiol Renal Physiol. 2016;310(9):F821-31. doi: 10.1152/ajprenal.00522.2015.

47. Xu D, Zhang J, Zhang Q, Fan Y, Liu C, You G. PKC/Nedd4-2 Signaling Pathway Regulates the Cell Surface Expression of Drug Transporter hOAT1. Drug Metab Dispos. 2017;45(8):887-95. doi: 10.1124/dmd.117.075861.

48. Gareau JR, Lima CD. The SUMO pathway: emerging mechanisms that shape specificity, conjugation and recognition. Nat Rev Mol Cell Biol. 2010;11(12):861-71. doi: 10.1038/nrm3011.

49. Babu E, Takeda M, Narikawa S, Kobayashi Y, Enomoto A, Tojo A, et al. Role of human organic anion transporter 4 in the transport of ochratoxin A. Biochim Biophys Acta. 2002;1590(1-3):64-75.

50. Ugele B, St-Pierre MV, Pihusch M, Bahn A, Hantschmann P. Characterization and identification of steroid sulfate transporters of human placenta. Am J Physiol Endocrinol Metab. 2003;284(2):E390-8. doi: 10.1152/ajpendo.00257.2002.

51. Rabe T, Hosch R, Runnebaum B. Diagnosis of intrauterine fetal growth retardation (IUGR) and placental insufficiency by a dehydroepiandrosterone sulfate (DHAS) loading test. Biol Res Pregnancy Perinatol. 1983;4(3):130-6.

52. Duan P, Li S, You G. Regulation of human organic anion transporter 4 by parathyroid hormone-related protein and protein kinase A. Int J Biochem Mol Biol. 2012;3(3):322-7.

53. Kusch-Poddar M, Drewe J, Fux I, Gutmann H. Evaluation of the immortalized human brain capillary endothelial cell line BB19 as a human cell culture model for the blood-brain barrier. Brain Res. 2005;1064(1-2):21-31. doi: 10.1016/j.brainres.2005.10.014.

54. Xu G, Bhatnagar V, Wen G, Hamilton BA, Eraly SA, Nigam SK. Analyses of coding region polymorphisms in apical and basolateral human organic anion transporter (OAT) genes [OAT1 (NKT), OAT2, OAT3, OAT4, URAT (RST)]. Kidney Int. 2005;68(4):1491-9. doi: 10.1111/j.1523-1755.2005.00612.x.

55. Buse P, Tran SH, Luther E, Phu PT, Aponte GW, Firestone GL. Cell cycle and hormonal control of nuclear-cytoplasmic localization of the serum- and glucocorticoid-inducible protein kinase, Sgk, in mammary tumor cells. A novel convergence point of anti-proliferative and proliferative cell signaling pathways. J Biol Chem. 1999;274(11):7253-63.

56. Chen SY, Bhargava A, Mastroberardino L, Meijer OC, Wang J, Buse P, et al. Epithelial sodium channel regulated by aldosterone-induced protein sgk. Proc Natl Acad Sci U S A. 1999;96(5):2514-9.

57. Leong ML, Maiyar AC, Kim B, O'Keeffe BA, Firestone GL. Expression of the serum- and glucocorticoid-inducible protein kinase, Sgk, is a cell survival response to multiple types of environmental stress stimuli in mammary epithelial cells. J Biol Chem. 2003;278(8):5871-82. doi: 10.1074/jbc.M211649200.

58. Naray-Fejes-Toth A, Canessa C, Cleaveland ES, Aldrich G, Fejes-Toth G. sgk is an aldosterone-induced kinase in the renal collecting duct. Effects on epithelial na+ channels. J Biol Chem. 1999;274(24):16973-8.

59. Rozansky DJ, Wang J, Doan N, Purdy T, Faulk T, Bhargava A, et al. Hypotonic induction of SGK1 and Na+ transport in A6 cells. Am J Physiol Renal Physiol. 2002;283(1):F105-13. doi: 10.1152/ajprenal.00176.2001.

60. Waldegger S, Barth P, Forrest JN, Jr., Greger R, Lang F. Cloning of sgk serine-threonine protein kinase from shark rectal gland - a gene induced by hypertonicity and secretagogues. Pflugers Arch. 1998;436(4):575-80. doi: 10.1007/s004240050674.

61. Pao AC, Bhargava A, Di Sole F, Quigley R, Shao X, Wang J, et al. Expression and role of serum and glucocorticoid-regulated kinase 2 in the regulation of Na+/H+ exchanger 3 in the mammalian kidney. Am J Physiol Renal Physiol. 2010;299(6):F1496-506. doi: 10.1152/ajprenal.00075.2010.

62. Rotin D, Staub O. Nedd4-2 and the regulation of epithelial sodium transport. Front Physiol. 2012;3:212. doi: 10.3389/fphys.2012.00212.

63. Yang B, Kumar S. Nedd4 and Nedd4-2: closely related ubiquitin-protein ligases with distinct physiological functions. Cell Death Differ. 2010;17(1):68-77. doi: 10.1038/cdd.2009.84.

64. Sorkina T, Miranda M, Dionne KR, Hoover BR, Zahniser NR, Sorkin A. RNA interference screen reveals an essential role of Nedd4-2 in dopamine transporter ubiquitination and endocytosis. J Neurosci. 2006;26(31):8195-205. doi: 10.1523/JNEUROSCI.1301-06.2006.

65. Garcia-Tardon N, Gonzalez-Gonzalez IM, Martinez-Villarreal J, Fernandez-Sanchez E, Gimenez C, Zafra F. Protein kinase C (PKC)-promoted endocytosis of glutamate transporter GLT-1 requires ubiquitin ligase Nedd4-2-dependent ubiquitination but not phosphorylation. J Biol Chem. 2012;287(23):19177-87. doi: 10.1074/jbc.M112.355909.

66. Naray-Fejes-Toth A, Snyder PM, Fejes-Toth G. The kidney-specific WNK1 isoform is induced by aldosterone and stimulates epithelial sodium channel-mediated Na+ transport. Proc Natl Acad Sci U S A. 2004;101(50):17434-9. doi: 10.1073/pnas.0408146101.

67. Macias MJ, Hyvonen M, Baraldi E, Schultz J, Sudol M, Saraste M, et al. Structure of the WW domain of a kinase-associated protein complexed with a proline-rich peptide. Nature. 1996;382(6592):646-9. doi: 10.1038/382646a0.

68. Staub O, Dho S, Henry P, Correa J, Ishikawa T, McGlade J, et al. WW domains of Nedd4 bind to the proline-rich PY motifs in the epithelial Na+ channel deleted in Liddle's syndrome. EMBO J. 1996;15(10):2371-80.

69. Duan P, Li S, You G. Angiotensin II inhibits activity of human organic anion transporter 3 through activation of protein kinase Calpha: accelerating endocytosis of the transporter. Eur J Pharmacol. 2010;627(1-3):49-55. doi: 10.1016/j.ejphar.2009.10.048.

70. Lamothe SM, Zhang S. The serum- and glucocorticoid-inducible kinases SGK1 and SGK3 regulate hERG channel expression via ubiquitin ligase Nedd4-2 and GTPase Rab11. J Biol Chem. 2013;288(21):15075-84. doi: 10.1074/jbc.M113.453670.

71. Boehmer C, Henke G, Schniepp R, Palmada M, Rothstein JD, Broer S, et al. Regulation of the glutamate transporter EAAT1 by the ubiquitin ligase Nedd4-2 and the serum and glucocorticoid-inducible kinase isoforms SGK1/3 and protein kinase B. J Neurochem. 2003;86(5):1181-8.

72. Klaus F, Palmada M, Lindner R, Laufer J, Jeyaraj S, Lang F, et al. Up-regulation of hypertonicity-activated myo-inositol transporter SMIT1 by the cell volume-sensitive protein kinase SGK1. J Physiol. 2008;586(6):1539-47. doi: 10.1113/jphysiol.2007.146191.

73. Snyder PM, Olson DR, Kabra R, Zhou R, Steines JC. cAMP and serum and glucocorticoid-inducible kinase (SGK) regulate the epithelial Na(+) channel through convergent phosphorylation of Nedd4-2. J Biol Chem. 2004;279(44):45753-8. doi: 10.1074/jbc.M407858200.

74. Hall BA, Kim TY, Skor MN, Conzen SD. Serum and glucocorticoid-regulated kinase 1 (SGK1) activation in breast cancer: requirement for mTORC1 activity associates with ER-alpha expression. Breast Cancer Res Treat. 2012;135(2):469-79. doi: 10.1007/s10549-012-2161-y.

75. Pearce D. The role of SGK1 in hormone-regulated sodium transport. Trends Endocrinol Metab. 2001;12(8):341-7.

76. Wang H, You G. SGK1/Nedd4-2 signaling pathway regulates the activity of human organic anion transporters 3. Biopharm Drug Dispos. 2017. doi: 10.1002/bdd.2085.

77. Wang H, Xu D, Toh MF, Pao AC, You G. Serum- and glucocorticoid-inducible kinase SGK2 regulates human organic anion transporters 4 via ubiquitin ligase Nedd4-2. Biochem Pharmacol. 2016;102:120-9. doi: 10.1016/j.bcp.2015.11.024.

78. Dallman MF, la Fleur SE, Pecoraro NC, Gomez F, Houshyar H, Akana SF. Minireview: glucocorticoids--food intake, abdominal obesity, and wealthy nations in 2004. Endocrinology. 2004;145(6):2633-8. doi: 10.1210/en.2004-0037.

79. Schacke H, Docke WD, Asadullah K. Mechanisms involved in the side effects of glucocorticoids. Pharmacol Ther. 2002;96(1):23-43.

80. Yang YX, Lichtenstein GR. Corticosteroids in Crohn's disease. Am J Gastroenterol. 2002;97(4):803-23. doi: 10.1111/j.1572-0241.2002.05596.x.

81. Di Pietro N, Panel V, Hayes S, Bagattin A, Meruvu S, Pandolfi A, et al. Serum- and glucocorticoid-inducible kinase 1 (SGK1) regulates adipocyte differentiation via forkhead box O1. Mol Endocrinol. 2010;24(2):370-80. doi: 10.1210/me.2009-0265.

82. Wang D, Zhang H, Lang F, Yun CC. Acute activation of NHE3 by dexamethasone correlates with activation of SGK1 and requires a functional glucocorticoid receptor. Am J Physiol Cell Physiol. 2007;292(1):C396-404. doi: 10.1152/ajpcell.00345.2006.

83. Miyata S, Koyama Y, Takemoto K, Yoshikawa K, Ishikawa T, Taniguchi M, et al. Plasma corticosterone activates SGK1 and induces morphological changes in oligodendrocytes in corpus callosum. PLoS One. 2011;6(5):e19859. doi: 10.1371/journal.pone.0019859.

84. Alamares-Sapuay JG, Martinez-Gil L, Stertz S, Miller MS, Shaw ML, Palese P. Serum- and glucocorticoid-regulated kinase 1 is required for nuclear export of the ribonucleoprotein of influenza A virus. J Virol. 2013;87(10):6020-6. doi: 10.1128/JVI.01258-12.

85. Chen W, Chen Y, Xu BE, Juang YC, Stippec S, Zhao Y, et al. Regulation of a third conserved phosphorylation site in SGK1. J Biol Chem. 2009;284(6):3453-60. doi: 10.1074/jbc.M807502200.

86. Christy NP, Laragh JH. Pathogenesis of hypokalemic alkalosis in Cushing's syndrome. N Engl J Med. 1961;265:1083-8. doi: 10.1056/NEJM196111302652203.

87. Ali R, Amlal H, Burnham CE, Soleimani M. Glucocorticoids enhance the expression of the basolateral Na+:HCO3- cotransporter in renal proximal tubules. Kidney Int. 2000;57(3):1063-71. doi: 10.1046/j.1523-1755.2000.00933.x.

88. Dagan A, Gattineni J, Cook V, Baum M. Prenatal programming of rat proximal tubule Na+/H+ exchanger by dexamethasone. Am J Physiol Regul Integr Comp Physiol. 2007;292(3):R1230-5. doi: 10.1152/ajpregu.00669.2006.

89. Zeng Y, Zhang R, Wu J, Liu M, Peng W, Yu X, et al. Organic anion transporter 1 (OAT1) involved in renal cell transport of aristolochic acid I. Hum Exp Toxicol. 2012;31(8):759-70. doi: 10.1177/0960327111424302.

90. Xue X, Gong LK, Maeda K, Luan Y, Qi XM, Sugiyama Y, et al. Critical role of organic anion transporters 1 and 3 in kidney accumulation and toxicity of aristolochic acid I. Mol Pharm. 2011;8(6):2183-92. doi: 10.1021/mp100418u.

91. Rodiger M, Zhang X, Ugele B, Gersdorff N, Wright SH, Burckhardt G, et al. Organic anion transporter 3 (OAT3) and renal transport of the metal chelator 2,3-dimercapto-1-propanesulfonic acid (DMPS). Can J Physiol Pharmacol. 2010;88(2):141-6. doi: 10.1139/Y09-123.

92. El-Sheikh AA, Greupink R, Wortelboer HM, van den Heuvel JJ, Schreurs M, Koenderink JB, et al. Interaction of immunosuppressive drugs with human organic anion transporter (OAT) 1 and OAT3, and multidrug resistance-associated protein (MRP) 2 and MRP4. Transl Res. 2013;162(6):398-409. doi: 10.1016/j.trsl.2013.08.003.

93. Spoorenberg SM, Deneer VH, Grutters JC, Pulles AE, Voorn GP, Rijkers GT, et al. Pharmacokinetics of oral vs. intravenous dexamethasone in patients hospitalized with community-acquired pneumonia. Br J Clin Pharmacol. 2014;78(1):78-83. doi: 10.1111/bcp.12295.

94. Lanevskij K, Dapkunas J, Juska L, Japertas P, Didziapetris R. QSAR analysis of blood-brain distribution: the influence of plasma and brain tissue binding. J Pharm Sci. 2011;100(6):2147-60. doi: 10.1002/jps.22442.

95. Xu D, Huang H, Toh MF, You G. Serum- and glucocorticoid-inducible kinase sgk2 stimulates the transport activity of human organic anion transporters 1 by enhancing the stability of the transporter. Int J Biochem Mol Biol. 2016;7(1):19-26.

96. Furu K, Kilvik K, Gautvik KM, Haug E. The mechanism of [3H]dexamethasone uptake into prolactin producing rat pituitary cells (GH3 cells) in culture. J Steroid Biochem. 1987;28(6):587-91.

97. Caceres-del-Carpio J, Costa RD, Haider A, Narayanan R, Kuppermann BD. Corticosteroids: Triamcinolone, Dexamethasone and Fluocinolone. Dev Ophthalmol. 2016;55:221-31. doi: 10.1159/000431198.

98. Franco M, William L, Poon P, Azad A. Dexamethasone for cancer-related fatigue. J Clin Oncol. 2014;32(6):608-9. doi: 10.1200/JCO.2013.53.7878.

99. Wang H, You G. SGK1/Nedd4-2 signaling pathway regulates the activity of human organic anion transporters 3. Biopharm Drug Dispos. 2017;38(8):449-57. doi: 10.1002/bdd.2085.

100. Barros SA, Srimaroeng C, Perry JL, Walden R, Dembla-Rajpal N, Sweet DH, et al. Activation of protein kinase Czeta increases OAT1 (SLC22A6)- and OAT3 (SLC22A8)-mediated transport. J Biol Chem. 2009;284(5):2672-9. doi: 10.1074/jbc.M808078200.

101. Lungkaphin A, Arjinajarn P, Pongchaidecha A, Srimaroeng C, Chatsudthipong L, Chatsudthipong V. Impaired insulin signaling affects renal organic anion transporter 3 (Oat3) function in streptozotocin-induced diabetic rats. PLoS One. 2014;9(5):e96236. doi: 10.1371/journal.pone.0096236.

102. Lee IH, Dinudom A, Sanchez-Perez A, Kumar S, Cook DI. Akt mediates the effect of insulin on epithelial sodium channels by inhibiting Nedd4-2. J Biol Chem. 2007;282(41):29866-73. doi: 10.1074/jbc.M701923200.

103. Wang J, Barbry P, Maiyar AC, Rozansky DJ, Bhargava A, Leong M, et al. SGK integrates insulin and mineralocorticoid regulation of epithelial sodium transport. Am J Physiol Renal Physiol. 2001;280(2):F303-13. doi: 10.1152/ajprenal.2001.280.2.F303.

104. Song C, Liu D, Yang S, Cheng L, Xing E, Chen Z. Sericin enhances the insulin-PI3K/AKT signaling pathway in the liver of a type 2 diabetes rat model. Exp Ther Med. 2018;16(4):3345-52. doi: 10.3892/etm.2018.6615.

105. Avramoglu RK, Basciano H, Adeli K. Lipid and lipoprotein dysregulation in insulin resistant states. Clin Chim Acta. 2006;368(1-2):1-19. doi: 10.1016/j.cca.2005.12.026.

106. Fry MJ. Structure, regulation and function of phosphoinositide 3-kinases. Biochim Biophys Acta. 1994;1226(3):237-68.

107. MacKay KB, Lowenson JD, Clarke SG. Wortmannin reduces insulin signaling and death in seizure-prone Pcmt1-/- mice. PLoS One. 2012;7(10):e46719. doi: 10.1371/journal.pone.0046719.

108. Zhou X, Zhao Y, Xu L, Li X, Chen P, Zou H, et al. [Wortmannin and U0126 inhibit the promoting effect of insulin on differentiation of skeletal myoblasts in rats]. Xi Bao Yu Fen Zi Mian Yi Xue Za Zhi. 2014;30(7):717-20.

109. Debonneville C, Flores SY, Kamynina E, Plant PJ, Tauxe C, Thomas MA, et al. Phosphorylation of Nedd4-2 by Sgk1 regulates epithelial Na(+) channel cell surface expression. EMBO J. 2001;20(24):7052-9. doi: 10.1093/emboj/20.24.7052.

110. Brewer PD, Habtemichael EN, Romenskaia I, Mastick CC, Coster AC. Insulin-regulated Glut4 translocation: membrane protein trafficking with six distinctive steps. J Biol Chem. 2014;289(25):17280-98. doi: 10.1074/jbc.M114.555714.

111. Klisic J, Hu MC, Nief V, Reyes L, Fuster D, Moe OW, et al. Insulin activates Na(+)/H(+) exchanger 3: biphasic response and glucocorticoid dependence. Am J Physiol Renal Physiol. 2002;283(3):F532-9. doi: 10.1152/ajprenal.00365.2001.

112. Mansley MK, Watt GB, Francis SL, Walker DJ, Land SC, Bailey MA, et al. Dexamethasone and insulin activate serum and glucocorticoid-inducible kinase 1 (SGK1) via different molecular mechanisms in cortical collecting duct cells. Physiol Rep. 2016;4(10):e12792. doi: 10.14814/phy2.12792.

113. Liu H, Yu J, Xia T, Xiao Y, Zhang Q, Liu B, et al. Hepatic serum- and glucocorticoid-regulated protein kinase 1 (SGK1) regulates insulin sensitivity in mice via extracellular-signal-regulated kinase 1/2 (ERK1/2). Biochem J. 2014;464(2):281-9. doi: 10.1042/BJ20141005.

114. Ng SSW, Tsao MS, Chow S, Hedley DW. Inhibition of phosphatidylinositide 3-kinase enhances gemcitabine-induced apoptosis in human pancreatic cancer cells. Cancer Res. 2000;60(19):5451-5.

115. Criscitiello C, Viale G, Curigliano G, Goldhirsch A. Profile of buparlisib and its potential in the treatment of breast cancer: evidence to date. Breast Cancer (Dove Med Press). 2018;10:23-9. doi: 10.2147/BCTT.S134641.

116. Ulrich HD. The fast-growing business of SUMO chains. Mol Cell. 2008;32(3):301-5. doi: 10.1016/j.molcel.2008.10.010.

117. Gill G. SUMO and ubiquitin in the nucleus: different functions, similar mechanisms? Genes Dev. 2004;18(17):2046-59. doi: 10.1101/gad.1214604.

118. Plant LD, Dementieva IS, Kollewe A, Olikara S, Marks JD, Goldstein SA. One SUMO is sufficient to silence the dimeric potassium channel K2P1. Proc Natl Acad Sci U S A. 2010;107(23):10743-8. doi: 10.1073/pnas.1004712107.

119. Rajan S, Plant LD, Rabin ML, Butler MH, Goldstein SA. Sumoylation silences the plasma membrane leak K+ channel K2P1. Cell. 2005;121(1):37-47. doi: 10.1016/j.cell.2005.01.019.

120. Rajan S, Dickson LM, Mathew E, Orr CM, Ellenbroek JH, Philipson LH, et al. Chronic hyperglycemia downregulates GLP-1 receptor signaling in pancreatic beta-cells via protein kinase A. Mol Metab. 2015;4(4):265-76. doi: 10.1016/j.molmet.2015.01.010.

121. Kang JS, Saunier EF, Akhurst RJ, Derynck R. The type I TGF-beta receptor is covalently modified and regulated by sumoylation. Nat Cell Biol. 2008;10(6):654-64. doi: 10.1038/ncb1728.

122. Tang Z, El Far O, Betz H, Scheschonka A. Pias1 interaction and sumoylation of metabotropic glutamate receptor 8. J Biol Chem. 2005;280(46):38153-9. doi: 10.1074/jbc.M508168200.

123. Minami S, Ito K, Honma M, Ikebuchi Y, Anzai N, Kanai Y, et al. Posttranslational regulation of Abcc2 expression by SUMOylation system. Am J Physiol Gastrointest Liver Physiol. 2009;296(2):G406-13. doi: 10.1152/ajpgi.90309.2008.

124. Giorgino F, de Robertis O, Laviola L, Montrone C, Perrini S, McCowen KC, et al. The sentrin-conjugating enzyme mUbc9 interacts with GLUT4 and GLUT1 glucose transporters and regulates transporter levels in skeletal muscle cells. Proc Natl Acad Sci U S A. 2000;97(3):1125-30.

125. Ulrich HD. Mutual interactions between the SUMO and ubiquitin systems: a plea of no contest. Trends Cell Biol. 2005;15(10):525-32. doi: 10.1016/j.tcb.2005.08.002.

126. Desterro JM, Rodriguez MS, Hay RT. SUMO-1 modification of IkappaBalpha inhibits NF-kappaB activation. Mol Cell. 1998;2(2):233-9.

127. Soodvilai S, Chatsudthipong V, Evans KK, Wright SH, Dantzler WH. Acute regulation of OAT3-mediated estrone sulfate transport in isolated rabbit renal proximal tubules. Am J Physiol Renal Physiol. 2004;287(5):F1021-9. doi: 10.1152/ajprenal.00080.2004.

128. Subramaniam S, Shahani N, Strelau J, Laliberte C, Brandt R, Kaplan D, et al. Insulin-like growth factor 1 inhibits extracellular signal-regulated kinase to promote neuronal survival via the phosphatidylinositol 3-kinase/protein kinase A/c-Raf pathway. J Neurosci. 2005;25(11):2838-52. doi: 10.1523/JNEUROSCI.5060-04.2005.

129. Isobe K, Jung HJ, Yang CR, Claxton J, Sandoval P, Burg MB, et al. Systems-level identification of PKA-dependent signaling in epithelial cells. Proc Natl Acad Sci U S A. 2017;114(42):E8875-E84. doi: 10.1073/pnas.1709123114.

130. Muller S, Matunis MJ, Dejean A. Conjugation with the ubiquitin-related modifier SUMO-1 regulates the partitioning of PML within the nucleus. EMBO J. 1998;17(1):61-70. doi: 10.1093/emboj/17.1.61.

131. Yang SH, Jaffray E, Senthinathan B, Hay RT, Sharrocks AD. SUMO and transcriptional repression: dynamic interactions between the MAP kinase and SUMO pathways. Cell Cycle. 2003;2(6):528-30. doi: 10.4161/cc.2.6.597.

132. Hietakangas V, Ahlskog JK, Jakobsson AM, Hellesuo M, Sahlberg NM, Holmberg CI, et al. Phosphorylation of serine 303 is a prerequisite for the stress-inducible SUMO modification of heat shock factor 1. Mol Cell Biol. 2003;23(8):2953-68.

133. Bach LA, Hale LJ. Insulin-like growth factors and kidney disease. Am J Kidney Dis. 2015;65(2):327-36. doi: 10.1053/j.ajkd.2014.05.024.

134. Yakar S, Adamo ML. Insulin-like growth factor 1 physiology: lessons from mouse models. Endocrinol Metab Clin North Am. 2012;41(2):231-47, v. doi: 10.1016/j.ecl.2012.04.008.

135. Giustina A, Chanson P, Kleinberg D, Bronstein MD, Clemmons DR, Klibanski A, et al. Expert consensus document: A consensus on the medical treatment of acromegaly. Nat Rev Endocrinol. 2014;10(4):243-8. doi: 10.1038/nrendo.2014.21.

136. Janecka A, Kolodziej-Rzepa M, Biesaga B. Clinical and Molecular Features of Laron Syndrome, A Genetic Disorder Protecting from Cancer. In Vivo. 2016;30(4):375-81.

137. Bang P, Polak M, Woelfle J, Houchard A, Group EIRS. Effectiveness and Safety of rhIGF-1 Therapy in Children: The European Increlex(R) Growth Forum Database Experience. Horm Res Paediatr. 2015;83(5):345-57. doi: 10.1159/000371798.

138. Wu W, Dnyanmote AV, Nigam SK. Remote communication through solute carriers and ATP binding cassette drug transporter pathways: an update on the remote sensing and signaling hypothesis. Mol Pharmacol. 2011;79(5):795-805. doi: 10.1124/mol.110.070607.

139. Bush KT, Wu W, Lun C, Nigam SK. The drug transporter OAT3 (SLC22A8) and endogenous metabolite communication via the gut-liver-kidney axis. J Biol Chem. 2017;292(38):15789-803. doi: 10.1074/jbc.M117.796516.

140. Wu W, Jamshidi N, Eraly SA, Liu HC, Bush KT, Palsson BO, et al. Multispecific drug transporter Slc22a8 (Oat3) regulates multiple metabolic and signaling pathways. Drug Metab Dispos. 2013;41(10):1825-34. doi: 10.1124/dmd.113.052647.

141. Wang H, Zhang J, You G. The mechanistic links between insulin and human organic anion transporter 4. Int J Pharm. 2019;555:165-74. doi: 10.1016/j.ijpharm.2018.11.040.

142. Wang H, Zhang J, You G. Activation of Protein Kinase A Stimulates SUMOylation, Expression, and Transport Activity of Organic Anion Transporter 3. AAPS J. 2019;21(2):30. doi: 10.1208/s12248-019-0303-4.

143. Yeh ET, Gong L, Kamitani T. Ubiquitin-like proteins: new wines in new bottles. Gene. 2000;248(1-2):1-14.

144. Yeh ET. SUMOylation and De-SUMOylation: wrestling with life's processes. J Biol Chem. 2009;284(13):8223-7. doi: 10.1074/jbc.R800050200.

145. Zhang J, Liu C, You G. AG490, a JAK2-specific inhibitor, downregulates the expression and activity of organic anion transporter-3. J Pharmacol Sci. 2018;136(3):142-8. doi: 10.1016/j.jphs.2018.01.006.

146. Duan P, You G. Novobiocin is a potent inhibitor for human organic anion transporters. Drug Metab Dispos. 2009;37(6):1203-10. doi: 10.1124/dmd.109.026880.

147. Toh MF, Suh W, Wang H, Zhou P, Hu L, You G. Inhibitory effects of chemotherapeutics on human organic anion transporter hOAT4. Int J Biochem Mol Biol. 2016;7(1):11-8.

148. Akarawut W, Smith DE. Competitive inhibition of p-aminohippurate transport by quinapril in rabbit renal basolateral membrane vesicles. J Pharmacokinet Biopharm. 1998;26(3):269-87.

149. Burlingham BT, Widlanski TS. An intuitive look at the relationship of K-i and IC50: A more general use for the Dixon plot. J Chem Educ. 2003;80(2):214-8. doi: DOI 10.1021/ed080p214.

150. Cer RZ, Mudunuri U, Stephens R, Lebeda FJ. IC50-to-Ki: a web-based tool for converting IC50 to Ki values for inhibitors of enzyme activity and ligand binding. Nucleic Acids Res. 2009;37(Web Server issue):W441-5. doi: 10.1093/nar/gkp253.